

# **Myeloid corticoid receptors in CNS autoimmunity:**

## **Old targets for novel therapies**

Dissertation

In partial fulfillment of the requirements for the degree  
“Doctor rerum naturalium (Dr. rer. nat.)”  
of the Georg-August University Göttingen

within the “Molecular Medicine” Study Program  
at the Georg-August University School of Science (GAUSS)

submitted by

**Elena Victoria Montes Cobos**

born in

**Badajoz, Spain**

Göttingen, April 2016

## **THESIS COMMITTEE**

### **Prof. Dr. Holger M. Reichardt**

**(First referee)**

Institute for Cellular and Molecular Immunology  
University Medical Center, Göttingen

### **Prof. Dr. Lutz Walter**

**(Second referee)**

Dep. of Primate Genetics  
German Primate Center, Göttingen

### **PD Dr. Fred Lühder**

Dep. of Neuroimmunology  
Institute for Multiple Sclerosis Research and the Hertie Fondation  
University Medical Center, Göttingen

## **ADDITIONAL MEMBERS OF THE EXAMINATION BOARD**

### **Prof. Dr. Christine Stadelmann-Nessler**

Institute for Neuropathology  
University Medical Center, Göttingen

### **Prof. Dr. mult. Thomas Meyer**

Lab. for Molecular Psychocardiology  
University Medical Center, Göttingen

### **Prof. Dr. Hubertus Jarry**

Dep. of Clinical and Experimental Endocrinology  
University Medical Center, Göttingen

Date of the oral examination: 15<sup>th</sup> June 2016

## **AFFIDAVIT**

I hereby declare that I have written this PhD thesis entitled “Myeloid corticoid receptors in CNS autoimmunity: Old targets for novel therapies” independently and with no other sources and aids than quoted. This thesis has not been submitted elsewhere for any academic degree.

---

Elena Victoria Montes Cobos

April 2016  
Göttingen, Germany

# TABLE OF CONTENTS

ABSTRACT .....	viii
LIST OF FIGURES .....	ix
LIST OF TABLES .....	xi
ABBREVIATIONS .....	xii
<b>1 INTRODUCTION .....</b>	<b>1</b>
<b>1.1 Multiple Sclerosis: the paradigm of CNS autoimmunity.....</b>	<b>1</b>
1.1.1 Multiple Sclerosis .....	2
1.1.2 Animal models of MS - Experimental autoimmune encephalomyelitis .....	3
<b>1.2 The cellular players of CNS autoimmune inflammation .....</b>	<b>5</b>
1.2.1 T cells functions in MS and EAE.....	7
1.2.2 The role of myeloid cells in CNS autoimmunity .....	10
<b>1.3 Immunomodulatory therapies for MS: glucocorticoids .....</b>	<b>14</b>
1.3.1 Glucocorticoid treatment in MS patients .....	14
1.3.2 Molecular and cellular basis of GCs immunosuppression .....	16
1.3.3 Mineralocorticoid receptor-mediated activities of GCs.....	17
1.3.4 Side effects of GC therapies .....	18
1.3.5 Emerging GC therapies: from dissociating ligands to nanoparticles.....	20
<b>1.4 Objectives.....</b>	<b>21</b>
<b>2 MATERIAL AND METHODS.....</b>	<b>23</b>
<b>2.1 Material.....</b>	<b>23</b>
2.1.1 General equipment .....	23
2.1.2 Consumables .....	25
2.1.3 Chemicals and reagents .....	26
2.1.4 Media, buffers and solutions .....	28
2.1.5 Enzymes and commercial kits .....	30
2.1.6 FACS Antibodies .....	31
2.1.7 IHC Antibodies.....	32

2.1.8	Oligonucleotides .....	33
2.1.9	Software .....	33
<b>2.2</b>	<b>Animal experimentation.....</b>	<b>34</b>
2.2.1	Mouse strains.....	34
2.2.2	Mouse genotyping .....	35
2.2.3	Tamoxifen-induction of SLO1C1 knockout mice .....	36
2.2.4	Anesthesia.....	36
2.2.5	Blood sample processing .....	36
<b>2.3</b>	<b><i>In vivo</i> assays.....</b>	<b>37</b>
2.3.1	EAE induction .....	37
2.3.2	<i>In vivo</i> T cell priming and proliferation .....	38
2.3.3	GC treatment .....	38
2.3.4	<i>In vivo</i> T cell apoptosis .....	39
2.3.5	Analysis of glucose metabolism .....	39
<b>2.4</b>	<b>Cellular methods.....</b>	<b>40</b>
2.4.1	Cell isolation from secondary lymphoid organs.....	40
2.4.2	Mononuclear cell isolation from the spinal cord .....	40
2.4.3	T cell purification.....	41
2.4.3.1	EasySep™ kit .....	41
2.4.3.2	Magnetic Activated Cell Sorting (MACS) .....	41
2.4.4	Macrophage isolation and culture .....	42
2.4.4.1	Induction of Bone Marrow-Derived Macrophages (BMDMs) .....	42
2.4.4.2	Induction and isolation of peritoneal macrophages .....	43
2.4.4.3	<i>In vitro</i> macrophage stimulation .....	43
2.4.5	CFSE staining .....	43
2.4.6	Flow cytometry (FACS).....	44
2.4.6.1	Extracellular staining .....	44
2.4.6.2	Intracellular staining.....	44
2.4.6.3	Annexin V apoptosis staining.....	44
<b>2.5</b>	<b><i>In vitro</i> assays .....</b>	<b>45</b>
2.5.1	<i>In vitro</i> T cell apoptosis .....	45
2.5.2	<i>In vitro</i> nanoparticle distribution in mixed cultures.....	45
2.5.3	<i>Ex vivo</i> re-stimulation of MOG-specific effector T cells .....	45
2.5.4	BMDM-mediated activation of MOG-specific T cells .....	46
<b>2.6</b>	<b>Histology.....</b>	<b>46</b>

2.6.1	Isolation and fixation of spinal cords .....	46
2.6.2	Immunohistochemistry (IHC) .....	47
2.6.3	Luxol fast blue Periodic acid-Schiff (LFB-PAS) .....	47
2.6.4	Bielschowsky silver staining .....	48
<b>2.7</b>	<b>Molecular methods .....</b>	<b>48</b>
2.7.1	DNA isolation from biopsies.....	48
2.7.2	Polymerase chain reaction (PCR) .....	49
2.7.3	RNA isolation.....	49
2.7.4	cDNA synthesis.....	50
2.7.5	Quantitative real-time PCR (qRT-PCR) .....	50
2.7.6	Enzyme-linked immuno-absorbent assay (ELISA) .....	51
2.7.7	Cytometric Bead Array (CBA) .....	51
<b>2.8</b>	<b>Statistical analysis.....</b>	<b>52</b>
<b>3</b>	<b>RESULTS .....</b>	<b>53</b>
<b>3.1</b>	<b>EAE therapy with betamethasone nanoparticles .....</b>	<b>53</b>
3.1.1	BNPs are preferentially taken up by myeloid cells.....	53
3.1.2	BNPs are more potent in modulating macrophages than T cell activity <i>in vivo</i> .....	55
3.1.3	BNPs modulate macrophage and T cell functions via the GR .....	58
3.1.4	BNPs efficiently ameliorate EAE in mice .....	61
3.1.5	Myeloid cells are essential targets of BNPs in EAE therapy .....	64
3.1.6	BNPs and Dex act synergistically in the treatment of EAE .....	67
3.1.7	BNPs partially circumvent GC-associated side-effects.....	68
3.1.7.1	Glucose metabolism .....	69
3.1.7.2	Muscle wasting.....	70
3.1.7.3	Stomach emptying.....	71
3.1.7.4	Bone re-sorption.....	72
<b>3.2</b>	<b>Role of the MR in myeloid cells in EAE.....</b>	<b>74</b>
3.2.1	MR <sup>lysM</sup> mice develop a milder EAE disease .....	74
3.2.2	MR deletion alters the activation state of circulating and CNS-infiltrating monocytes.....	79
3.2.3	Monocytes and neutrophils in secondary lymphoid organs are not affected by the MR deletion ...	81
3.2.4	T cell interactions with MR <sup>lysM</sup> macrophages.....	82
3.2.4.1	The cytokine secretion profile is altered in MR-deficient BMDMs.....	83
3.2.4.1	MR <sup>lysM</sup> macrophages are potent APCs in vitro .....	83
3.2.5	The role of T cells in the pathogenesis of EAE in MR <sup>lysM</sup> mice.....	85
3.2.5.1	MR-deficiency does not impair MOG-specific T cell priming in vivo .....	85

3.2.5.2	Secretion of Th1 and Th17 cytokines during EAE is impaired in MR <sup>lysM</sup> mice .....	86
3.2.5.3	MR deficiency in myeloid cells leads to increased numbers of peripheral Treg cells.....	87
3.2.6	The phenotype of microglia during EAE is altered in MR <sup>lysM</sup> mice .....	89
<b>4</b>	<b>DISCUSSION .....</b>	<b>92</b>
<b>4.1</b>	<b>EAE therapy with betamethasone nanoparticles .....</b>	<b>92</b>
4.1.1	BNPs are anti-inflammatory in different immune cell types, albeit with different efficacy .....	93
4.1.2	Myeloid cells are major targets of BNPs in EAE therapy.....	94
4.1.3	Are BNPs a potential solution to GC-derived side effects? .....	96
4.1.4	BNP therapy: open questions and perspectives .....	98
<b>4.2</b>	<b>The role of the MR in myeloid cells during EAE .....</b>	<b>100</b>
4.2.1	MR deficiency in myeloid cells promotes M2-like polarization and causes a milder EAE phenotype.....	101
4.2.2	MR deletion in myeloid cells alters T cell responses during EAE .....	102
4.2.3	MR deletion in myeloid cells partially restores peripheral tolerance .....	105
<b>4.3</b>	<b>Conclusions.....</b>	<b>107</b>
<b>5</b>	<b>REFERENCES .....</b>	<b>108</b>
<b>6</b>	<b>ACKNOWLEDGEMENTS .....</b>	<b>127</b>

## ABSTRACT

Since the 1950s, glucocorticoids (GCs) have been the most widely employed drugs in the treatment of inflammatory and autoimmune disorders, such as multiple sclerosis (MS). Short-time application of high-dose GCs is the first line therapy for acute relapses of MS. Several clinical studies even suggest that prolonged GC pulsed therapy may slow down MS disease progression as well. However, a plethora of GC-associated side effects derived from the ubiquitous expression of the glucocorticoid receptor (GR) restricts the use of these drugs. Therefore, to assess the full potential of GCs new pharmacological formulations and more insights about their mechanisms of action are needed.

For many years, T cells were proposed to be major targets of GCs in the treatment of neuroinflammation. In contrast, the relevance of myeloid cells for GC therapy is highlighted in this doctoral thesis. Using experimental autoimmune encephalomyelitis (EAE) as a mouse model of CNS autoimmunity, we directed GC therapy to the myeloid compartment by means of state-of-the-art inorganic-organic hybrid nanoparticles (IOH-NPs). Although IOH-NPs loaded with betamethasone (BNPs) modulated both T cell survival and macrophage activation *in vitro*, *in vivo* BNPs selectively targeted myeloid cells. Moreover, BNPs achieved a therapeutic efficacy comparable to free GCs in the treatment of EAE. In this study BNPs were also proposed as an alternative to circumvent GC-derived side effects, however our data did not provide conclusive information in this respect yet.

Additionally, the roles of the two different GC-responsive nuclear receptors, the GR and the mineralocorticoid receptor (MR), were investigated in myeloid cells. In this cell compartment, GCs can act either via the GR in a deactivating manner, or via the MR promoting a pro-inflammatory state. Hence, we hypothesized that altering the balance between the GR and the MR might influence the course of EAE. Indeed, mice selectively devoid of MR in myeloid cells developed a milder EAE disease course compared to their littermate controls, and presented with a lower degree of demyelination. Consistent with these results, monocytes/macrophages exhibited a M2 phenotype in both the CNS and the periphery, and the proportion of reactive microglia in the spinal cord was reduced as well. Furthermore, our experiments revealed that, in consequence of the general myeloid anti-inflammatory state, Treg cell numbers increased in secondary lymphoid organs, where cytokine release by effector T cells was consequently impaired.

Taken together, this study provides evidence of the important implications of myeloid cells in the response to GCs during autoimmune inflammation, and supports the targeted delivery to the myeloid compartment as an alternative to improve the therapeutic features of synthetic GCs.



## LIST OF FIGURES

<b>Figure 1.1</b>   Immune cells participating in MS and EAE pathology. ....	6
<b>Figure 1.2</b>   Macrophage polarization induced by different stimuli. ....	12
<b>Figure 2.1</b>   EAE induction protocol. ....	37
<b>Figure 2.2</b>   FACS gating strategy for different T cell subsets .....	39
<b>Figure 3.1</b>   BNPs are efficiently but differentially taken up by immune cells <i>in vitro</i> .....	54
<b>Figure 3.2</b>   BNPs exert potent immunosuppressive activity on peritoneal macrophages <i>in vivo</i> ... ..	56
<b>Figure 3.3</b>   BNPs do not efficiently induce T cell apoptosis <i>in vivo</i> .....	58
<b>Figure 3.4</b>   BNPs do not reduce MHC class II expression on GR <sup>lysM</sup> macrophages <i>in vivo</i> . ....	59
<b>Figure 3.5</b>   BNPs depend on the presence of the GR for the induction of T cell apoptosis.....	60
<b>Figure 3.6</b>   The therapeutic efficacy of BNPs in the treatment of EAE is similar to free GCs. ....	62
<b>Figure 3.7</b>   BNPs improve myelin pathology during EAE. ....	63
<b>Figure 3.8</b>   BNPs reduce macrophage infiltration during EAE therapy.....	65
<b>Figure 3.9</b>   Myeloid cells are essential targets of BNPs in the treatment of EAE. ....	67
<b>Figure 3.10</b>   Combined treatment with BNPs and Dex synergistically improves EAE.. ....	68
<b>Figure 3.11</b>   Short treatment with BNPs affects glucose metabolism similarly to Dex. ....	70
<b>Figure 3.12</b>   Short treatment with BNP hardly affects muscle wasting.....	71
<b>Figure 3.13</b>   Short treatment with BNPs and Dex has a mild effect on gastric emptying .....	72
<b>Figure 3.14</b>   Short treatment with BNPs does not affect the osteoporosis marker osteocalcin.....	73
<b>Figure 3.15</b>   MR <sup>lysM</sup> mice develop a milder EAE phenotype.. ....	75
<b>Figure 3.16</b>   Macrophage infiltration into the spinal cord is reduced in MR <sup>lysM</sup> mice during EAE.....	77
<b>Figure 3.17</b>   Demyelination and axonal damage in MR <sup>lysM</sup> mice during EAE are not as severe as in MR <sup>fl</sup> mice. ....	78

**Figure 3.18** | The percentage of inflammatory monocytes in blood and spinal cord of MR<sup>lysM</sup> mice is reduced during EAE. .... 80

**Figure 3.19** | Inflammatory monocytes and neutrophils are unaffected in secondary lymphoid organs of MR<sup>lysM</sup> mice during EAE.. .... 82

**Figure 3.20** | MR-deficient BMDMs secrete less M1 cytokines, whereas M2 cytokine release is increased. .... 83

**Figure 3.21** | MR<sup>lysM</sup> BMDMs stimulate MOG<sub>35-55</sub>-specific stimulation of 2D2 T cell proliferation *in vitro*..... 84

**Figure 3.22** | T cell priming in MR<sup>lysM</sup> mice in the early phases of EAE is unaffected..... 86

**Figure 3.23** | Secretion of pro-inflammatory cytokines by effector T cells is reduced in the secondary lymphoid organs of MR<sup>lysM</sup> mice before the onset of EAE. .... 87

**Figure 3.24** | The frequency of Treg cells in peripheral lymphoid organs is increased in MR<sup>lysM</sup> mice.. .... 89

**Figure 3.25** | The frequency of reactive microglia in the spinal cord of MR<sup>lysM</sup> mice is reduced. .... 91

## LIST OF TABLES

<b>Table 1.1</b>   General equipment.....	23
<b>Table 1.2</b>   Consumables .....	25
<b>Table 1.3</b>   Chemicals and reagents.....	26
<b>Table 1.4</b>   Media.....	28
<b>Table 1.5</b>   Buffers and solutions.....	29
<b>Table 1.6</b>   Enzymes and commercial kits.....	30
<b>Table 1.7</b>   Antibodies for flow cytometry.....	31
<b>Table 1.8</b>   Antibodies for immunohistochemistry.....	32
<b>Table 1.9</b>   Primers for qRT-PCR .....	33
<b>Table 1.10</b>   Software .....	33
<b>Table 1.11</b>   PCR reagents and thermocycler program.....	49
<b>Table 1.12</b>   qRT-PCR reagents and thermocycler program.....	50

## ABBREVIATIONS

11 $\beta$ -HSD II	11-Beta hydroxysteroid dehydrogenase type II
2-PM	2-photon microscopy
Abs	Antibodies
AIA	Adjuvant-induced experimental arthritis
AP-1	Activator protein 1
APC	Antigen presenting cell
APC	Allophycocyanine
Arg-1	Arginase 1
BBB	Blood Brain Barrier
Bcl-2	B cell lymphoma 2
BMDM	Bone marrow-derived macrophage
BMZ	Betamethasone
BNP	Betamethasone nanoparticle
CBA	Cytometric bead assay
CCL	CC chemokine ligand
CD	Cluster of differentiation
CCR	CC chemokine receptor
cDNA	Complementary DNA
CFA	Complete Freund's adjuvant
CFSE	Carboxyfluorescein succinimidyl ester
CNS	Central nervous system
CSF	Cerebrospinal fluid
CXCL	CXC chemokine ligand
CXCR	CXC chemokine receptor
DC	Dendritic cell
ddH <sub>2</sub> O	Double-distilled water
Dex	Dexamethasone
DMEM	Dulbecco modified Eagle's medium
DNA	Deoxyribonucleic acid

EAE	Experimental autoimmune encephalomyelitis
ELISA	Enzyme linked immunoadsorbent assay
EMA	European Medicines Agency
ENP	Empty phosphate nanoparticles
FACS	Fluorescence-activated cell sorting
FDA	Food and drug administration
FITC	Fluorescein isothiocyanate
FMN	Flavin mononucleotide
FoxP3	Forkhead box P3
g	Gram
GA	Glatiramer acetate
GFP	Green fluorescent protein
GC	Glucocorticoid
GILZ	Glucocorticoid-induced leucine zipper
GM-CSF	Granulocyte-macrophage colony stimulating factor
GR	Glucocorticoid receptor
GRE	Glucocorticoid responsive element
h	Hour
HRP	Horseradish peroxidase
ICAM-1	Intercellular adhesion molecule 1
IFN $\gamma$	Interferon gamma
Ig	Immunoglobuline
IHC	Immunohistochemistry
IL-	Interleukine
iNOS	Inducible nitric oxide synthase
IOH-NPs	Inorganic-organic hybrid nanoparticles
i.p.	Intraperitoneal
i.v.	Intravenously
IVC	Individually ventilated cages
IVMP	Intravenous methylprednisolone
LCCM	L-929 conditioned medium
LFB-PAS	Luxol fast-blue periodic acid-Schiff
LN	Lymph node
LPS	Lipopolysaccharide
M	Molar

MACS	Magnetic-activated cell sorting
MBP	Myelin basic protein
MCP-1	Monocyte chemoattractant protein 1
MFI	Mean fluorescence intensity
MHC	Major histocompatibility complex
min	Minute
ml	Milliliter
MM	Meningeal macrophage
MMP	Matrix metalloproteinase
MR	Mineralocorticoid receptor
MRI	Magnetic resonance imaging
mRNA	Messenger ribonucleic acid
M-CSF	Macrophage colony-stimulating factor
MOG	Myelin oligodendrocyte glycoprotein
MS	Multiple sclerosis
NFκB	Nuclear factor κB
NO	Nitric oxide
O/N	Overnight
PBS	Phosphate buffered saline
PCR	Polymerase chain reaction
PE	Phycoerythrin
PEG	Polyethylen glycol
PFA	Paraformaldehyde acid
PL	Liposomal prednisolone
PPMS	Primary progressive MS
PRMS	Progressive relapsing MS
PRR	Pattern-recognition receptor
PVM	Perivascular macrophage
qRT-PCR	Quantitative real time PCR
ReMed	Re-stimulation medium
RFP	Red fluorescent protein
ROS	Reactive oxygen species
RRMS	Relapsing-remitting MS
RT	Room Temperature
SEM	Standard error of the mean

s.c.	Subcutaneously
SFP	Specific pathogen-free
SPMS	Secondary progressive MS
Th cell	T helper cell
TLR	Toll-like receptor
TNF $\alpha$	Tumor necrosis factor alpha
Treg cell	Regulatory T cell
VCAM-1	Vascular adhesion molecule 1
wt	Wild type
ZrO <sub>2</sub>	Zirconium oxide

# 1 INTRODUCTION

## 1.1 Multiple Sclerosis: the paradigm of CNS autoimmunity

In the beginning of the 20th century, Paul Ehrlich (awarded in 1908 with the Nobel Prize for his work in immunology) described for the first time the responses of the immune system to its own organism, what he defined as '*horror autotoxicus*'. His observations set the basis of the concept of **autoimmunity** (Ehrlich P. and Morgenroth J. 1957).

Autoimmune responses arise as a consequence of the breakdown of self-tolerance, a process tightly regulated in the lymphoid organs. Once self-reactive lymphocytes escape central tolerance in the thymus or bone marrow, the mechanisms of peripheral tolerance, like regulatory immune cells, become crucial to prevent exacerbated immune responses against self antigens. Failure of these regulatory mechanisms due to genetic factors or external triggers alters innate immunity and results in the development of autoimmune diseases.

Certain organs, defined as immune privileged, lack conventional lymphatic vasculature and are delimited by functional and anatomical barriers that restrict the access of immune cells. One example of immune privileged organ is the **central nervous system (CNS)**, which is surrounded by the blood-brain barrier (BBB). Although nowadays the view of the CNS as immune privileged is in question (Carson et al. 2006; Iliff et al. 2015), for many years this organ was believed to be exempt from immune responses (Medawar 1948; Barker and Billingham 1972). However, in some cases the brain also becomes target of auto-reactive immune cells. CNS antigens are constantly released to induce peripheral tolerance (Harris et al. 2014), but if antigen-specific lymphocytes recognize them as non-self and get activated, these antigens are able to induce changes in the BBB permeability to enter the CNS, thereby starting an inflammatory process that may result in autoimmunity. This situation is clearly reflected by the autoimmune pathology in multiple sclerosis (MS).



### 1.1.1 Multiple Sclerosis

MS is the most common inflammatory disease of the CNS and is characterized by focal myelin loss and axonal damage within the white matter. This neurodegenerative process leads to severe motor, sensory and cognitive deficits. The disorder affects around 2.5 million people worldwide (Compston and Coles 2002), with a particularly increasing prevalence in North America and Europe, where >100/100.000 inhabitants suffer from it (Leray et al. 2016). The first symptoms, which include blurred vision and muscle weakness, normally appear between 20 and 40 years of age, and the disease is two times more prevalent in females than in male individuals.

It was Jean Martin Charcot who in 1868 first described the symptomatology associated with sclerotic plaques in patients with neurologic dysfunction, although those neuroanatomic observations had already been depicted years before by Robert Carswell (1838) and Jean Cruveilhier (1842). MS lesions are defined by four histopathological features: inflammation, astrogliosis, demyelination and axonal loss, the latter being the direct cause of the neurological disabilities in MS patients. Nevertheless, depending on the patient and the disease stage the lesions can present with different demyelination patterns, and the contribution of distinct immune infiltrates may vary (Lucchinetti et al. 2000; Lassmann et al. 2007). This complexity is also reflected by the high inter-individual variability of symptoms and disease progression. Based on that, patients can be grouped in four different modalities of MS (Hauser and Goodwin 2008):

- *Relapsing-remitting MS (RRMS)*: this is the most prevalent form of MS (85% of the cases), in which patients suffer from sporadic episodes of neurological impairment with full or partial recovery. In this phase of the disease, inflammatory infiltrates are the major component of the lesion.
- *Secondary progressive MS (SPMS)*: also characterized by a relapsing fashion but with persistence of disability after each relapse with periods of no remission. It often develops in patients with a previous history of RRMS, and at this stage inflammation gives its leading role up to a more prominent demyelinating pathology and the subsequent axonal damage.

- *Primary progressive MS (PPMS)*: affects 10% of MS patients and is the most severe variant due to its unresponsiveness to conventional therapies. These patients accumulate deficits progressively from the beginning of the disease, and no remission phases occur.
- *Progressive relapsing MS (PRMS)*: this rare form of MS shares the progressive course of PPMS with flare-ups that lead to acute worsening of the symptoms.

Despite the efforts made to determine the causes of MS, little is known about the etiology of the disease. As other autoimmune disorders, MS is believed to arise from a combination of genetic and environmental factors. Among all possible environmental triggers, epidemiological studies show that high-salt diet, Vitamin D deficiency and smoking are most relevant (Kleinewietfeld et al. 2013; Hedström et al. 2015; Hucke et al. 2016; Mimura et al. 2016). Some bacterial and viral infections have also been linked to MS, particularly infection with Epstein-Barr virus (Fernández-Menéndez et al. 2016). Apart from the external factors, the higher incidence of MS among relatives suggests a genetic component of the disease (Sadovnick 1993). Different polymorphisms of genes involved in immune responses have been identified as risk factors in genome-wide association studies. The strongest association with a higher MS susceptibility was found in the DRB1\*15:01 allele of the human leukocyte antigen (HLA) complex (Sawcer et al. 2011), but also specific allelic variants of genes coding for cytokines receptors (IL2RA and IL7R) or co-stimulatory molecules (CD58, CD80 and CD86) have been reported to increase the predisposition to MS (Hafler et al. 2007; Sawcer et al. 2011; Traboulsee et al. 2014).

### **1.1.2 Animal models of MS - Experimental autoimmune encephalomyelitis**

The complexity and the wide heterogeneity of MS make it a difficult matter of study. Nevertheless, throughout the years several rodent and non-human primate models resembling different aspects of MS pathology have provided useful information for the understanding of the disease, and have been essential tools for the development of the current MS therapies.

Damage of the myelin sheaths of the nerves followed by only partial re-myelination is a hallmark of MS. To study the mechanisms involved in myelin loss and regeneration, there are several animal models available based on toxic or viral agents. Toxic-induced demyelination is achieved with lysolecithin or cuprizone, a copper chelating compound that induces oligodendroglial cell death, affecting almost exclusively this cell type (Matsushima and Morell 2001). As an alternative, neurotropic viral infection with Theiler's murine encephalitis virus (TMEV) has the advantage of including the inflammatory component typical from MS, as CNS infiltrates are found in the TMEV-infected mice (Tsunoda et al. 2006).

Despite not being the model of choice for demyelination studies, **experimental autoimmune encephalomyelitis (EAE)** is most extensively employed and mimics more aspects of the autoimmune pathology from MS patients. This model was developed by Rivers and colleagues using monkeys that were immunized with rabbit brain extracts, which resulted in paralysis associated with perivascular infiltrates and demyelination (Rivers et al. 1933). Nowadays, the immunogens used for EAE induction in rodents and non-human primates are components of the myelin sheaths, mostly myelin basic protein (MBP), proteolipid protein (PLP), myeloid oligodendrocyte glycoprotein (MOG), or peptides derived from the latter one. The disease course is characterized by progressive paralysis from the tail up to the forelimbs (Berard et al. 2010), and can be induced in different mouse and rat strains either via active immunization or adoptive transfer of encephalitogenic T cells. Similarly to the human disease, the progression pattern is highly variable: depending on the genetic background and the immunizing agent, EAE can follow a relapsing-remitting course (Lublin et al. 1981) or develop in a chronic-progressive way (Tuohy et al. 1989).

Noteworthy, EAE cannot be properly induced without the help of adjuvants. Complete Freund's Adjuvant (CFA), an oily solution containing heat-inactivated *M. tuberculosis* (Freund et al. 1947), induces Th1 responses thereby providing an immunological environment that favors the initiation of the disease (Smith et al. 2011). Additionally, *Pertussis* toxin facilitates the permeabilization of the BBB, and has other boosting effects like increasing adhesion molecules in lymphocytes, inducing maturation of dendritic cells (DCs) and suppressing regulatory T cells (Treg cells) (Hou et al. 2003; Kerfoot et al. 2004; Chen et al. 2006).

The EAE model has been a valuable tool to study MS pathomechanisms, nevertheless EAE is an artificially generated entity that differs in many aspects from human MS (Procaccini et al. 2015). First of all, the use of inbred strains does not reflect the complex human heterogeneity. Furthermore, disease initiation is controlled and induced under the effect of strong adjuvants, thus we cannot obtain information about the natural causes of MS. Another limiting factor is that inflammation and demyelination in EAE are restricted to the spinal cord white matter, while MS lesions are mostly found in the brain and cerebellar cortex. And moreover, EAE is mainly driven by CD4<sup>+</sup> T cells, and little information about the role of CD8<sup>+</sup> T cells or B cells can be obtained. Some of these issues were addressed in the recent years thanks to alternative EAE models with transgenic animals and different induction protocols (Litzenburger et al. 1998; Ford and Evavold 2005; Bettelli 2007); nevertheless, new approaches are still needed to answer these questions.

## 1.2 The cellular players of CNS autoimmune inflammation

Although the mechanisms that initiate MS in humans remain elusive, many years of study on EAE models have provided a quite accurate picture of how the disease starts in rodents. In rough outlines, myelin peptides derived from the immunizing agents are presented by DCs in the lymph nodes and stimulate auto-reactive T cells that have escaped negative selection in the thymus. Afterwards, the autoantigen-specific activated T cells proliferate quickly and circulate until they encounter their cognate antigen in the CNS. Once there, they promote the open up of the BBB and secrete cytokines and chemokines that attract subsequent waves of immune cells, including more T cells, B cells and myeloid cells. The chronic inflammatory response established in the spinal cord damages the myelin cover of the nerves and, in some EAE models, eventually disrupts axonal structures. All this leads to the described symptomatology in the animals.

In summary, MS and EAE are complex entities where the interplay of different immune cells, belonging to both the innate and the adaptive immune system, determines their progression and final outcome (**Figure 1.1**). The specific roles of the key cell mediators of these CNS autoimmune reactions will be described below in more detail.

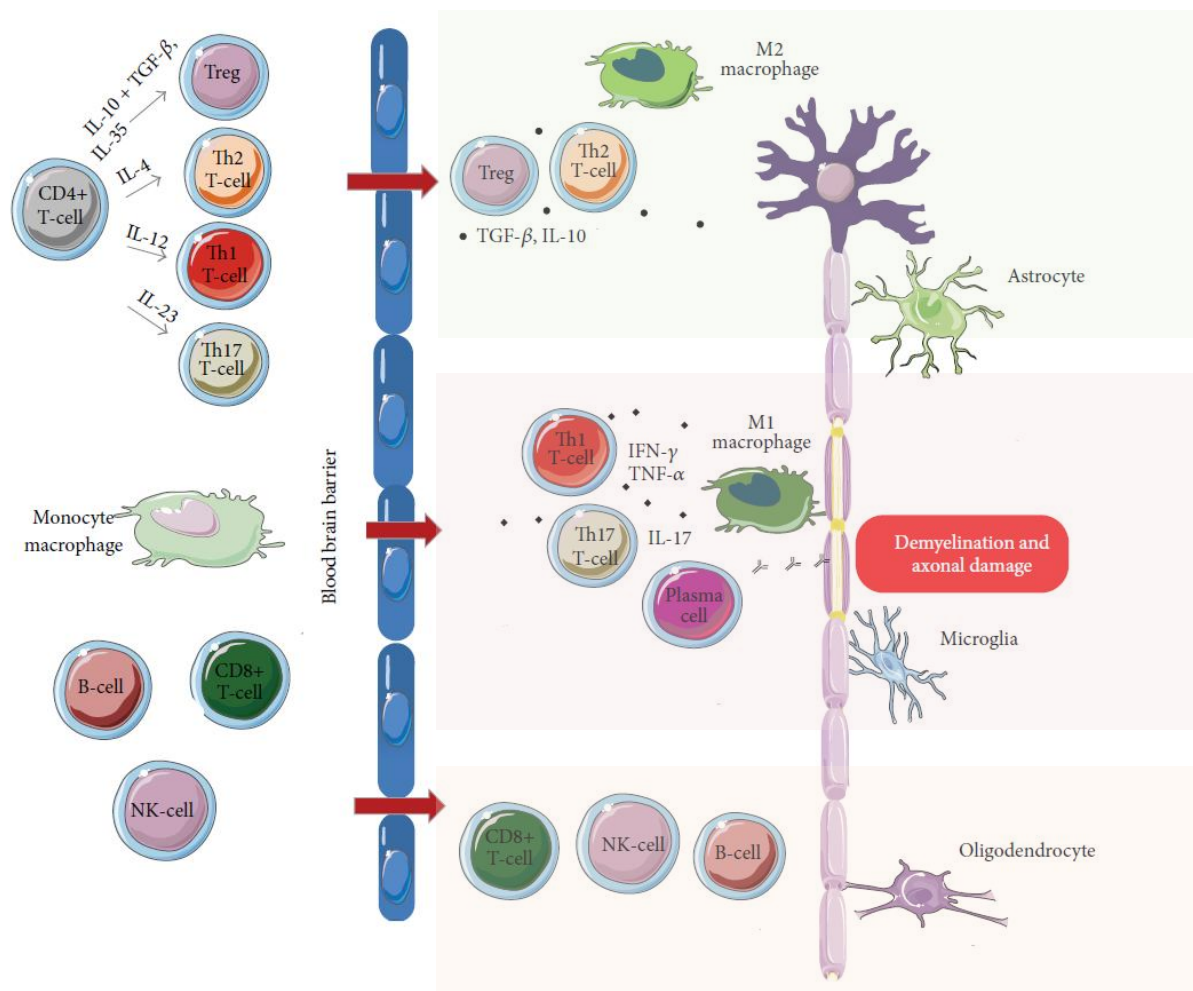


**Figure 1.1 | Immune cells participating in MS and EAE pathology.** In the initial stages of EAE, soluble mediators secreted by auto-reactive T cells facilitate the opening of breaches in the BBB, allowing the access of different immune cell types to the CNS. These cells can be subdivided into three groups according to their contribution to the disease. The first group consists of effector cells, with the mission of promoting inflammation, and includes Th1, Th17, antibody-secreting plasma cells and M1 macrophages. Another group of cells fulfill regulatory functions, important to control the exacerbation of the immune response; to this section belong Th2 cells, Treg cells, and M2 macrophages. Finally, the third part of this classification refers to cells with both inflammatory and regulatory activities, the roles of which in the context of EAE have not been fully elucidated yet: these are CD8<sup>+</sup> cells, NK cells and B cells. Beyond infiltrating leukocytes, also cells residing in the CNS, like microglia, astrocytes and oligodendrocytes, contribute to MS and EAE progression. *Adapted from Duffy et al. 2014.*

### 1.2.1 T cells functions in MS and EAE

MS and EAE have always been described as T cell-driven diseases. Evidence for this is that adoptive transfer of encephalitogenic T cells isolated from immunized mice is capable of inducing a strong disease course in healthy animals (Ben-Nun et al. 1981; Zamvil et al. 1985). T cells are, together with B cells, the major effectors of the adaptive immune response. Depending on the class of the MHC molecules encountered during thymic selection, naïve T cells can adopt two major phenotypes. On the one hand, T cells expressing the CD4 co-receptor, denominated T helper (Th) cells, are in charge of modulating immune responses via expression of membrane-bound molecules and secretion of cytokines and chemokines. Upon encounter with their cognate antigen (phenomenon defined as priming), signals provided by the antigen-presenting cell (APC) will determine their further differentiation into the Th1, Th2 or Th17 subsets, each one with specific effector functions (Mosmann et al. 1986; Langrish et al. 2005). On the other hand, CD8<sup>+</sup> T cells are specialized in eliminating harmful target cells, e.g. virally-infected cells, via direct cytotoxicity. Although both T cell types can be found in the CNS of animals with EAE, apparently CD4<sup>+</sup> T cells are the main mediators of the disease. In contrast, in human MS CD8<sup>+</sup> T cells are generally more abundant in the CSF of the patients (Koh et al. 1992; Babbe et al. 2000).

Since interferon gamma (IFN $\gamma$ )-secreting cells were present in the CNS of mice after immunization with MBP (Ando et al. 1989; Renno et al. 1994), EAE was initially considered a Th1-mediated pathology. In agreement with the Th1/Th2 dichotomy, Th2 cells (characterized by the production of IL-4, IL-5 and IL-13) were then proposed to protect from EAE (Adorini et al. 1996). This notion was confronted by other publications showing that TCR-engineered Th2 cells were also capable of inducing autoimmune CNS responses (Lafaille et al. 1997). **Th1 cells** secrete a cytokine profile that includes tumor necrosis factor alpha (TNF $\alpha$ ) and IFN $\gamma$ . Despite the active participation of these cytokines during neuroinflammation, their contribution to EAE and MS is under debate. Certain experiments performed with TNF $\alpha$ -deficient mice showed a delayed EAE onset and reduced infiltration into the CNS parenchyma (Körner et al. 1997), whereas other investigations pointed to a dispensable role of TNF $\alpha$  for EAE initiation and severity (Kassiotis et al. 1999; Batoulis et al. 2011). The contribution of IFN $\gamma$  to EAE and MS is equally controversial. Blockade of IFN $\gamma$ , but

not TNF $\alpha$ , reduced the number of active lesions in patients with SPMS (Skurkovich et al. 2001). Additionally, MS treatment with IFN $\gamma$  resulted in disease exacerbation (Panitch et al. 1987). However, in the late 90s several studies showed that IFN $\gamma$  deficiency aggravated the course EAE, suggesting a protective effect of the molecule (Ferber et al. 1996; Krakowski and Owens 1996; Chu et al. 2000). This hypothesis was further investigated with similar outcome in mice devoid of IL-12, the cytokine responsible of Th1 differentiation, or its different subunits (Becher et al. 2002; Gran et al. 2002; Zhang et al. 2003). But surprisingly, the deletion of the IL-12p40 subunit rendered the mice resistant to EAE, revealing the essential role of a new cytokine: IL-23 (Oppmann et al. 2000; Becher et al. 2003; Cua et al. 2003). IL-23 shares with IL-12 the p40 subunit and is responsible for the stability of a different Th phenotype, the Th17 subset (Langrish et al. 2005). These findings drastically changed the view of EAE as a Th1-driven disease and established the new lines of EAE research.

**Th17 cells** are now believed to be the initiators of EAE (Korn et al. 2007a). These cells are defined by the production of cytokines from the IL-17 family, especially IL-17A and IL-17F, although they secrete IL-6, IL-22, TNF $\alpha$  and GM-CSF as well. IL-17 exerts different activities during the early phases of EAE. First, it acts locally on the near tissues inducing the expression of cytokines and chemokines that are important for the mobilization and migration of myeloid cells to the inflamed CNS (e.g. CCL-7 and CCL-2). Moreover, IL-17 has a direct impact on the integrity of the BBB by disorganizing tight-junctions, inducing reactive oxygen species (ROS) and increasing the expression of adhesion molecules, such as ICAM-1, by endothelial cells (Huppert et al. 2010). Deletion of IL-17 or its receptor has been reported to significantly improve disease progression (Komiyama et al. 2006), however, it does not result in resistance to EAE (Haak et al. 2009; Kroenke and Segal 2011).

Noteworthy, Th17 cells have the ability to switch their phenotype to the Th1 subtype once they reach the CNS, and this plasticity appears to be controlled by IL-23 (Kurschus et al. 2010; Hirota et al. 2011). Hence, Th1 and Th17 responses complement each other rather than competing during EAE (Stromnes et al. 2008), and therefore the simultaneous secretion of IFN $\gamma$  and IL-17 can be found in the CNS of animals with EAE (Abromson-Leeman et al. 2009). The common denominator between these two T helper subsets is GM-CSF, a cytokine produced downstream to IL-23 that has been identified as the only molecule produced by T

cells strictly necessary for the development of EAE (Codarri et al. 2011; El-Behi et al. 2011). Probably the importance of this cytokine resides in its function as link between T cells and myeloid cells, since it promotes the release of myeloid progenitors from the bone marrow and influences the differentiation and polarization of cells from both immune cell types.

But not all T cell activities are detrimental for the CNS. The balance between effector and regulatory functions is essential to prevent autoimmune disorders, and to maintain this balance the adaptive immune system relies on **Treg cells**. This additional T cell subpopulation is originated either by thymic selection (naturally occurring Treg cells, nTreg cells) or in peripheral lymphoid organs during priming of naïve T cells (inducible Treg cells, iTreg cells). Induction of iTreg cells is strongly influenced by the cytokine milieu, and TGF $\beta$  is necessary for this differentiation. Importantly, TGF $\beta$  in combination with IL-6 also participates in the induction of Th17 cells, meaning that presumably the presence or absence of IL-6 determines the differentiation of naive CD4<sup>+</sup> T cells into either the Th17 or the Treg cell compartment (Xu et al. 2007; Korn et al. 2009). Moreover, the local environment may direct the conversion between both cell types (Xu et al. 2007; Koenen et al. 2008) and, in fact, some publications claimed that part of the Treg cells found in the CNS of mice with EAE originated from encephalitogenic T cells (Liu et al. 2006).

Treg cells are generally characterized by the expression of the phenotypic markers CD4, IL-2 receptor  $\alpha$ -chain (CD25) and the transcription factor FoxP3. Their potent suppression of immune effector functions is achieved via different mechanisms: first, indirect suppression via secretion of regulatory cytokines, such as IL-10, IL-35 and TGF $\beta$ , and second, cell-to-cell contact with effector T cells resulting in disrupted TCR-induced proliferation and reduced IL-2 secretion (Groux et al. 1997; Thornton and Shevach 2000; Sakaguchi et al. 2008).

Given the importance of Treg cells for the maintenance of tolerance, it was not surprising to find dysfunctional Treg cells in MS patients and mice with EAE (Viglietta et al. 2004; Haas et al. 2005). Treg cells have been shown to prevent the development of CNS inflammation and ameliorate EAE disease course (Kohm et al. 2003). Additionally, it has been described that during the remission phase of MS and EAE the number of Treg cells increases (Korn et al. 2007a; O'Connor et al. 2007), which highlights their participation in disease resolution.



### 1.2.2 The role of myeloid cells in CNS autoimmunity

The inflammatory activities of T cells would not be possible without the help of myeloid cells. Myeloid cells constitute the first line of defense against infections and moreover, establish the connection between innate and adaptive immune responses. These cells are especially relevant in EAE, since they recognize components of the adjuvants employed for immunization via pattern recognition receptors (PRRs), e.g. Toll-like receptors (TLRs) and provide a pre-activated cytokine milieu that is necessary for disease induction (Imrich and Harzer 2001).

All myeloid cells derive from a pluripotent common myeloid progenitor in the bone marrow, and differentiate into the different lineages (DCs, monocytes/macrophages and granulocytes) in response to signals from peripheral tissues. In the context of MS and EAE the three subsets of myeloid cells fulfill essential functions in the sequence of events leading to CNS inflammation. **DCs**, defined by the expression of CD11c and considered professional APCs, are the first ones to present myelin antigens to naïve T cells in the lymph nodes. Thus, fully functional DCs are strictly required for EAE initiation (Greter et al. 2005; Hertenberg et al. 2013). After activation and migration of Th17 cells, **neutrophils** (a granulocyte subtype characterized by the surface expression of Ly6G) are the next line of immune mediators. In SJL and Balb/C mice, impaired neutrophil migration to the CNS or treatment with neutrophil-depleting antibodies (Abs) resulted in delayed EAE onset and attenuated disease severity (McColl et al. 1998; Carlson et al. 2008). In the MOG<sub>35-55</sub>-induced EAE model, abundant Ly6G<sup>+</sup> infiltrates were found in the perivascular space during the asymptomatic phase of the disease (Soulaka et al. 2009). It is known that just before the onset of clinical symptoms, neutrophils are able to permeabilize the BBB via secretion of matrix metalloproteinase (MMPs) (Folgueras et al. 2008; Soulaka et al. 2009) and are neurotoxic in a contact-dependent and paracrine manner (Dinkel et al. 2004). In addition, because of their production of pro-inflammatory cytokines, neutrophils promote DC and monocyte maturation within the CNS, thereby supporting APC functions (Steinbach et al. 2013).

From all myeloid cells, the monocyte/macrophage compartment (defined by the expression of the phenotypic marker CD11b) is particularly interesting for MS and EAE, since it participates in all stages of disease progression either in an inflammatory or regulatory way.

Furthermore, they are the only immune cells with permanent representation within the CNS, where perivascular macrophages (PVMs), meningeal macrophages (MMs) and microglia are located.

Produced under the effect of GM-CSF in the bone marrow, **monocytes** circulate in blood and secondary lymphoid organs, and express chemokine receptors and adhesion molecules that mediate their infiltration into the inflamed tissue. There, they can differentiate into macrophages or DCs depending on the cytokine environment and the activation of PRRs. Monocytes can be subdivided into two different groups, CCR2<sup>+</sup> Ly6C<sup>high</sup> inflammatory monocytes, and CX3CR1<sup>+</sup> Ly6C<sup>low</sup> resting ones (Geissmann et al. 2003). It has been shown that deletion of CCR2 from these myeloid cells strongly ameliorates EAE clinical symptoms, which reveals a crucial role of inflammatory monocytes in CNS autoimmunity (Mildner et al. 2009).

**Macrophages**, due to their prominent phagocytic capacity, are essential elements of the host defense against pathogens, but also fulfill important homeostatic functions by clearing cellular debris allowing tissue remodeling (Mosser and Edwards 2008). Hence they function in a dual manner in the context of MS as well, contributing to both tissue injury and repair. Macrophages derive from blood monocytes (van Furth et al. 1972) that migrate to inflammatory sites following chemokine-traced paths. Some monocytes also replenish tissue-resident macrophages, populations that function as immune sentinels in specific niches. The main feature of macrophages is their remarkable plasticity. They have the appropriate receptor machinery to sense a wide diversity of signals and dynamically change their phenotype accordingly. Mirroring the Th1/Th2 classification, initially these phenotypes were divided into classically activated macrophages (M1) and alternatively activated ones (M2). This terminology, however, didn't reflect the real heterogeneity of macrophage activation. Nowadays, a full spectrum of polarization states ranging from M1 to M2 has been proposed, and every intermediate state should be independently defined depending on the specific activating stimuli (Mosser and Edwards 2008; Martinez and Gordon 2014; Hume 2015). In a simplified way (**Figure 1.2**), M1 polarization is primarily induced by INF $\gamma$ , TNF $\alpha$  and GM-CSF coming from Th1 cells, NK cells or macrophages themselves. Recognition of bacterial elements by PRRs, e.g. LPS through TLR4, can also trigger macrophage classical

activation. These stimuli promote elimination of pathogens by increasing phagocytosis and antigen presentation, a process that involves up-regulation of MHC class II and the co-stimulatory molecules CD80 and CD86. M1 macrophages also enhance their expression of the inducible nitric oxide synthase (iNOS, NOS2) and secrete pro-inflammatory cytokines such as IL-1 $\beta$ , IL-6, IL-12, IL-23 and TNF $\alpha$ . Conversely, alternative macrophage activation by IL-4 and IL-13 supports clearance of parasites via expression of the mannose receptor (CD206), an important mediator of endocytosis, and secretion of polyamines. Additional markers of this macrophage phenotype are Arginase-1 (Arg-1), Fizz1 and Ym1 (R szer 2015). In parallel, IL-10 and glucocorticoids (GCs) have the ability to induce a different alternative phenotype involved in immune regulation and tissue remodeling, defined by Mantovani as M2c or deactivated state (Mantovani et al. 2004; Kleiman et al. 2012; R szer 2015). This phenotype is characterized by the expression of IL-10, TGF $\beta$ , CD206 and CD163.

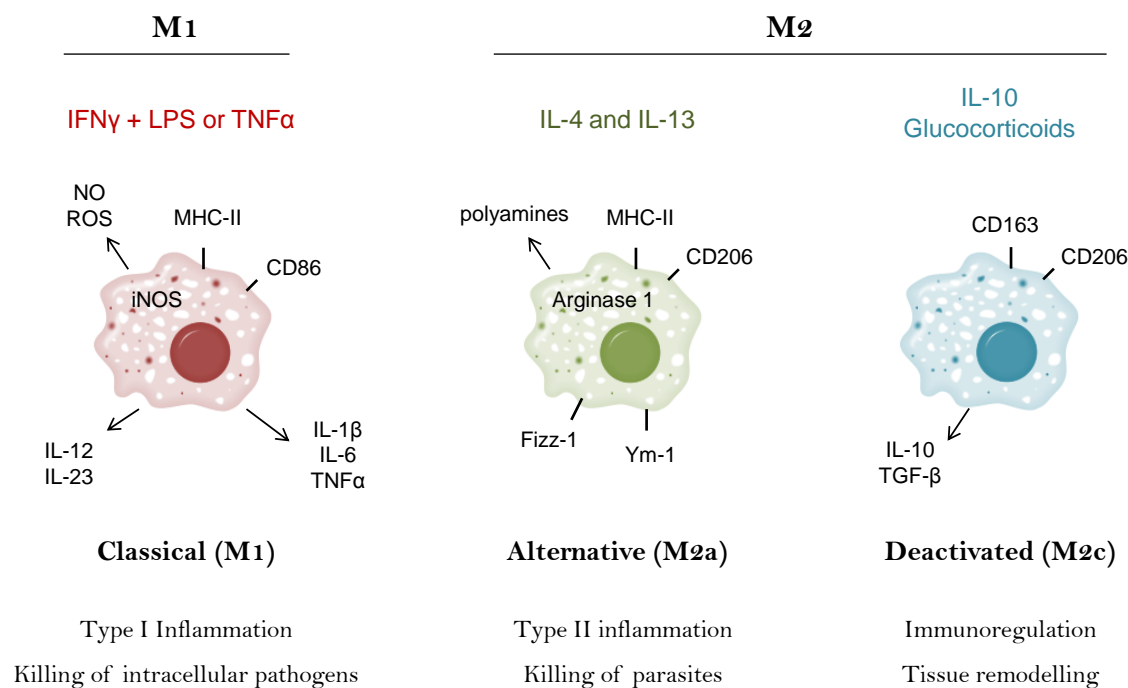


**Figure 1.2 | Macrophage polarization induced by different stimuli.** Classification of macrophage activation states according to Mantovani et al. The figure depicts the specific inducing stimuli, typical markers and cytokines, as well as immune functions of each macrophage phenotype. *Adapted from Mantovani et al. 2004.*

The participation of different subsets of macrophages during MS and EAE has been extensively reported. It is known that the number of monocyte-derived pro-inflammatory macrophages increases progressively in the CNS until the peak of the disease (Mikita et al. 2011). In this stage of CNS inflammation, however, macrophages are difficult to be distinguished from **microglia**, their counterparts in the CNS parenchyma. Microglia, in contrast to infiltrating monocyte-derived macrophages, derive from myeloid precursors originating in the yolk sac that populate the CNS during embryonic development (Kierdorf and Prinz 2013). After birth, these populations are self-sustained by local progenitor cells (Ajami et al. 2011). All in all, activated macrophages/microglia play an important detrimental role at disease onset and are a prominent component of active demyelinating MS lesions (Barnett and Prineas 2004). In the first place, microglia are the major source of chemokines for T cell recruitment. Peripheral macrophages do not seem to be involved in this T cell chemoattraction, since their depletion with clodronate liposomes does not impair T cell migration (Tran et al. 1998). However, in mice where macrophages were depleted, T cells could not access the CNS parenchyma and EAE induction was abrogated (Huitinga et al. 1990; Tran et al. 1998), probably due to the lack of MMPs (Toft-Hansen et al. 2004). Additionally, macrophages/microglia up-regulate MHC II molecules and secrete pro-inflammatory cytokines during neuroinflammation, thereby collaborating in the reactivation of T cells (Murphy et al. 2010). These cytokines, in combination with ROS, NO and glutamate are also neurotoxic, leading to axonal damage and oligodendroglial death (Shijie et al. 2009).

Nevertheless, the alternatively-activated variants of these myeloid cells have a regulatory function during MS and EAE. The presence of M2 macrophages/microglia has been associated with disease resolution (Mikita et al. 2011), and these cells have been shown to contribute to neuronal regeneration via secretion of neurotrophic factors (Elkabes et al. 1996; Batchelor et al. 1999). These cells also participate in the removal of myelin debris, which are known to be neurotoxic and to inhibit re-myelination (Kotter 2006). Moreover, several publications correlate the benefits of M2 polarized macrophages with increased Treg cell-mediated immunosuppression (Weber et al. 2007; Keating et al. 2009)

## 1.3 Immunomodulatory therapies for MS: glucocorticoids

Up to now there is no cure for MS. Nevertheless, in the past 20 years the better understanding of the disease pathomechanisms provided by animal models has led to the development of different therapies approved by the Food and Drug Administration (FDA) and the European Medicines Agency (EMA). Most of these drugs, so called **disease-modifying therapies (DMTs)**, are immunomodulatory compounds that have proven to successfully reduce MS relapse rate and slow down the development of neuronal damage associated with disease progression, especially in the early phases of RRMS. Classical first line therapies for RRMS patients are IFN $\beta$  (Paty and Li 1993) and glatiramer acetate (GA) (Johnson et al. 1995); in the case of patients not responding to these drugs, the use of the monoclonal antibodies Natalizumab (Polman et al. 2006) and Alemtuzumab (Brown and Coles 2013) is recommended. Despite the efficacy of IFN $\beta$  and GA, their application via subcutaneous (s.c.) or intramuscular (IM) injection often affects patient compliance; to solve this problem, in recent years new oral drugs like dimethyl fumarate (Gold et al. 2012), teriflunomid (Papadopoulou et al. 2012) and fingolimod (Kappos et al. 2010) have been also approved by the FDA and are currently in use, although the latter just as second line treatment. Unfortunately, finding the appropriate therapy for the progressive forms of the disease is still a challenge for the clinicians. In these cases, the immunosuppressive drug Mitoxantrone is often the treatment of choice in spite of its associated side effects (Boster et al. 2008).

### 1.3.1 Glucocorticoid treatment in MS patients

Complementary to the approved DMTs, high-dose **GCs** are the first line therapy to treat acute exacerbations of MS. Cortisol, the natural GC in humans, is a steroid hormone produced by the adrenal glands that participates in many different physiological processes, such as embryonic development, response to stress or glucose metabolism. It also has effects on the immune system, e.g. controlling the differentiation and survival of leukocytes. Due to their potent immunosuppressive properties, natural and synthetic GCs have been extensively used during decades for the treatment of numerous inflammatory and

autoimmune disorders (Hench et al. 1950), like rheumatoid arthritis, allergic asthma, inflammatory bowel disease, MS and psoriasis. Still nowadays, GCs are the most commonly prescribed anti-inflammatory drugs.

Administration of 1 g/day intravenous (i.v.) methylprednisolone (IVMP) for 3-5 days is the standard treatment for acute relapses of RRMS (Goodin 2014). Acute relapses are defined as episodes longer than 24h of neurological impairment caused by active inflammatory demyelinating lesions (McDonald et al. 2001). These episodes are mostly followed by resolution of the symptoms, but unfortunately this is not always the case, and an incomplete recovery is often associated with a worse prognosis (Renoux 2011). Hence, on time and efficient management of the relapses is critical for the patients. Different clinical trials have confirmed the benefits of GCs in terms of relapse recovery (Milligan et al. 1987; Filippini et al. 2000; Miller et al. 2000). Moreover, the results of the “Optic Neuritis Treatment Trial” (Beck et al. 1993) showed that optic neuritis patients receiving high-dose IVMP appeared to have a lower risk of developing MS than the placebo controls, suggesting that GCs might have long-lasting immunosuppressive effects. To shed light on this question some studies tested the administration of GCs over longer time periods. In one of these studies, prolonged administration of low-dose oral GCs did not appear to influence relapse rate or progression of disability (Miller et al. 1961). However, a second trial using similar doses indicated improved neuronal deterioration after 18 months daily treatment (Tourtellotte and Haerer 1965). Using an alternative approach, pulsed high-dose IVMP treatment in patients with RRMS significantly prevented the accumulation of disability (Zivadinov et al. 2001). In accordance with these results, another clinical trial showed that a single monthly dose of 500mg IVMP reduced the number of lesions for 12 months (Then Bergh et al. 2006), and also studies on SPMS patients have reported an improvement in the disease progression with pulsed GC therapy (Goodkin et al. 1998). None of these treatments seemed to influence the frequency of relapse, but in another trial in 2009 this positive effect was indeed observed when pulsed IVMP was applied as an add-on to IFN $\beta$  therapy (Sorensen et al. 2009). Collectively, these studies indicate that pulsed GC therapy might also offer an alternative to interfere with the natural history of the disease, but further research is required to confirm this hypothesis.

### 1.3.2 Molecular and cellular basis of GCs immunosuppression

The immunosuppressive properties of GCs rely on a complex **molecular mechanism**. GCs diffuse through the plasma membrane and act predominantly by binding to the GR, which is located in the cytosol in association with chaperones and immunophilins that keep it in an inactive state (Hutchison et al. 1996). After GC binding, the GR is released from these proteins and translocates into the nucleus, where it can act both as a monomer or a dimer. GR homodimers recognize DNA palindromic sequences in promotor or enhancer regions called GC-responsive elements (GREs) (Chandler et al. 1983). GC-activation of these GREs modulate the transcription of genes either positively, e.g. IL-10, GILZ and Bcl-X<sub>L</sub> (D'Adamio et al. 1997; Hodge et al. 1999; Gascoyne et al. 2003), or negatively, e.g. IL-1 $\beta$ , osteocalcin and prolactin (Sakai et al. 1988; Strömstedt et al. 1991; Zhang et al. 1997). In contrast, in its monomeric form the GR binds to transcription factors, such as AP-1 or NF $\kappa$ B, that participate in inflammatory signaling cascades, resulting in the trans-repression of pro-inflammatory genes via tethering interactions. Studies with GR<sup>dim</sup> mice, in which dimerization of the receptor is impaired (Reichardt et al. 1998), revealed that both mechanisms act separately and fulfill different functions depending on the cell type and the physiological context (Kleiman et al. 2012; Reichardt et al. 2012). In addition, GCs have also rapid non-genomic effects mediated by non-specific interactions with cellular membranes, or with membrane-bound GRs (Bartholome et al. 2004). However, the consequences of these interactions are still not well understood (Strehl et al. 2011).

Regarding the activities of GCs in the context of MS and EAE, five different **immunosuppressive mechanisms** have been proposed:

- 1) GCs have a pro-apoptotic effect on immune cells, especially T cells, involving members of the Bcl-2 family and caspases (Leussink et al. 2001; Tuckermann et al. 2005).
- 2) Furthermore, they alter the overall inflammatory cytokine milieu. GCs are known to reduce the expression of several pro-inflammatory cytokines, such as TNF $\alpha$ , IFN $\gamma$  and IL-2 (Almawi et al. 1996). Apart from direct genomic effects, this inhibition can be partially explained by the simultaneous down-regulation of IL-12 and IL-6 in myeloid cells, hindering Th1 and Th17 differentiation (Blotta et al. 1997). In contrast, higher levels of IL-10, an

important cytokine for the negative control of autoimmune responses, were found in MS patients after MP treatment (Gayo et al. 1998).

3) In EAE models, GCs have also been reported to influence T cell chemotaxis via modulation of chemokines like CXCL12 and its receptor CXCR4 (Schweingruber et al. 2014).

4) GCs have the ability to partially restore the BBB, preventing the extravasation of leukocytes into the CNS. These benefits derive from the up-regulation of molecules such as occludin and claudin (Kashiwamura et al. 2011), and down-regulation of adhesion molecules both in leukocytes (LFA-1) and endothelial cells (ICAM-1, VCAM-1) (Pitzalis et al. 2002). The reduced expression of MMPs also contributes to the maintenance of the BBB stability (Rosenberg et al. 1996).

5) Finally, GCs diminish the release of NO and ROS by macrophages and microglia (Lim et al. 2007), directly preventing neurotoxicity. Furthermore, additional positive effects resulting from M2 polarization of these cells have been described (Kiefer and Kreutzberg 1991; Varga et al. 2008).

### 1.3.3 Mineralocorticoid receptor-mediated activities of GCs

It is known that, in certain situations, GCs also activate the **mineralocorticoid receptor (MR)** via similar molecular mechanisms as the GR. The MR and the GR share 57% homology in their ligand-binding domain, 94% in the DNA-binding domain (Funder 1997), and have similar affinities for cortisol (Funder 1993). But in contrast to the ubiquitously present GR, MR expression is confined to certain epithelial tissues such as kidney and colon, some non-epithelial tissues like hippocampus and heart, and specific immune cell subsets, mostly myeloid cells. Furthermore, some of these tissues co-express the 11 $\beta$ -hydroxysteroid dehydrogenase type II (11 $\beta$ -HSD II), an enzyme that locally inactivates GCs, making the MR mostly sensitive to aldosterone instead of cortisol and corticosterone. Aldosterone-mediated effects of the MR are, for instance, the regulation of electrolyte homeostasis in the kidney epithelium (Funder 1997); in the heart, MR signaling leads to hypertrophy and fibrosis. Therefore MR antagonists are commonly used for the treatment of hypertension and other cardiovascular diseases (Pitt et al. 1999). However, since GCs circulate in the organism at a much higher concentration than mineralocorticoids do, in cells devoid of 11 $\beta$ -



HSD II expression, e.g. macrophages and microglia, the MR is preferentially occupied by GCs rather than by aldosterone. This means that in myeloid cells both the GR and the MR are responsible for GC activities.

Importantly, the two receptors drive macrophage/microglia polarization in opposite directions. While GR-GC binding triggers a deactivating phenotype in macrophages (see **Figure 1.2**), GC binding to the MR has been associated with M1 macrophage polarization. Various experimental evidences support this hypothesis. Aldosterone treatment of peritoneal macrophages cultured in steroid-depleted medium resulted in increased expression of the pro-inflammatory markers TNF $\alpha$ , MCP-1 or IL-12, effect that could be reverted by MR-blockade using eplerenone (Usher et al. 2010). Moreover, *in vitro* LPS stimulation of MR-deficient macrophages induced lower mRNA levels of M1 genes and higher expression of M2 markers compared to the wild type (wt) controls (Usher et al. 2010). In another study, MR activation by aldosterone in a microglial cell line also potentiated LPS induction of TNF $\alpha$  and IL-6, in line with the previous data. Additionally, it was shown that aldosterone binding to the MR activated NF $\kappa$ B, whereas the GR repressed it (Chantong et al. 2012). All in all, the balance between MR and GR appears to play a relevant role in macrophage polarization. Whether this is also the case for other immune cells, like T cells or B cells, remains unclear and needs to be further investigated (Bene et al. 2014).

### 1.3.4 Side effects of GC therapies

A major drawback of GCs is the concurrence with adverse side effects (Moghadam-Kia and Werth 2010; Weinstein 2012; Ciriaco et al. 2013; Hunter et al. 2014a; Hwang and Weiss 2014). This problem derives from the ubiquitous expression of the glucocorticoid receptor (GR) (Rhen and Cidlowski 2005), that makes GCs important players in numerous homeostatic and metabolic processes. Although GC side effects in MS patients are rare due to the short duration of the treatment, in some clinical trials that tested pulsed long-term IVMP certain symptoms derived from the treatment were reported (Zivadnov et al. 2001). In fact, in other pathologies where regular GC application is the conventional therapy, this is a critical negative aspect that can even force the withdrawal of the treatment.

One important side effect of GC therapy is **hyperglycemia**. This complication, defined as an abnormal increase in post-prandial and basal blood glucose, affects almost 50 % of GC-treated patients and can lead to type II diabetes. GCs increase glucose levels via promotion of gluconeogenesis in the liver and reduction of glucose uptake in the skeletal muscle. They also affect pancreatic  $\beta$  cells, diminishing insulin secretion, and can act as insulin antagonists leading to insulin resistance (Kuo et al. 2015). Another complication observed after GC therapy is **skeletal muscle atrophy**. Steroid myopathy is characterized by a reduction in the diameter of type II muscle fibers and lower myofibrillar protein content, due to a deregulation between protein synthesis and proteasomal degradation (Schakman et al. 2013; Braun and Marks 2015). Additionally, the occurrence of gastric ulcers in patients under GC therapy is also frequently reported. Recent studies demonstrated that dexamethasone (Dex) administration to mice leads to **gastroparesis**. This effect appears to be a result of a decreased production of NO, which is essential for gastric motility (Reichardt et al. 2014). As a consequence, stomach emptying is impaired and the weight of the filled stomach increases. Last but not least, the reduction in bone mineral density leading to **osteoporosis** is possibly the most severe GC-derived adverse symptom. Just a few weeks after low dose GC-treatment, the risk of bone fractures can increase up to 75%, especially in post-menopausal women (Steinbuch et al. 2004). The GR is expressed in osteoblasts, osteocytes and osteoclasts, and can therefore alter bone production and re-sorption. However, studies using cell type-specific GR knock-out mice revealed that osteoblasts were the major targets of GCs in the context of osteoporosis, whereas the role of osteoclasts was of minor importance (Rauch et al. 2010). Among other effects, GCs diminish the production of new osteoblast progenitors interfering with the Wnt-signaling pathway, and induce premature osteoblast apoptosis, leading to a reduction of bone density.

Because of these and others clinical symptoms, GCs must be prescribed carefully, and the balance between the benefits and the disadvantages of the therapy must always be evaluated.

### 1.3.5 Emerging GC therapies: from dissociating ligands to nanoparticles

As mentioned above, GCs are a mainstay for the treatment of MS as well as other inflammatory and autoimmune conditions, but their widespread effects are an important limiting factor for their clinical use. In recent years, big efforts have been made to improve the pharmacological features of GCs, and although many of the alternatives have shown good results in animal models, none of these formulations reached the market so far.

The results obtained from GR<sup>dim</sup> studies pointed to the trans-activation mechanism of the GR as the responsible mechanism for some of the metabolic adverse effects following GC treatment. Thus, taking advantage of the dual molecular pathway employed by the GR, different **dissociating ligands** were designed to act predominantly via the GR trans-repression mechanism, among them, AL-438 (Coghlan et al. 2003) or Compound A (CpdA) (Louw et al. 1997). CpdA was shown to be effective in the treatment of EAE, however, its neurotoxic effects at high concentrations discarded it as a suitable drug for patients (Wüst et al. 2009).

In the design of drug delivery systems for the treatment of MS, the CNS compartment poses an additional challenge, since the formulation must be able to cross the BBB. This obstacle can be circumvented using biocompatible micro-/nanoparticles such as **liposomes**. Liposomes do not only cross the BBB due to their lipophilic character, but also have the right size to be taken up by phagocytic immune cells, such as macrophages and DCs, that will carry the drug to the CNS achieving a local therapeutic effect. The safety and tolerability of liposome-encapsulated drugs have been successfully evaluated in several clinical trials (Gordon et al. 2001; Alberts et al. 2004). In fact, liposomal doxorubicin is currently approved for the treatment of certain cancers and seems to overcome the signs of cardiopathy associated with the free drug (Tahover et al. 2015). Regarding GCs, some studies confirmed the therapeutic potential of liposomal corticosteroids in animal models of autoimmune inflammatory disorders, such as arthritis and MS (Metselaar et al. 2003; Linker et al. 2008; Schweingruber et al. 2011). Furthermore, liposomal encapsulation of GCs was shown to significantly increase the potency of the drug in the EAE mouse model (Schweingruber et al. 2011).

As an alternative delivery system, current research focuses on the development of state of the art biocompatible **nanoparticles** with sizes ranging from 10 to 100 nm. Due to this feature, nanoparticles are preferentially pinocytosed by inflammatory monocytes and macrophages, allowing the specific targeting of these immune cells. Larger particles, on the contrary, accumulate in the lungs and the liver and are phagocytosed mainly by peripheral DCs (Weissleder et al. 2014). Nanoparticles can be obtained from different organic materials, such as poly(lactic-co-glycolic acid), chytosan, alginate or silica, and can be additionally coated with antibodies (Abs) or other targeting molecules (Tabansky et al. 2015). Recently, a new modality of inorganic-organic hybrid nanoparticles (IOH-NPs) for the delivery of corticosteroids was developed (Heck et al. 2015). From a molecular point of view, IOH-NPs are composed of an inorganic bivalent cation reacting with equimolar amounts of an organic functional anion. In this case, betamethasone (BMZ) phosphate constitutes the organic part of the compound, and zirconium oxide ( $ZrO_2$ ) was chosen as cation due to its stability and lack of physiological activity. In solution, this compound crystalizes in particles with a diameter of 40 to 90 nm, and moreover, the combination with flavin mononucleotide (FMN) provides a fluorescent signal that allows their detection via flow cytometry or fluorescence microscopy. Preliminary *in vitro* experiments with these nanoparticles showed a good cell tolerability and proper delivery of the drug, however their therapeutic potential has not been evaluated in detail yet (Heck et al. 2015; Ring, unpublished data).

## 1.4 Objectives

T cells were for a long time believed to be major targets of the GC-therapy for acute relapses of MS (Wüst et al. 2008). However, myeloid cells like macrophages and microglia are affected by endogenous and therapeutic GCs as well, and their importance for the maintenance of tolerance and the pathogenesis of MS has gained attention over the years. Macrophage/microglia phenotypes are highly dynamic, and changes in their polarization state may determine the course of MS and EAE. In these myeloid cells, GCs can act either via the GR in a deactivating manner, or via the MR promoting a pro-inflammatory state (Usher et al. 2010), and this dual role of GCs makes the myeloid compartment particularly

interesting in the context of neuroinflammation. In this doctoral thesis I aimed to define the roles of the GR and the MR in myeloid cells for the response to GCs during EAE. Furthermore, I propose that targeting GC therapy specifically to these immune cells might represent a strategy to improve the therapeutic features of the drug. To address these issues, two different approaches were employed:

- The first part of the project aimed to evaluate the *in vitro* and *in vivo* effects of BMZ-phosphate ZrO<sub>2</sub> IOH-NPs (BNPs) (Heck et al. 2015). BNPs are expected to preferentially target myeloid cells due to their size, therefore their effects on different cell types and their *in vivo* cell specificity were analyzed. Furthermore, the therapeutic potential of the BNPs in the MOG<sub>35-55</sub>-induced EAE mouse model and possible GC-derived side effects were studied.
- The second part of the project dealt with the role of the MR in myeloid cells in the context of CNS autoimmunity. Since MR-mediated responses counteract the immunosuppressive effect that GCs induce via the GR, the blockade of the MR might potentiate macrophage polarization towards a deactivated phenotype, thereby reducing CNS inflammation during EAE. To test this hypothesis, mice harboring a myeloid-specific MR deletion were studied after disease induction, and the different cellular events involved in disease initiation and progression were investigated.

## 2 MATERIAL AND METHODS

### 2.1 Material

#### 2.1.1 General equipment

**Table 1.1** | *General equipment*

<b>Instrument</b>	<b>Model</b>	<b>Manufacturer</b>
Blood glucose meter	Ascensia CONTOUR	Bayer, Leverkusen
Centrifuges	5417R for reaction tubes	Eppendorf, Hamburg
	5804 for FACS tubes	Eppendorf, Hamburg
	Multifuge 4 KR for Falcon tubes	Heraeus, Hanau
	Sigma 2-5 for 96-well plates	Sigma Laborzentrifugen GmbH, Osterode am Harz
Dehydration system	TP1020	Leica Microsystems, Nussloch
Electrophoresis chamber		Peqlab Biotechnology, Erlangen
Electrophoresis power supply	EPS 301	Amersham Biosciences, Freiburg
FACS machines	BD FACS Canto II	Beckton Dickinson Biosciences, Heidelberg
	BD FACS Sorter FACSAria	Beckton Dickinson Biosciences, Heidelberg
Gel imager	Chemostar	Intas GmbH, Goettingen
Incubator	HERACell 240	Heraeus, Hanau
Infrared Lamp	Balance 100W	Philips, Amsterdam, Netherlands
Laminar airflow cabinet	HERASafe	Heraeus, Hanau
	Interactive Safe Change station	Tecniplast GmbH, Hohenpeissenberg
MACS	AutoMACS	Miltenyi Biotech, Bergisch Gladbach

Micropipettes	2.5, 20, 200 and 1000 $\mu$ L	Gilson, Middleton, Wisconsin, USA
Microscopes	Primo Star	Zeiss, Jena
	Telaval 31	Zeiss, Jena
	Olympus BX51	Olympus, Tokio, Japan
Microtome	Leica SM2000R	Leica Microsystems, Nussloch
Microwave oven	R-212	Sharp, Osaka, Japan
Neubauer improved haemocytometer		Henneberg-Sander GmbH, Giessen
Ph-meter	766 Calimatic	Knick Elektronische Messegerate GmbH, Berlin
Photometers	Nanodrop 2000	ThermoScientific, Erlangen
	BioTek®Power Wave 340 plate reader	BioTek, Bad Friedrichshall
Pipette controller	Accu-jet® pro	Brand GmbH, Wertheim
Refrigerators	Freezer Hera -80°C	Heraeus, Hanau
	Freezer Liebherr Comfort -20°C	Liebherr International GmbH, Biberach an der Riss
	Freezer VIP plus -150°C	Sanyo Electric Co. Moriguchi, Osaka
Scale	TE313S	Sartorius AG, Göttingen
Shaker	3006	Gesellschaft fuer Labortechnik, Burgwedel
Tuberculin glass/metal syringes (1, 2 ml)		Hartenstein
Thermocyclers	Thermocycler	Heraeus, Hanau
	7500 Real-Time PCR	AB Applied Biosciences, Applied Biosystems GmbH, Darmstadt
	Thermomixer Comfort	Eppendorf, Hamburg
Tissue Embedding System	EG1160	Leica Microsystems, Nussloch
UV system camera and gel imager		Intas GmbH, Göttingen
Vortex mixer	Vortex Genie2	Bohemia , NY, USA
Water bath	W12	Labortechnik Medigen, Dresden

Water purification system	Arium®611	Sartorius AG, Göttingen
	Millipore purification system	Millipore GmbH, Schwalbach

Unless otherwise indicated, all companies are located in Germany

## 2.1.2 Consumables

**Table 1.2** | *Consumables*

Product description		Manufacturer
96-well Optical Reaction Plates		Applied Biosystems, Foster City, California, USA
Gavage cannula		Cadence Science, Cranston, USA
Cell Culture Plates	4 cm, 10 cm	Sarstedt, Nümbrecht
	6-well, 24-well, 48-well, 96-well flat bottom	Greiner bio-one GmbH, Frickenhausen
	96-well round bottom	Greiner bio-one GmbH, Frickenhausen
Cell strainer	20 µm, 40 µm	BD Biosciences, Heidelberg
ELISA plates	Nunc Maxisorb flat bottom 96 well plate	eBioscience, San Diego, USA
FACS tubes		BD Biosciences, Heidelberg
Microscope slides	SuperFrost Plus	Menzel Glaeser, Braunschweig
Needles	24G 1", 20G 1½", 27G¾", 25G 1"	B. Braun Melsungen AG, Melsungen
Optical adhesive covers		Applied Biosystems, Foster City, California, USA
Pasteur pipettes	3 mL	Th. Geyer GmbH, Renningen
Pipettes	Cellstar® 5 mL, 10 mL, 25 mL	Greiner bio-one GmbH, Frickenhausen
Pipette tips	10 µL, 200 µL, 1000 µL	Greiner bio-one GmbH, Frickenhausen
Reaction tubes	0.5 mL	Sarstedt, Nümbrecht
	1.5 mL, 2 mL	Greiner bio-one GmbH, Frickenhausen
	15 mL, 50 mL	Greiner bio-one GmbH, Frickenhausen



Syringes	1 mL	Henke Sass Wolf, Tuttlingen
	2 mL, 5 mL, 60 mL	BD Biosciences, Heidelberg
Serum separation tubes	STT™ BD Microtainer®	BD Biosciences, Franklin Lakes, USA
Tissue cassettes	MacrOfFlow	Microm International, Waldorf

Unless otherwise indicated, all companies are located in Germany

### 2.1.3 Chemicals and reagents

**Table 1.3** | *Chemicals and reagents*

Chemical	Manufacturer
2-β-Mercaptoethanol	Invitrogen, Paisley, UK
Acetic acid glacial 100%	Carl Roth, Karlsruhe
Agarose UltraPure	Sigma-Aldrich, Taufkirchen
Betamethasone phosphate (Celestan®)	MSD Sharp and Dohme GmbH, Haar
Bovine Serum Albumin (BSA)	Carl Roth, Karlsruhe
CaCl <sub>2</sub> x 2 H <sub>2</sub> O	Merk, Darmstadt
Carboxyfluorescein succinimidyl ester (CFSE)	Life Technologies, Darmstadt
Citric acid	Merk, Darmstadt
Complete Freund's Adjuvant (CFA)	Difco Laboratories, Detroit, USA
Dexa-ratiopharm® 100mg Injektionlösung	Ratiopharm GmbH, Ulm
D-Glucose	Merk, Darmstadt
3,3'-Diaminobenzidine tetrahydrochloride (DAB)	Sigma-Aldrich, Taufkirchen
Dimethyl sulfoxide (DMSO)	Carl Roth, Karlsruhe
DNA ladder 1kb	Fermentas GmbH, St. Leon-Rot
dNTPs	Genaxxon bioscience, Ulm

Entellan	Merck, Darmstadt
Ethanol $\geq 99,8\%$	Carl Roth, Karlsruhe
Ethylendiaminetetraacetic acid (EDTA)	Sigma-Aldrich, Taufkirchen
Ethidium Bromide	Carl Roth, Karlsruhe
10% stripped Fetal Calf Serum (FCS)	Invitrogen, Paisley, UK
H <sub>2</sub> O <sub>2</sub> 30%	Carl Roth, Karlsruhe
H <sub>2</sub> SO <sub>4</sub>	Merk, Darmstadt
4-(2-hydroxyethyl)-1-piperacine-thane-sulfonic acid (HEPES)	Merk, Darmstadt
iScript Reaction Mix	BIO-Rad, USA
Ketamine 10%	MediStar, Aschenberg
KCl	Merk, Darmstadt
KH <sub>2</sub> PO <sub>4</sub>	Merk, Darmstadt
Na <sub>2</sub> HPO <sub>4</sub> x12H <sub>2</sub> O	Merk, Darmstadt
Na <sub>3</sub> C <sub>6</sub> H <sub>5</sub> O <sub>7</sub>	Carl Roth, Karlsruhe
NaCl	Carl Roth, Karlsruhe
Na <sub>2</sub> HPO <sub>4</sub> x H <sub>2</sub> O	Merk, Darmstadt
NaN <sub>3</sub>	Carl Roth, Karlsruhe
Myelin Oligodendrocyte Glycoprotein 35-55 peptide (MOG <sub>35-55</sub> )	Charité, Berlin
Orange G	Sigma-Aldrich, Taufkirchen
Optilyse®	Immunotech, Marseille, France
Paraformaldehyde Histofix 4%	Carl Roth, Karlsruhe
Penicillin/ Streptomycin	GIBCO® Invitrogen, Paisley, UK
Percoll®	Sigma, St. Louise, USA
Sodium dodecyl sulfate (SDS)	SERVA GmbH, Heidelberg
3,3',5,5'-Tetramethylbenzidin (TMB)	Sigma-Aldrich, Taufkirchen

Thioglycolate	Sigma-Aldrich, Taufkirchen
Tris	Carl Roth, Karlsruhe
Trypan blue	Sigma Aldrich, Taufkirchen
Tween 20	Carl Roth, Karlsruhe
Xylarium® (Xylazine 2%)	Riemser, Greifswald-Insel Riems
Xylol	Carl Roth, Karlsruhe

Unless otherwise indicated, all companies are located in Germany

## 2.1.4 Media, buffers and solutions

Table 1.4 | *Media*

Medium	Composition or additives	Manufacturer
<b>DMEM+GlutaMAX™</b>	+ 10% FCS	GIBCO® Invitrogen, Paisley, UK
	+ 0.01% Penicillin/Streptomycin	
<b>RPMI Medium 1640 + GlutaMAX™</b>	+ 10% FCS	GIBCO® Invitrogen, Paisley, UK
	+ 0.01% Penicillin/Streptomycin	
<b>Re-stimulation medium (ReMed)</b>	RPMI Medium 1640	GIBCO® Invitrogen, Paisley, UK
	+ 5% FCS	
	+ 0.01% Penicillin/Streptomycin	
	+ 1% Sodium pyruvat	
	+ 0.2% β-mercaptoethanol	

Unless otherwise indicated, all companies are located in Germany

Table 1.5 | *Buffers and solutions*

<b>Buffer or solution</b>	<b>Composition</b>
<b>Alsevers</b>	27 mM NaCl
	125 mM D-Glucose
	3 mM Citric Acid
	30 mM Na <sub>3</sub> C <sub>6</sub> H <sub>5</sub> O <sub>7</sub> in ddH <sub>2</sub> O
<b>Annexin binding buffer</b>	10 mM HEPES/NaOH pH7.4
	140 mM NaCl
	2.5 mM CaCl <sub>2</sub> in ddH <sub>2</sub> O
<b>Citrate buffer pH 6</b>	109 mM Citric Acid in ddH <sub>2</sub> O
<b>ELISA Assay diluent</b>	10% FCS in PBS
<b>ELISA Carbonate coating buffer pH 9.5</b>	0.1M Na <sub>2</sub> CO <sub>3</sub> in ddH <sub>2</sub> O
<b>ELISA Phosphate coating buffer pH 6.5</b>	0.1M Na <sub>2</sub> HPO <sub>4</sub> in ddH <sub>2</sub> O
<b>ELISA Substrate buffer</b>	0.1M Citric Acid
	0.2M Na <sub>2</sub> HPO <sub>4</sub> in ddH <sub>2</sub> O
<b>ELISA Developing solution</b>	Substrate buffer
	1% TMB in DMSO
	0.2% H <sub>2</sub> O <sub>2</sub>
<b>FACS buffer</b>	0.1% BSA
	0.01% NaN <sub>3</sub> in PBS
<b>MACS buffer</b>	0.5% BSA
	2mM EDTA in PBS
<b>Phosphate Saline Buffer pH 7.4 (PBS)</b>	137 mM NaCl
	2.7 mM KCl
	10 μM Na <sub>2</sub> HPO <sub>4</sub>
	2.0 mM KH <sub>2</sub> PO <sub>4</sub> in ddH <sub>2</sub> O

<b>PBS/BSA</b>	0.1% BSA	in PBS
<b>PBS/Tween</b>	0.1% Tween 20	in PBS
<b>Percoll diluent</b>	0.1% BSA	
	1% Glucose	in PBS
<b>Spinal cord suspension buffer</b>	0.1% BSA	
	1% Glucose	
	100 µg/mL DNase	in PBS
<b>Sulfite wash</b>	1% HCl	
	0.4% K <sub>2</sub> S <sub>2</sub> O <sub>5</sub>	in ddH <sub>2</sub> O
<b>TAC buffer pH 7.2</b>	155 mM NH <sub>4</sub> Cl	
	20mM Tris	in ddH <sub>2</sub> O
<b>Tail buffer</b>	1% SDS	
	100 mM NaCl	
	100 mM EDTA	
	5 mM Tris	in ddH <sub>2</sub> O

## 2.1.5 Enzymes and commercial kits

**Table 1.6** | *Enzymes and commercial kits*

<b>Product</b>	<b>Manufacturer</b>
Cytometric Bead Array (CBA)	BD Bioscience
Mouse Th1, Th2, Th17 cytokine kit	
Easy Sep™ Mouse T cell Isolation Kit	StemCell™ Technologies
Intracellular FACS Staining Kit	eBioscience, San Diego USA
iScript cDNA Synthesis Kit	Bio-Rad Laboratories, Munich
Mouse IFNγ ELISA MAX™ Standard Set	BioLegend, San Diego, USA

Mouse TNF $\alpha$ ELISA MAX™ Standard Set	
Mouse IL-17A ELISA MAX™ Standard Set	
Mouse Insuline ELISA	RayBiotech Inc., Heidelberg
Osteocalcin ELISA	R&D Systems, USA
Mouse Renin ELISA	RayBiotech Inc., Heidelberg
Mouse GM-CSF ELISA reagents	R&D Systems, USA
Mouse IL-17A ELISA reagents	
Pan T cell isolation Kit II, Mouse	Miltenyi Biotech, Bergisch Gladbach
Phusion® DNA Polymerase and 5x Reaction Buffer HF	Thermo Scientific, Waltham, USA
Power SYBR® Green PCR Master Mix	Applied Biosystems, Foster City, USA
RNeasy Mini Kit	Qiagen, Hilden
Proteinase K	AppliChem GmbH, Darmstadt
Quick-RNA MiniPrep	Zymo Research, Irvine, USA

Unless otherwise indicated, all companies are located in Germany

## 2.1.6 FACS Antibodies

**Table 1.7** | *Antibodies for flow cytometry*

Specificity	Clone	Fluorochrome	Isotype	Manufacturer
CD3 $\epsilon$	17A2	PerCP	Rat IgG2b, $\kappa$	BioLegend
		APC		
CD4	RM4-5	PerCP	Rat IgG2a, $\kappa$	BD Biosciences
		APC-Cy7		
CD8 $\alpha$	53-6.7	PE	Rat IgG2a, $\kappa$	BioLegend
CD11b	M1/70	PE-Cy7	Rat IgG2b, $\kappa$	BioLegend

CD11c	N418	bio	Armenian Hamster IgG	BD Biosciences
CD25	PC61	APC-Cy7	Rat IgG1, λ	BioLegend
CD45.2	104	APC	Mouse IgG2a, κ	BD Biosciences
CD45R/B220	RA3-6B2	PE	Rat IgG2a, κ	BD Biosciences
CD86	GL-1	PE	Rat IgG2a, κ	BioLegend
CD206	C068C2	APC	Rat IgG2a, κ	BioLegend
Ly6C	HK1.4	FITC	Rat IgG2c, κ	BD Biosciences
Ly6G	1A8	PE	Rat IgG2a, κ	BD Biosciences
I-A <sup>b</sup> (MHC-II)	AF6-120.1	PE	Mouse (BALB/c) IgG2a, κ	BioLegend
FoxP3	FJK-16s	APC	FJK-16s	eBioscience
Annexin V		Cy5		BD Biosciences
CD16/CD32 (Fc-block)	2.4G2		Rat IgG2a, λ	BioLegend

### 2.1.7 IHC Antibodies

**Table 1.8** | *Antibodies for immunohistochemistry*

Specificity	Clone	Isotype	Manufacturer
Human CD3	CD3-12	Rat IgG1	AbD Serotec®
Mouse MAC3	M3/84	Rat IgG1	BD Pharmingen®
Rat IgG (biotinilated)		Rabbit	Vector Laboratories

## 2.1.8 Oligonucleotides

**Table 1.9** | *Primers for qRT-PCR*

Target gene		Sequence (5' - 3')
mHP-1	<i>fwd</i>	GCC CAA GAT GGA CGC AAT C
	<i>rev</i>	CCG AGG CGC CAG TCT TC
mFKBP51	<i>fwd</i>	GAA CCT GGC CAT GTG CTA CCT
	<i>rev</i>	GTC CAG TCC AAG GGC CTT GT
mPEPCK	<i>fwd</i>	AAA GCA TTC AAC GCC AGG TT
	<i>rev</i>	TGC TGA ATG GGA TGA CAT ACA TG
mTAT	<i>fwd</i>	CCT CTG GAA GCT AAG GAT GTC ATT
	<i>rev</i>	AAC ACG GCT AGA CAC AGC TCA A

## 2.1.9 Software

**Table 1.10** | *Software*

Software	Developer
analySIS <sup>B</sup>	Olympus, Tokio, Japan
BD FACSDiva Software v6.1.2	BD Biosciences, Heidelberg
FCAP Array Software v3.0.1	BD Biosciences, Heidelberg
FlowJo Software v 7.6	Tree Star, Inc., Ashland, Oregon, USA
Gen5 v1.09.8	BioTek Instruments, Bad Friedrichshall
GraphPad Prism for Windows v5.04	GraphPad Software, La Jolla, CA, USA
ImageJ 1.46r	Wayne Rasband Nat. Inst. Of Health, USA
Intas GDS	Intas, Göttingen

Unless otherwise indicated, all companies are located in Germany



## 2.2 Animal experimentation

All the mice used during this project had a C57BL/6 background and were either purchased from Charles River Laboratories (Sulzfeld, Germany) or bred in the breeding facilities of the University Medical Center in Göttingen. The animals were housed in individually ventilated cages (IVC) under specific pathogen-free conditions (SFP) with 12 hours day/night cycle, and water and food were given *ad libitum*. The mice used for experimentation were at least 10 weeks old. All experiments were approved by the responsible authorities of Lower Saxony and conducted in accordance to the ethical standards of humane animal care.

### 2.2.1 Mouse strains

- **C57BL/6**: wt, background strain (Charles River Laboratories, Wilmington, USA).
- **GR<sup>fl</sup>**:  $Nr3c1^{tm2Gsc}$  (Tronche et al. 1999). This mouse strain contains *loxP* sites flanking exon 3 of the nuclear receptor subfamily 3, group C, member 1 (*Nr3c1*) gene, coding for the GR.
- **GR<sup>Lck</sup>**:  $Nr3c1^{tm2Gsc}Tg(Lck-cre)548Jxm/J$ . Generated by crossing  $Nr3c1^{tm2Gsc}$  mice with  $Tg(Lck-cre)548Jxm/J$  mice (Baumann et al. 2005). These mice express the Cre recombinase under the control of the lymphocyte protein tyrosine kinase (Lck) promoter, which mediates T cell-specific excision of the GR sequence.
- **GR<sup>LysM</sup>**:  $Nr3c1^{tm2Gsc}Lyz2tm1(cre)lfo/J$ . Generated by crossing  $Nr3c1^{tm2Gsc}$  mice with  $Lyz2tm1(cre)lfo/J$  mice (Clausen et al. 1999). In these mice, the Cre recombinase is expressed under the control of the lysozyme 2 gene promoter (*lyz2*), mediating the targeted deletion of the GR in monocytes, mature macrophages and granulocytes.

- **GR<sup>Lck/LysM</sup>** : *Nr3c1<sup>tm2Gsc</sup>Tg(Lck-cre)548Jxm/J Lyz2tm1(cre)lfo/J*. This mouse strain expresses the Cre recombinase under both the Lck and the Lyz2 promoters, mediating the excision of the GR in T cells and cells from the myeloid lineage.
- **MR<sup>fl</sup>** : *Nr3c2<sup>tm2Gsc</sup>* (Berger et al. 2006). This mouse strain contains *loxP* sites flanking exon 3 of the nuclear receptor subfamily 3, group C, member 2 (*Nr3c2*) gene, coding for the MR.
- **MR<sup>LysM</sup>** : *Nr3c2<sup>tm2Gsc</sup>Lyz2tm1(cre)lfo/J*. Generated by crossing *Nr3c2<sup>tm2Gsc</sup>* mice with *Lyz2tm1(cre)lfo/J* mice (Rickard et al. 2009). In these mice, the Cre recombinase is expressed under the control of the lysozyme 2 gene promoter (*lyz2*), mediating the targeted deletion of the MR in monocytes, mature macrophages and granulocytes.
- **GR<sup>SLCO1C1</sup>**: *Nr3c1<sup>tm2Gsc</sup>Tg(Slco1c1-icre/ERT2)1Mrks*. Generated by crossing *Nr3c1<sup>tm2Gsc</sup>* mice with *Tg(Slco1c1-icre/ERT2)1Mrks* mice (Ridder et al. 2011). These mice carry a tamoxifen-inducible gene to express the Cre recombinase in brain endothelial cells, but not in other endothelial cells, mediating the deletion of the GR in this cell type.
- **2D2 RFP**: (*Tcra2D2,Tcrb2D2*)1Kuch/J (Bettelli et al. 2003). Transgenic mouse strain expressing a fully competent, MOG<sub>35-55</sub> specific TCR. This strain was back-crossed with RFP mice (*Gt(ROSA)26Sor<sup>tm1Hjf</sup>*, Luche et al. 2007), expressing the red-fluorescent protein to confer red fluorescence to the carrying cells.

### 2.2.2 Mouse genotyping

In order to assess the genotype of the newborns from our inbred transgenic strains, tail biopsies were collected four weeks after birth and DNA was isolated and used for PCR with the correspondent primers (see 2.7.1). Generally, *Cre* negative animals were used as a control to their respective knock-out for our experiments.

### **2.2.3 Tamoxifen-induction of SLO1C1 knockout mice**

The deletion of the GR from endothelial cells of the BBB was achieved via tamoxifen treatment 4 weeks prior to starting the experiment. Tamoxifen was dissolved in sunflower oil and left overnight (O/N) at 37°C. Three consecutive doses of 3 mg of tamoxifen were administered every other day via oral gavage with a bulb-tipped gastric gavage needle.

### **2.2.4 Anesthesia**

Mice subjected to EAE experiments were anesthetized before subcutaneous injection of the immunizing agent. A preparation of 1% Ketamine and 0.01% Xylazine (Xylarium®) diluted in 0.9% NaCl solution was injected i.p. at a dose of 10 µl per gram of body weight. Mice under anesthesia were kept warm to prevent hypothermia and a moistening balm was applied over the eyes to maintain hydration.

### **2.2.5 Blood sample processing**

Blood was obtained either from the tail of living mice, or via heart puncture on CO<sub>2</sub>-sacrificed animals when higher blood volumes were needed.

Blood samples analyzed by FACS were collected directly on Alsevers, centrifuged 5 min at 350 x g, and stained for surface markers with the correspondent fluorescent-labeled antibodies (Abs). After washing with FACS buffer (350 x g, 5 min), cells were incubated with 100 µl Optilyse® for 12 min. Then, 1 ml ddH<sub>2</sub>O was added and samples were kept for at least 2 h in the dark before they could be analyzed in the FACS device.

For serum extraction, at least 200 µl blood obtained by heart puncture were left to clot in a Microtainer™ serum collection tube for 20 min. Then tubes were centrifuged at 350 x g for 2 min, and serum was removed with the help of a pipette. Serum samples were stored at -20°C.

## 2.3 *In vivo* assays

### 2.3.1 EAE induction

For all the experiments described here, EAE was induced by active immunization with 50 µg MOG<sub>35-55</sub> peptide. First, an emulsion of 1 mg/ml MOG<sub>35-55</sub> in 1 mg/ml CFA at a 1:1 ratio was prepared and left for 1 h at 4°C. Once the mice were anesthetized, 50 µl of the antigen-containing emulsion were injected s.c. in each flank at the beginning of the tail. Additionally, 200 ng of *Pertussis* toxin diluted in 200 µl of a 0,9% NaCl solution were i.p. injected to help disrupting the BBB and boost immunization. Two days later, a second dose of *Pertussis* toxin was applied (**Figure 2.1**).

From day 9 on following immunization, mice were weighted daily and disease progression was monitored. EAE symptoms were evaluated according to the following 0 to 10 scoring scale: 0= Healthy; 1= Reduced tone of the tail; 2= Total paralysis of the tail; 3= Gait disturbance; 4= Gait ataxia in hind limbs; 5= Mild paresis of the hind limbs; 6= Moderate paraparesis; 7= Severe paraparesis or paraplegia; 8= Tetraparesis; 9= Moribund; 10= Death (Linker et al. 2008). Due to ethical reasons, mice with score 6 or higher were provided with special bedding and wet food, and mice reaching a score over 7 were sacrificed.



**Figure 2.1 | EAE induction protocol.** The timeline for EAE induction in C57BL/6 mice considers the day of immunization as day 0. *Pertussis* toxin is given as an adjuvant on days 0 and 2 after immunization, and the first symptoms of the disease typically appear from day 9 on, reaching the peak of disease around day 14-16.

### 2.3.2 *In vivo* T cell priming and proliferation

To test the ability of MR<sup>lysM</sup> APCs to prime T cells and promote their proliferation during the early phases of EAE the following protocol was carried out. T cells were purified from lymphoid organs of RFP 2D2 mice and labeled with CFSE as described below (see 2.4.5). 1·10<sup>6</sup> CFSE-labeled RFP 2D2 T cells were then i.v. injected into either MR<sup>fl</sup> (control) or MR<sup>lysM</sup> mice. Two days later, mice were immunized according to our standard protocol (see 2.3.1). At day 3 and 5 after immunization the mice were sacrificed and lymphoid organs were isolated to analyze the proliferation cycles of the previously injected T cells via flow cytometric analysis of the RFP<sup>+</sup> CFSE<sup>+</sup> cells.

### 2.3.3 GC treatment

Mice were injected i.p. daily on three consecutive days with 10 mg/kg of Dex, a corticosteroid 25 more potent than cortisol with minimal mineralocorticoid activity. In exceptional cases, BMZ was used at the same dose parallel to Dex. The equivalent volume of PBS was injected as a vehicle control.

One of the aims of this thesis work was to evaluate a novel corticoid drug where the corticosteroid, in this case BMZ, is delivered by an inorganic compound (ZrO<sub>2</sub>) in the form of nanoparticles (BNPs). To test the efficacy of BNPs, 100 µl of the nanoparticle suspension, equivalent to 10 mg/kg of BMZ, were injected i.p. during either one or three consecutive days. The same volume of nanoparticles without betamethasone (ENP) was used as a control.

When applied therapeutically on animals with EAE, the treatment was started once the animals showed the first symptoms (score ≥ 1).

### 2.3.4 *In vivo* T cell apoptosis

The potential of the BNPs to induce T cell apoptosis *in vivo* was evaluated treating wt B57BL/6 mice for one and three days with PBS, Dex, ENPs and BNPs. One day after the last injection, spleens were removed and total splenocyte numbers were determined under the microscope. Additionally, cells were stained with fluorophore-coupled Abs against CD3, CD4 and CD8 and analyzed via FACS (**Figure 2.2**).

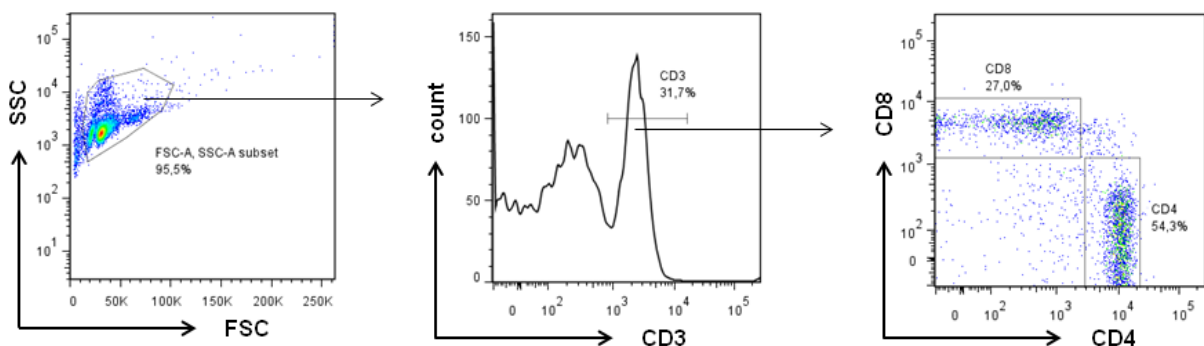


**Figure 2.2 | FACS gating strategy for different T cell subsets.** First, living cells were identified in the FSC/SSC panel. T cells were defined as CD3<sup>+</sup> cells, and within this population Th cells could be distinguished from cytotoxic T cells by the expression of the co-receptors CD4 and CD8, respectively.

### 2.3.5 Analysis of glucose metabolism

To analyze the effects of Dex and BNPs in glucose release and metabolism, mice were treated with PBS, 10 mg/kg Dex, ENPs and 10 mg/kg BNPs i.p. on four consecutive days. Following the last treatment, food pellets were removed O/N. Fasting blood sugar levels were determined in the morning with an Ascensia CONTOUR glucose-meter in blood droplets obtained via tail puncture.

Following glucose measurement, mice received an additional dose of the correspondent drug; 2.5 h later mice were sacrificed and plasma, serum and liver samples were obtained

and snap frozen. Circulating insulin levels were analyzed via ELISA, and expression of gluconeogenic enzymes in the liver via qRT-PCR

## **2.4 Cellular methods**

### **2.4.1 Cell isolation from secondary lymphoid organs**

Mice were sacrificed via CO<sub>2</sub> inhalation. Afterward, spleens and cervical, axillary, mesenteric, inguinal and lumbar lymph nodes were removed and placed on a Petri dish with PBS/BSA. Single cell suspensions were obtained by homogenizing the tissue with the help of a syringe plunger and passing it through a 40 µm cell strainer to avoid cell clumps. Cells were washed in PBS/BSA and centrifuged at 300 x g, 4°C for 7 minutes. In the case of splenocytes, erythrocytes were additionally lysed by incubation with 6 ml TAC buffer/ml of cell suspension for 12 min, followed by centrifugation at 300 x g, 4°C for 7 min. Pellets were re-suspended in 1-2 ml PBS/BSA or the corresponding buffer. Subsequently, 10 µL of the cell suspension were diluted in a Trypan-blue solution and living cell numbers were determined under the microscope using a Neubauer haemocytometer.

### **2.4.2 Mononuclear cell isolation from the spinal cord**

Mice were euthanized with CO<sub>2</sub> and perfused with 20 ml of saline solution to clean vessels from blood. Then, the spine of the mice was removed and vertebrae were cut open in order to obtain the spinal cords, which were homogenized with a syringe plunger in spinal cord suspension buffer. The suspension was washed and centrifuged at 350 x g, 4°C for 10 min, and the pellet was re-suspended in 6 ml of 30% Percoll. Mononuclear cells were separated on a three-phase Percoll gradient (70%, 40%, 30% Percoll) by centrifugation at 350 x g, 4°C for 20 min without stopping break, and collected with the help of a syringe. Cells were washed with PBS (350 x g, 4°C, 10 min) and re-suspended in 1 ml PBS or the corresponding buffer.

### **2.4.3 T cell purification**

#### **2.4.3.1 *EasySep™ kit***

CD3<sup>+</sup> T cells were purified by negative selection using the Easy Sep™ Mouse T cell Isolation Kit according to the manufacturer's instructions. In brief, the volume of the single cell suspension was adjusted to a concentration of  $1 \cdot 10^8$  cells/ml with PBS/2% FCS supplemented with 2% normal rat serum and placed in a 5mL polystyrene tube. Per ml of cell suspension, 50  $\mu$ l T cell enrichment cocktail were added and incubated for 15 min at 4°C. Then, cells were incubated for 15 min with 100  $\mu$ l of the biotin selection cocktail at 4°C, followed by a last incubation step of 5 min with 75  $\mu$ l of magnetic beads. The cell suspension was brought to a volume of 2.5 ml with PBS/2% FCS, and the tube was placed into an Easy Sep™ magnet. After 5 min, the liquid content of the tube was decanted without removing it from the magnet. The collected suspension, corresponding to the negative fraction containing the purified T cells, was washed with PBS (300 x g, 4°C, 7 min) and the pellets were re-suspended in the corresponding buffer to determine cell numbers.

#### **2.4.3.2 *Magnetic Activated Cell Sorting (MACS)***

For MACS separation, single cell suspensions were washed with MACS buffer and the Pan T cell isolation Kit II was employed according to the manufacturer's instructions. For  $1 \cdot 10^7$  total cells, suspensions were incubated for 10 min at 4°C with 10  $\mu$ l of Biotin-Antibody Cocktail in 40  $\mu$ l MACS buffer. Without washing, 30  $\mu$ l of MACS buffer and 20  $\mu$ l of anti-biotin magnetic beads were added and incubated for 15 more min. After incubation, cells were washed in 2ml MACS buffer (300 x g, 4°C, 7 min), re-suspended in 600  $\mu$ l MACS buffer and filtered to avoid cell clusters. The negative cell fraction, corresponding to T cells, was collected with the AutoMACS device, and the purified T cells were subsequently washed (300 x g, 4°C, 7 min) and re-suspended in PBS.



## 2.4.4 Macrophage isolation and culture

### 2.4.4.1 Induction of Bone Marrow-Derived Macrophages (BMDMs)

BMDMs were obtained by culturing bone marrow extracted from mouse tibiae and femur in the presence of macrophage colony-stimulating factor (M-CSF), a lineage-specific growth factor responsible for differentiation of committed myeloid progenitors into cells of the monocyte/macrophage lineage. M-CSF is secreted by L929 cells, and therefore L929-conditioned medium (LCCM) can be used to achieve macrophage maturity. In order to produce LCCM for our experiments, L929 cells were cultured in DMEM in a 5% CO<sub>2</sub> atmosphere at 37 °C. Cells were split once they reached confluence, and the culture medium was collected, filtered and stored at -20°C.

*Bone Marrow isolation.* Mice were sacrificed with CO<sub>2</sub> and the muscle tissue from the hind limbs was removed using a scalpel to obtain clean femur and tibiae. Both ends of the bone were cut and the bone marrow was flushed with ice-cold PBS/BSA using a 5 ml syringe and collected in a Petri dish. Bone marrow cells were homogenized with the help of the syringe in order to obtain a single-cell suspension, which was filtered through a 40 µm nylon strainer.

*Macrophage culture and maturation.* The cell suspensions were washed with PBS/BSA (300 x g, 4°C, 7 min). The pellet was re-suspended in pre-warmed DMEM at a density of 1·10<sup>6</sup> cells/ml and the bone marrow hematopoietic precursors were incubated O/N on cell culture dishes to allow fibroblasts and stromal cells to adhere. Non-adherent cells were collected in the morning, washed and plated in LCCM at a concentration of 2·10<sup>6</sup> cells/ml in 10 cm Petri dishes. The myeloid progenitors were incubated at 37°C and 5% CO<sub>2</sub> for 7-9 days, and 4 ml of fresh LCCM was added at day 4 to boost maturation. When macrophage differentiation was complete (mature macrophages can be recognized under the light microscope by their spindle shape), the cells were harvested by incubating them with 2 ml PBS/BSA + 2mM EDTA for 20 min at 4°C. Afterwards, macrophages were washed and re-suspended in DMEM for further culturing or FACS analysis.

#### ***2.4.4.2 Induction and isolation of peritoneal macrophages***

Another source of macrophages for FACS analysis and cell culture is the peritoneum. Peritoneal macrophages were elicited by i.p. injection of 1 ml of thioglycolate, a monosaccharide frequently used to induce neutrophil and macrophage responses *in vivo*. 4 days after injection, a peritoneal lavage with PBS/BSA was performed with the help of a Pasteur pipette. The collected cell suspension was washed in PBS via centrifugation (300 x g, 4°C for 7 min) and pellets were re-suspended in 8 ml DMEM and plated in 10 cm plates to let macrophages adhere. After 1 h incubation at 37°C in a 5% CO<sub>2</sub> atmosphere, the plates were washed twice with PBS in order to remove non-adherent cells and debris, and 2 ml of PBS/EDTA were added to promote macrophage detachment. Plates were incubated for 20 min and macrophages were collected and washed with PBS (300 x g, 4°C for 7 min). Pellets were re-suspended in 1 ml PBS/BSA or the corresponding buffer, and cell numbers were determined as previously described.

#### ***2.4.4.3 In vitro macrophage stimulation***

When a pre-activated state of macrophages was needed, M1 polarization was induced on naive BMDMs incubating them for 24 h in DMEM supplemented with 20 ng/ml LPS and 50 ng/ml IFN $\gamma$ . Afterwards, cells were washed once with PBS/BSA and prepared for further use.

#### **2.4.5 CFSE staining**

CFSE is a fluorescent dye that covalently binds to lysine residues and other amines, cross-linking to intracellular proteins. Due to its high stability, it serves to track cell proliferation by FACS, since every cell division halves the fluorescence in the daughter cells. For the T cell proliferation experiments described in this thesis, purified T cells were diluted in PBS at a concentration of  $1 \cdot 10^6$  cells/ml and incubated in a water bath at 37°C with 0.25  $\mu$ M of CFSE for 10 min. Every minute, cells were gently mixed by inverting the tubes. The reaction was stopped by adding FCS till a final concentration of 2%. Subsequently, cells were washed twice (300 x g, 4°C for 7 min) and re-suspended in PBS or the corresponding medium.

## **2.4.6 Flow cytometry (FACS)**

### ***2.4.6.1 Extracellular staining***

Single cell suspensions subjected to FACS analysis were prepared at an approximate concentration of  $5 \cdot 10^5$  cells/ml in FACS buffer. Cells were firstly incubated with Fc Block™ (anti-mouse CD16/CD32) for 20 min to prevent unspecific binding. Subsequently, cells were incubated with the respective fluorescence-labeled Abs for 20 min in the dark. After incubation, cells were washed with 3 ml FACS buffer (350 x g, 5 min) and analyzed in the FACS machine.

### ***2.4.6.2 Intracellular staining***

For nuclear staining of FoxP3 the Intracellular Staining Kit from eBioscience was employed. First,  $1 \cdot 10^6$  cells were stained with the surface Abs (CD3, CD4 and CD25) following the above-mentioned protocol. Afterwards, cells were incubated for 30 min at 4 °C with 100 µl of cold Fix/Perm buffer and washed with 2ml PBS (7 min, 350 x g). Two more washing steps with 2 ml of freshly diluted Perm Wash buffer were done before incubation with the anti-mouse FoxP3 Abs (30 min, 4 °C in the dark). Finally, cells were washed once more with Perm Wash buffer and analyzed in the FACS machine.

### ***2.4.6.3 Annexin V apoptosis staining***

Apoptotic cells were detected by an additional incubation step after normal surface antigen staining. Cells were washed in FACS buffer (350 x g, 5 min) and incubated for 15 min with 100 µl of 1x Annexin-buffer containing 1 µl of fluorescent-labeled Annexin V, a protein which binds to phosphatidylserine residues that are exposed on the surface of early apoptotic cells. Cells were then analyzed in the FACS device without any additional washing.

## 2.5 *In vitro* assays

### 2.5.1 *In vitro* T cell apoptosis

$1 \cdot 10^5$  splenocytes from wt C57BL/6 mice were cultured in 96 well plates in the presence of PBS,  $1 \cdot 10^{-6}$  M and  $1 \cdot 10^{-7}$  M Dex, ENPs or  $1 \cdot 10^{-6}$  M and  $1 \cdot 10^{-7}$  M BNPs. Cells were collected 5 h, 10 h and 20 h post-treatment and the percentage of apoptotic T cells was determined via FACS analysis gating on  $CD3^+$  / AnnexinV<sup>+</sup> population.

### 2.5.2 *In vitro* nanoparticle distribution in mixed cultures

The cell distribution of the BNPs was analyzed *in vitro* in cultures of splenocytes and lymph node cells.  $1 \cdot 10^5$  cells were plated in 96 well plates and treated with  $1 \cdot 10^{-6}$  M BNPs. 6 h, 24 h and 48 h later, cells were collected and nanoparticle uptake was determined in different cell subsets ( $CD3^+$ ,  $B220^+$  and  $CD11b^+$  cells) by FACS analysis via quantification of the FITC fluorescence emitted by each population.

### 2.5.3 *Ex vivo* re-stimulation of MOG-specific effector T cells

MR<sup>fl</sup> (control) and MR<sup>lysM</sup> mice were immunized and at day 10 after immunization the mice were sacrificed to obtain single cell suspensions from spleens and lymph nodes.  $6 \cdot 10^5$  splenocytes and  $3 \cdot 10^5$  lymph node cells were incubated in ReMed in the presence of 20  $\mu$ M MOG<sub>35-55</sub> for 72 h (37°C, 5% CO<sub>2</sub>; 96-well U-bottom plates in a total volume of 110  $\mu$ l). After that, the supernatants were collected, centrifuged to remove cell debris (300 x g, 4°C for 7 min) and stored at -20°C to be used for ELISA.

### 2.5.4 BMDM-mediated activation of MOG-specific T cells

The antigen presenting capacity of MR<sup>lysM</sup> macrophages was evaluated with the following experimental setting. BMDMs from MR<sup>fl</sup> (control) and MR<sup>lysM</sup> mice at day 7 of their maturation state were plated in 96 well plates at  $1 \cdot 10^5$  cells/well. Afterwards,  $1 \cdot 10^5$  CFSE-labeled T cells, freshly isolated from 2D2 RFP mice, were added. Both cell types were co-cultured in Re-Med in the presence or absence of 20  $\mu$ M MOG<sub>35-55</sub>, and T cells were harvested after 24 h, 48 h and 72 h to analyze their proliferation by FACS. Cell culture supernatants were stored at -20°C for cytokine quantification.

With a similar setup regarding BMDMs culture and stimulation, additional experiments using *in vitro* re-stimulated RFP Th17 MOG-specific cells were also performed in order to analyze the IL-17A secretion potential upon MR<sup>lysM</sup> BMDM activation. RFP Th17 MOG-specific cells were kindly provided by Judith Strauß, from the IMSF in Göttingen.

## 2.6 Histology

### 2.6.1 Isolation and fixation of spinal cords

Mice were euthanized with CO<sub>2</sub> and perfused with 20 ml of saline solution to clean vessels from blood. Then, 4% PFA was circulated throughout the body to fix the tissue. Spinal cords were isolated, kept in 4% PFA for 48 h and stored in PBS at 4°C.

Whole spinal cords were cut in smaller sections, mounted in a grid in PBS and dehydrated O/N. Then the tissue was embedded in paraffin blocks and 3  $\mu$ m sections of the spinal cord were cut with the microtome.

### 2.6.2 Immunohistochemistry (IHC)

IHC staining of the sections was performed as follows: first, sections were re-hydrated immersing the slides through a decreasing alcohol gradient (xylol, ethanol 99%, ethanol 96%, ethanol 70% and ddH<sub>2</sub>O). For antigen retrieval, the slides were then boiled in citrate buffer for 15 min, washed with ddH<sub>2</sub>O and PBS, and endogenous peroxidase activity was blocked with 3% H<sub>2</sub>O<sub>2</sub> for 15 min at 4°C. Subsequently, another blocking step with PBS/FCS was performed at RT, and the slides were incubated O/N at 4°C with the primary Abs (1:200 in PBS/FCS). After washing with PBS, the slides were incubated 1 h at RT with the secondary Abs (anti-rat-IgG-biotin, 1:200 in PBS/FCS) and afterwards with Streptavidin-peroxidase (1:1000 in PBS/FCS) for one more hour. Then, the slides were developed with DAB at RT for 1-2 min, and the reaction was stopped with ddH<sub>2</sub>O. Finally, the sections were dehydrated again in an increasing alcohol gradient and the slides were covered with Entellan.

### 2.6.3 Luxol fast blue Periodic acid-Schiff (LFB-PAS)

To determine the de-myelination grade in the spinal cord of mice with ongoing EAE, LFB-PAS staining was performed. Firstly, the spinal cord sections were immersed in decreasing alcohol concentrations and the gradient was stopped at 96% ethanol. The slides were then incubated O/N at 56°C in a 0.1% LFB solution. LFB stains the myelin in blue. After washing the slides with 96% ethanol and ddH<sub>2</sub>O, excess of LFB was removed immersing them in 0.1% Li<sub>2</sub>CO<sub>3</sub> for 30 s, followed by washing in 70% ethanol and ddH<sub>2</sub>O. Then, slides were incubated during 10 min in 0.8% Periodic Acid, washed in ddH<sub>2</sub>O, and 20 more min in Schiff's reagent, the excess of which was washed away with a sulphite wash. Finally, the cuts were washed 10 min in tap water, dehydrated and mounted as previously described.

### **2.6.4 Bielschowsky silver staining**

Silver impregnation was performed to stain axonal fibers using a modified protocol based on Litchfield and colleagues (Litchfield and Nagy 2001). Slides were first de-parafined in a decreasing alcohol gradient and immersed for 15 min in a 20% AgNO<sub>3</sub> solution at 4°C. Then, slides were collected in ddH<sub>2</sub>O and 25% NH<sub>3</sub> solution was added drop by drop to the AgNO<sub>3</sub> until the brown precipitate disappeared. Slides were then incubated for 20 min at 4°C in the newly formed silver hydroxide solution, and washed in ammonium water for 5 min. The staining was then developed immersing the slides in the previously used ammoniacal silver solution with the developer (50 µl developer / 25 ml Ag solution). When the nerve fibers got dark, slides were washed with ammonium water and ddH<sub>2</sub>O. Finally, cuts were incubated 5 min in sodium thiosulfate at 4°C, dehydrated in an increasing alcohol gradient, and covered with Entellan.

All reagents needed for the various histological staining protocols were kindly provided by the IMSF in Göttingen.

## **2.7 Molecular methods**

### **2.7.1 DNA isolation from biopsies**

Tail samples were digested O/N by incubation at 56 °C in 750 µL of Tail buffer with 20 µL proteinase K. After vortexing, 300 µL from a saturated NaCl solution were added, incubated for 5 min at RT and the samples were centrifuged for 10 min at 20.800 x g. The upper phase of each sample was removed and mixed with 600 µL isopropanol, incubated for 3 min at RT and again centrifuged for 10 min at 20.800 x g. The supernatant was discarded and 500 µL of 70% EtOH were added, followed by further centrifugation for 5 min. The pellet was dried and dissolved in 100 µL TE buffer. The samples were stored at 4 °C.

### 2.7.2 Polymerase chain reaction (PCR)

DNA samples from newborn transgenic mice were subjected to PCR amplification with specific primers in order to determine their genotypes.

**Table 1.11 | PCR reagents and thermocycler program.**

PCR reaction mix	PCR program		
0.5 µL DNA	1 min	98.5 °C	Activation
4 µL High Fidelity buffer	20 s	98.5 °C	Denaturation
1 µL dNTPs 5mM	15 s	64 °C	Annealing
1 µL Primer mix	20 s	72 °C	Elongation
0.3 µL PhuS	2 min	72 °C	
13.2 µL dH <sub>2</sub> O			

} X 30

Amplification products were run together with 7 µL of the DNA loading dye Orange G on a 1.5% agarose gel at 120 V, 230 mA for 25 min.

### 2.7.3 RNA isolation

RNA extraction from frozen tissue was performed with the help of the RNeasy plus Universal Kit (Quiagen). The tissue samples were homogenized in 900 µL Quiazol using an Ultra-Turrax mixer, then 100 µL DNA Eliminator solution and 180 µL chloroform were added before centrifugation at 20.800 x g, 4°C for 15 min. The upper phase was mixed with 600 µL 70% EtOH by pipetting and poured into a RNA-separation column which was centrifuged for 15 s. Subsequently, 700 µL RWT buffer were added to the column, which was centrifuged for 20 s at 20.800 x g. The process was repeated with 500 µL RPE buffer for 2 min, plus 1 additional min to dry the membrane. The RNA was eluted from the membrane with 70 µL ddH<sub>2</sub>O. The RNA concentration was quantified with the Nanodrop. Additionally, 1 µg RNA was run on a 1% agarose gel to check its purity on the basis of the 18s and 28s rRNA bands.



In the case of RNA purification from cell cultures, cells were directly lysed on the wells with a lysing solution and the Quick-RNA MiniPrep kit (Zymo Research), with comparable steps as the above described, was used according to the manufacturer’s instructions.

### 2.7.4 cDNA synthesis

In order to quantify gene expression 1 µg RNA was reversely transcribed with the iScript Reaction Mix kit. 4 µl of iScript buffer and 0.25 µl Reverse Transcriptase were added per reaction tube, and volume was adjusted to 20 µl. The cDNA synthesis was performed in a thermocycler with a three-step incubation program: 5 min at 25°C, 30 min at 42°C and 5 min at 85°C.

### 2.7.5 Quantitative real-time PCR (qRT-PCR)

qRT-PCR was performed to determine the gene expression levels of certain genes (primers in **Table 1.9**) with the Power SYBR Green polymerase according to manufacturer's instructions.

**Table 1.12 | qRT-PCR reagents and thermocycler program**

qRT-PCR reaction mix	qRT-PCR program		
1 µL cDNA	2 min	50 °C	Activation
12.5 µL SYBR Green	10 min	95 °C	Denaturation
11 µL ddH <sub>2</sub> O	15 s	95 °C	Denaturation
0.5 µL Primer mix	1 min	60 °C	Annealing + Elongation
	15 s	95 °C	
	1 min	60 °C	Dissociation stage
	15 s	95 °C	

} X 40

### **2.7.6 Enzyme-linked immuno-absorbent assay (ELISA)**

ELISA was performed on appropriately diluted supernatants from re-stimulated T cell, macrophage or mixed cell cultures according to the manufacturer's instructions. In brief, 96-well optic plates were coated O/N with 100 µl capture antibody (1:200 dilution in coating-buffer). Between incubation steps, wells were washed 4 times with 200 µl PBS/Tween.

The following morning, plates were blocked with Assay Diluent for 1 h. Then, serial dilutions of the standard provided by the kit and the corresponding samples were loaded on the wells and incubated for 2 h (100 µl/well, all samples were run in triplicates). Afterwards, wells were incubated 1 h with the detection Abs (1:200 in Assay Diluent) and after subsequent washing steps, additionally 30 min with Horse Radish Peroxidase (HRP, 1:1000 in Assay Diluent). Finally, 100 µl/well of substrate solution were added and a blue color with an intensity proportional to the protein concentration developed along 20 min in the dark. To stop the reaction, 100 µl/well of 2N H<sub>2</sub>SO<sub>4</sub> were added and the plate was measured in the photometer. Final concentration of the protein in the samples was calculated via extrapolation of the absorbance values from the standard dilutions.

### **2.7.7 Cytometric Bead Array (CBA)**

Th1, Th2 and Th17 cytokines were quantified in undiluted cell culture supernatants with a CBA. This method allows the simultaneous detection of different cytokines thanks to bead populations with different PerCP-intensities coated with specific capture antibodies for each cytokine. All reagents used were provided by the kit. First, the capture beads for each cytokine were mixed in equal proportions, and standards were prepared performing 1:2 serial dilutions from the top standard. Then, a 96 well plate was pre-wet with 100 µl/well of wash buffer, and 20 µl/well of the mixed capture beads, together with 20 µl of the samples and 20 µl of the PE detection reagent were incubated for 2 h at RT in the dark. Then the plate was washed, samples were re-suspended in wash buffer and acquired in the FACS device. Data analysis was performed using the FCAP Array software v.3.0.1 (BD Bioscience).

## 2.8 Statistical analysis

Data was analyzed by two-tailed Student's t test for unpaired groups using GraphPad Prism 5.03 (San Diego, California, USA). The Mann Whitney test with the Wilcoxon correction was used in the case of the EAE scoring curves. Results are depicted as mean values  $\pm$  SEM; p values above 0.05 were considered as non-significant (n.s.); \*,  $p < 0.05$ ; \*\*,  $p < 0.01$ ; and \*\*\*,  $p < 0.001$ .

## 3 RESULTS

### 3.1 EAE therapy with betamethasone nanoparticles

In recent years, the use of new carriers for the selective delivery of drugs to treat cancer and inflammatory diseases, such as MS, has attracted widespread attention. Previous research from our group revealed that liposomal encapsulation altered the mechanism of action of GCs, now targeting macrophages to a larger extent than T cells (Schweingruber et al. 2011). In addition, the potency of the drug in the treatment of EAE was increased. It is against this background that we investigated IOH-NPs (Heck et al. 2015) as an alternative vehicle for the delivery of GCs specifically to myeloid cells. Hence, the first part of this work was aimed to explore the features of BNPs in different cellular contexts, their therapeutic efficacy and mechanism of action in the treatment of EAE, and potential side effects.

#### 3.1.1 BNPs are preferentially taken up by myeloid cells

Initial work from our group on this topic showed that the efficacy of the BNPs in macrophages was similar to the one of the free GC Dex in terms of expression of pro-inflammatory cytokines and molecules involved in antigen presentation (Ring, unpublished data). These experiments confirmed that BNPs were well tolerated *in vitro* and taken up by myeloid cells. Unexpectedly, however, they also induced T cell apoptosis to the same extent as free Dex, indicating that their effect *in vitro* was not limited to phagocytic cells. Thus I started to compare the uptake of BNPs by different cell types *in vitro* using 2-photon microscopy (2-PM) and FACS, taking advantage of the fact that the fluorescent dye FMN has been incorporated into the nanoparticles.

BMDMs, peritoneal lavage cells, splenocytes and lymph node cells were treated with BNPs for up to 48 h *in vitro*, and the uptake of the BNPs was monitored in different cell types. Analysis by 2-PM revealed the intracellular presence of the fluorescent nanoparticles in BMDMs, distributed in a homogeneous fashion (**Figure 3.1 A**). FACS analysis allowed to further distinguish the uptake efficacy between individual cell types. Although T cells, B cells and macrophages increasingly accumulated the fluorescent dye over time, CD11b<sup>+</sup> myeloid cells were the brightest, indicating that they took up the BNPs more efficiently than T and B cells (**Figure 3.1 B,C,D**). These data collectively indicate that the nanoparticles *in vitro* are able to target various types of immune cells albeit with different efficacy.

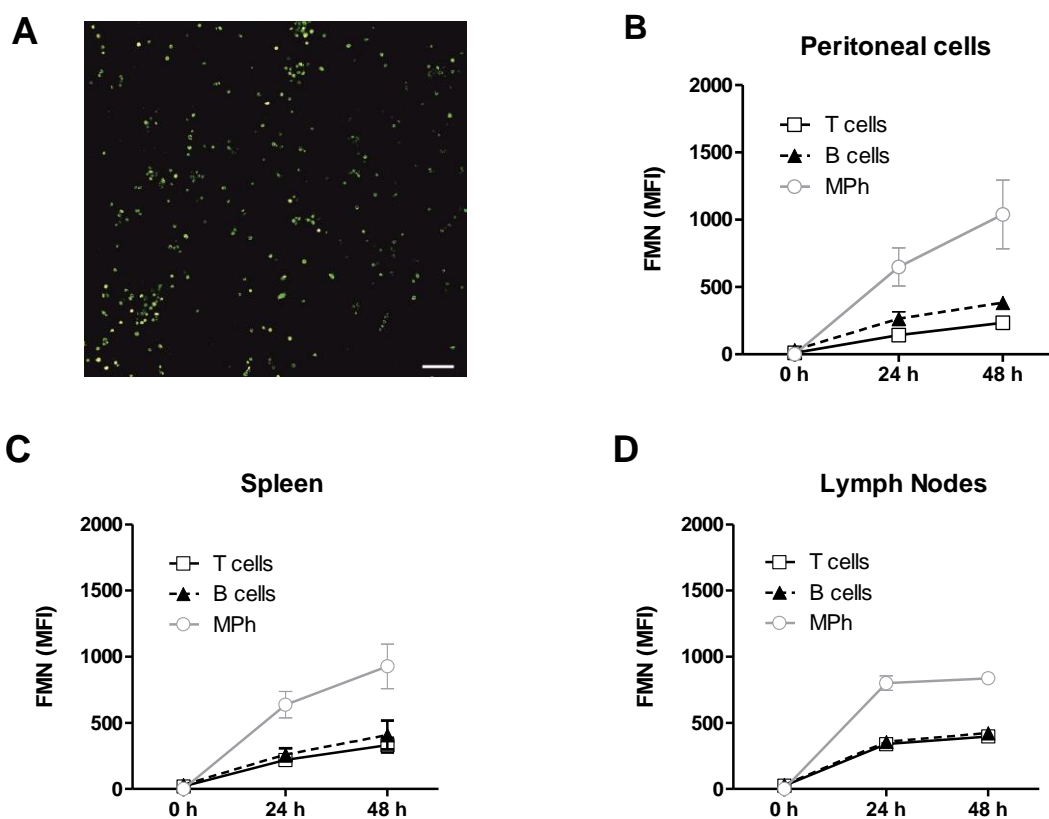


**Figure 3.1 | BNPs are efficiently but differentially taken up by immune cells *in vitro*.** (A) Analysis of BMDMs treated O/N with BNPs by 2-PM (*in collaboration with Judith Strauß, IMSF Göttingen*). (B,C,D) Peritoneal lavage cells, splenocytes and lymph nodes cells were isolated from wt C57BL/6 mice (n=6) and total cell suspensions were cultured in the presence of 10<sup>-6</sup>M BNPs. Cells were harvested after 24 h and 48 h,

---

incubated with monoclonal Abs against CD3, B220 and CD11b and analyzed by FACS. After electronic gating on the three subpopulations, nanoparticle uptake was quantified on the basis of the mean fluorescence intensity (MFI) of the FMN dye. Values are depicted as mean  $\pm$  SEM.

### **3.1.2 BNPs are more potent in modulating macrophages than T cell activity** *in vivo*

Previous *in vitro* analyses suggested that BNPs equally modulated T cell and macrophage function in a similar manner. However, in a competitive situation such as mixed cultures, the nanoparticles were preferentially internalized by myeloid cells. Thus we hypothesized that BNPs might exert a stronger anti-inflammatory effect on macrophages as compared to T cells when applied *in vivo*.

First, surface expression of molecules involved in antigen-presentation was studied on peritoneal macrophages by FACS (**Figure 3.2 A**). In all experiments, the same dose of free Dex and BNPs was employed (10 mg/kg) and administered on three consecutive days. PBS or empty nanoparticles without the drug (ENPs) served as controls. Expression of MHC class II and CD86 were both strongly reduced by Dex and BNPs compared to their respective controls. To confirm the efficacy of the BNPs, peritoneal macrophages were isolated from mice treated with Dex, BNPs, PBS or ENPs for three days, and subsequently stimulated *in vitro* with IFN $\gamma$  and LPS. Secretion of TNF $\alpha$  was then analyzed in the supernatants by ELISA (**Figure 3.2 B**). Similar to the results of the FACS analysis, *in vivo* applied Dex and BNPs resulted in a suppression of TNF $\alpha$  release compared to the controls. Taken together, BNPs and free Dex have a comparable immunomodulatory efficacy in macrophages *in vivo*.

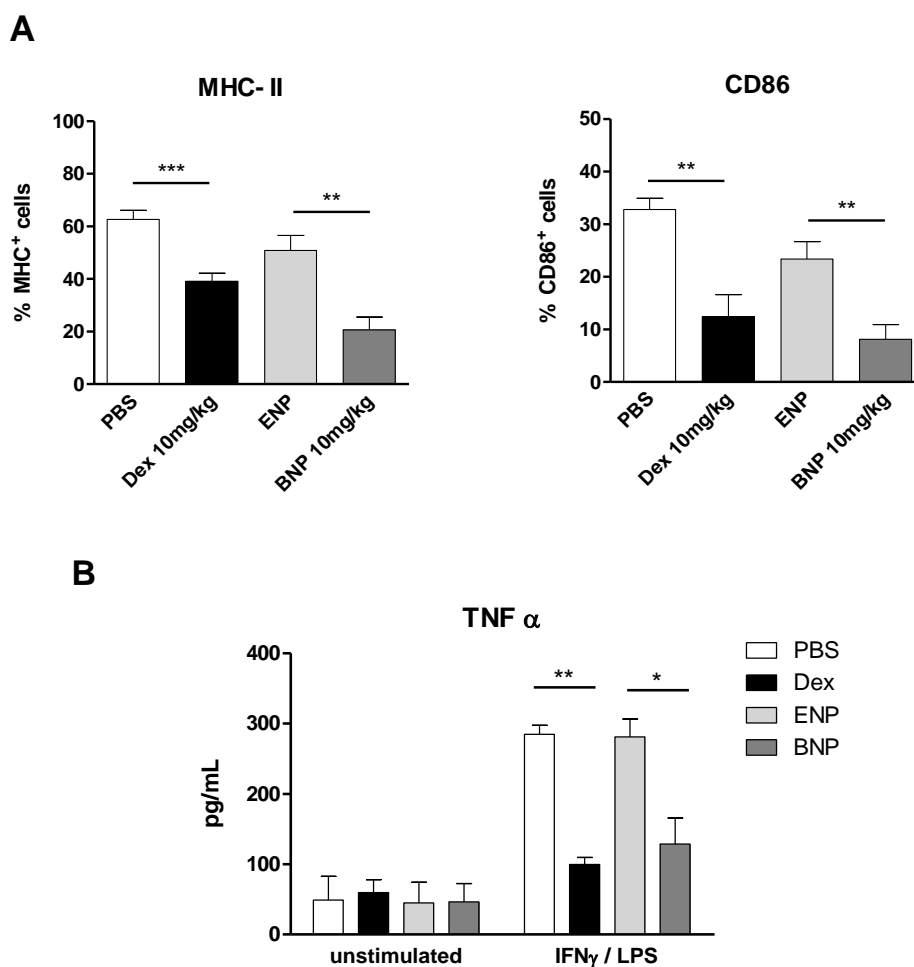


**Figure 3.2 | BNPs exert potent immunosuppressive activity on peritoneal macrophages *in vivo*.**

Thioglycolate-elicited macrophages were obtained by peritoneal lavage from wt C57BL/6 mice that received a daily injection of PBS (n=5), 10 mg/kg Dex (n=6), ENPs (n=8) or 10 mg/kg BNPs (n=6) for three consecutive days. **(A)** Cells were incubated with monoclonal Abs against CD11b, IA<sup>b</sup> (MHC II) and CD86 and analyzed by FACS. Cells expressing MHC II and CD86 were determined after gating on CD11b<sup>+</sup> cells. **(B)** 2·10<sup>5</sup> peritoneal macrophages/ml (n=3 per group) obtained from mice treated as in panel A were cultured in DMEM medium and half of the wells were stimulated with LPS and IFN $\gamma$ . After 48 h, cell culture supernatants were collected and the concentration of TNF $\alpha$  was determined by ELISA. Statistical significance was calculated using the unpaired Student's t-test and values are depicted as mean  $\pm$  SEM; \*, p <0.05; \*\*, p <0.01; and \*\*\*, p <0.001.

Having demonstrated the *in vivo* anti-inflammatory activity of the BNPs on macrophages, we wondered whether BNPs had a comparable effect regarding T cell apoptosis. Following the same protocol as for the analysis of macrophages, mice were injected daily up to three times

i.p. with the vehicles (PBS/ENPs) or 10 mg/kg GCs (Dex/BNPs). On day 0, 1 and 3 after treatment, total splenocytes were counted, stained for T cell markers and analyzed by FACS (**Figure 3.3**). *In vitro* it was shown that BNPs and Dex exerted a similar effect on T cell apoptosis as free GCs. *In vivo*, Dex induced a reduction of total splenocytes as well as CD4<sup>+</sup> and CD8<sup>+</sup> T cell numbers by almost 100% the third day of treatment. However, BNPs achieved only a 20% decrease in splenocyte numbers and a reduction around 30% in CD4<sup>+</sup> T cell numbers. The amount of CD8<sup>+</sup> cells was even unaffected. Unexpectedly, ENPs appeared to moderately increase total splenocyte numbers, in particular the CD8<sup>+</sup> T cell subset (**Figure 3.3 A**). The reason and implications of this observation, however, remain unclear.

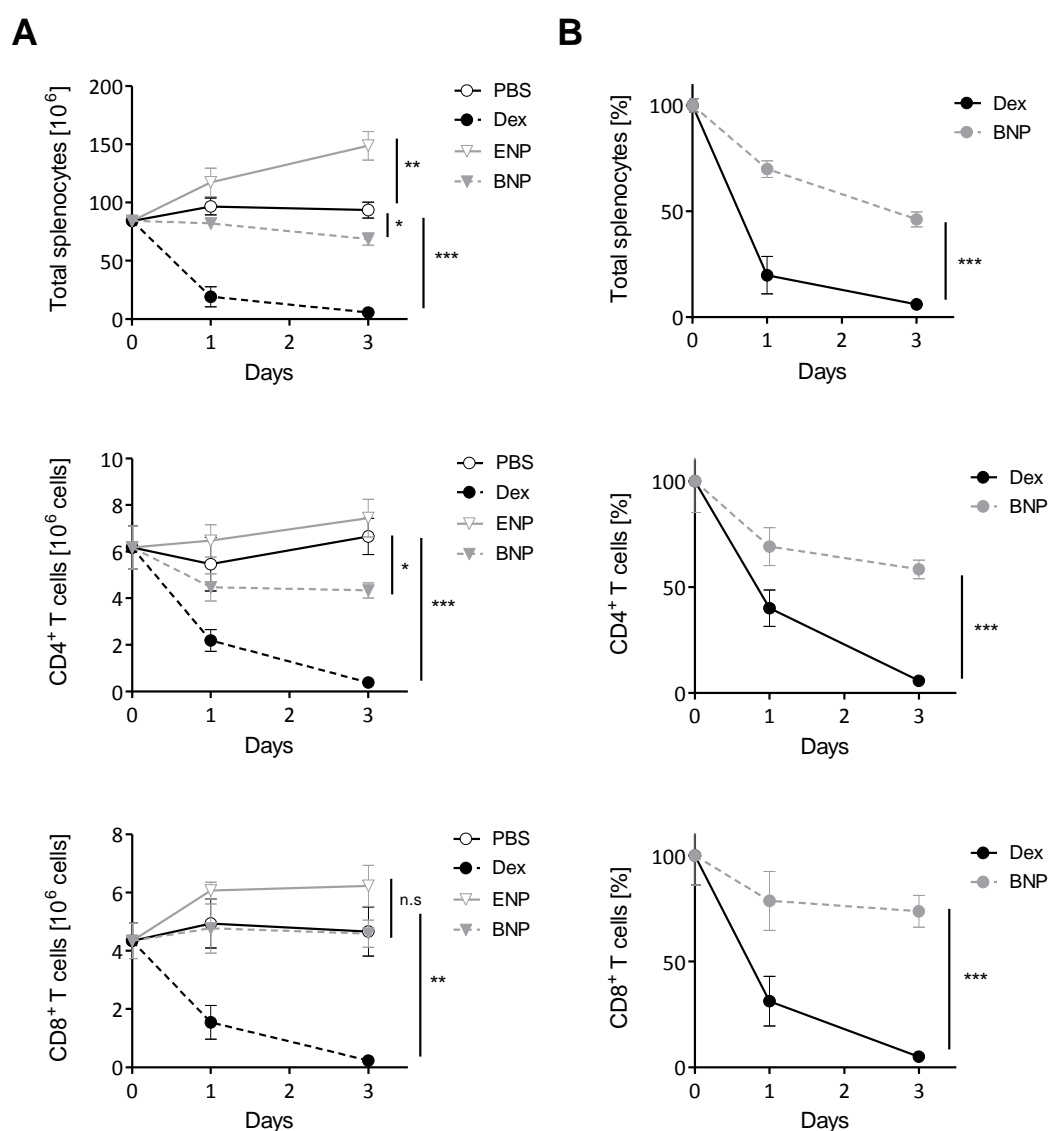




**Figure 3.3 | BNP**s do not efficiently induce T cell apoptosis *in vivo*. PBS, 10 mg/kg Dex, ENPs or 10 mg/kg BNPs were injected i.p. once per day into wt C57BL/6 mice during a three day period. On day 0 (n=5), 1 (n=3) and 3 (n=6) after treatment, total splenocytes were isolated, counted and stained with monoclonal Abs against CD3, CD4 and CD8. CD4<sup>+</sup> and CD8<sup>+</sup> populations were gated on total CD3<sup>+</sup> T cells. Total cell numbers were multiplied with the percentages of each cell population, and are presented either as absolute cell numbers (**A**) or referred to the corresponding vehicle controls (**B**). Statistical significance was calculated using the unpaired Student's t-test and values are depicted as mean ± SEM; (n.s.), p ≥ 0.05; \*, p <0.05; \*\*, p <0.01; and \*\*\*, p <0.001.

### 3.1.3 BNP

s modulate macrophage and T cell functions via the GR

Although the findings up to this point indicated that BNP

s were in principle able to modulate macrophage and T cell function, the mechanism was still unknown. It is generally accepted that free GCs exert their anti-inflammatory effects mostly through binding to the GR, but it is known that selective GC activities might also be mediated by some other receptors (Funder 1997). To corroborate that the activity of BNPs was GR-dependent, the GC-nanoparticles were tested in mice with specific deletions of the GR either in macrophages or T cells.

First, GR-deficient peritoneal macrophages were analyzed for MHC class II expression after *in vivo* treatment using a similar protocol as in **Figure 3.2**. Application of Dex or BNP

s to GR<sup>lysm</sup> mice had no effect on the surface levels of MHC class II, whereas the same treatments induced a reduction by 50% of this surface molecule in GR<sup>fl</sup> control animals, similarly to the previously shown experiments performed in mice with a wt phenotype (**Figure 3.4**). This indicates that the presence of the GR in macrophages is required for the function of BNPs.

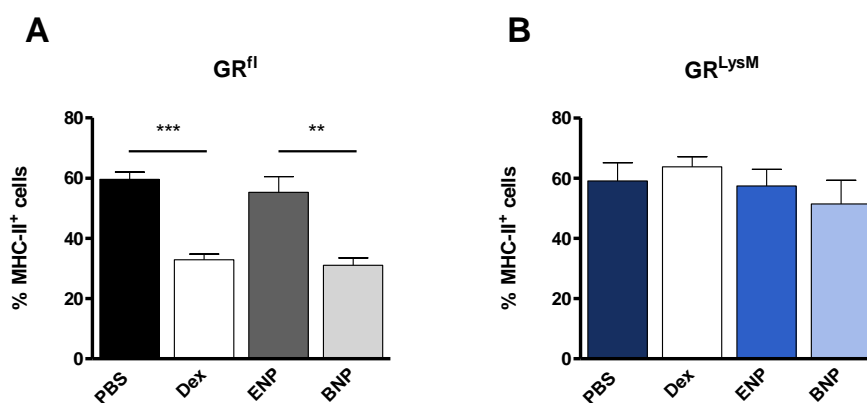


**Figure 3.4 | BNPs do not reduce MHC class II expression on GR<sup>lysM</sup> macrophages *in vivo*.** Thioglycolate-elicited macrophages were obtained by peritoneal lavage from GR<sup>fl</sup> (A) and GR<sup>lysM</sup> (B) mice that had received a daily injection of PBS (n=3/3), 10 mg/kg Dex (n=3/3), ENPs (n=3/4) or 10 mg/kg BNPs (n=6/4) during three consecutive days. The cells were incubated with monoclonal Abs against CD11b and IA<sup>b</sup> (MHC class II). Cells expressing MHC class II were gated within the CD11b<sup>+</sup> subpopulation. Statistical significance was calculated using the unpaired Student's t-test and values are depicted as mean ± SEM; \*\*, p < 0.01; and \*\*\*, p < 0.001.

Furthermore, induction of T cell apoptosis was analyzed *in vitro* and *in vivo*. GR<sup>fl</sup> control splenocytes treated *in vitro* with 10<sup>-7</sup>M BNPs underwent apoptosis to the same levels as Dex-treated ones, whereas the pro-apoptotic effect was abolished on splenocytes from the GR<sup>lck</sup> mice, with GR-deficient T cells, when they were treated with either Dex or BNPs (Figure 3.5 A,B). A similar effect was observed when Dex and BNPs were applied *in vivo* using a similar protocol as in Figure 1.3. The reduction in splenic T cell numbers by Dex and BNPs was more pronounced in GR<sup>lck</sup> mice compared to GR<sup>fl</sup> mice (Figure 3.5 C,D), indicating that their pro-apoptotic effect is partially abolished. The slight drop in T cells in the mutant mice after treatment might be due to the effect of GCs in other cell types in the spleen, such as B cells, thus causing a collateral decrease in T cell numbers.

Taken together, our data confirmed that not only free GCs but also BNPs require the GR in order to exert their immunomodulatory effects in T cells and macrophages.

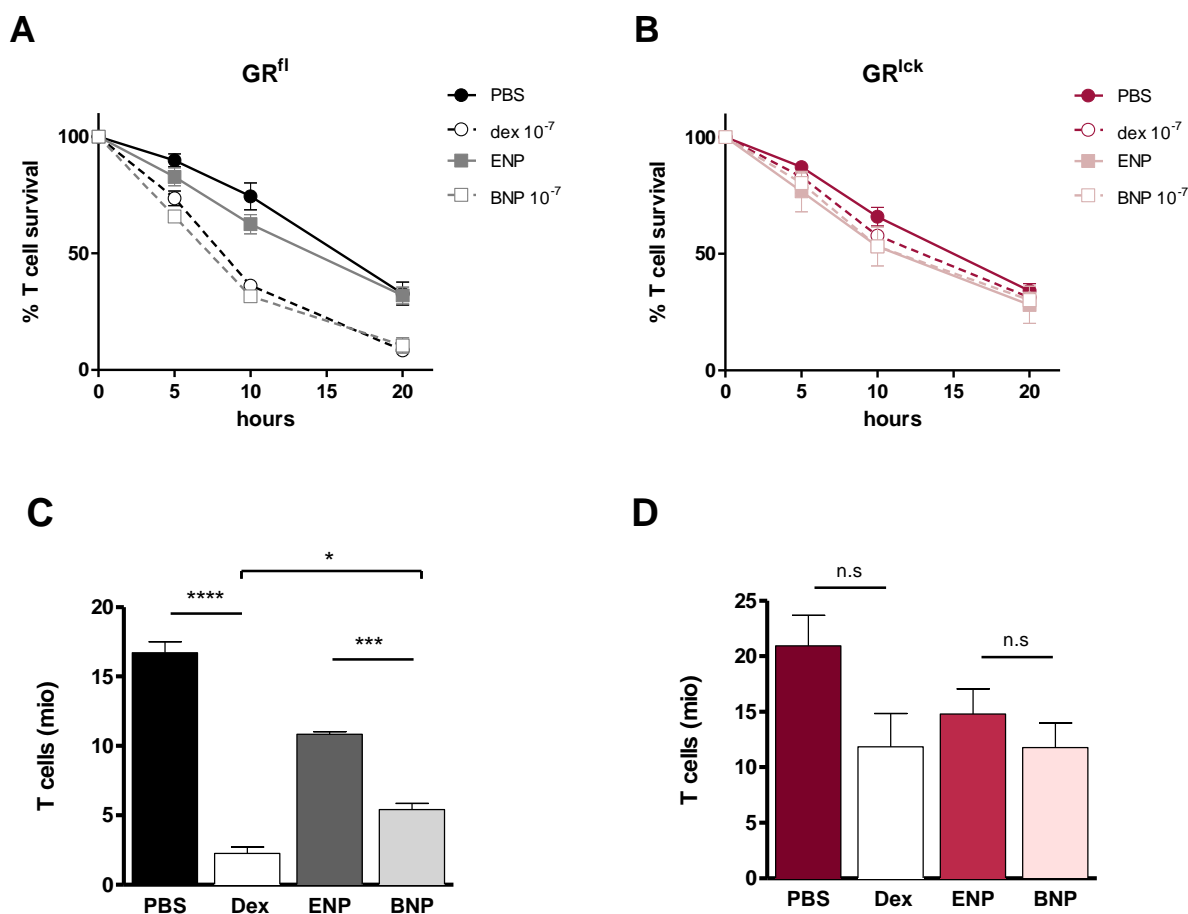
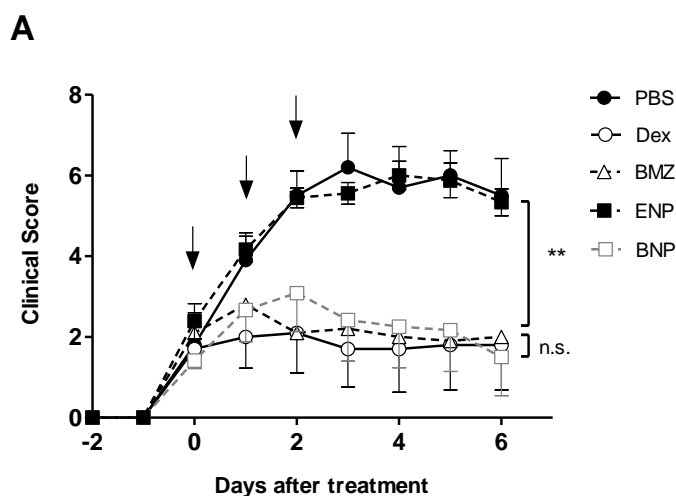


**Figure 3.5 | BNPs depend on the presence of the GR for the induction of T cell apoptosis.** The activity of BNPs in GR-deficient T cells was evaluated *in vitro* and *in vivo*. **(A, B)** Total splenocytes isolated from GR<sup>fl</sup> (n=6, A) and GR<sup>lck</sup> (n=6, B) mice were cultured *in vitro* with PBS, 10<sup>-7</sup>M Dex, ENPs or 10<sup>-7</sup>M BNPs, and harvested 5 h, 10 h and 20 h after treatment. Cells were stained with an anti-CD3 Ab and Annexin V, and analyzed by FACS. The percentage of surviving T cells was referred to the values obtained for freshly isolated splenocytes, which were set to 100%. **(C, D)** Splenocytes were isolated from GR<sup>fl</sup> (n=6, C) and GR<sup>lck</sup> (n=6, D) mice that had been treated with PBS, 10 mg/kg Dex, ENPs and 10 mg/kg BNPs once per day during a three day period. To determine total T cell numbers, the splenocytes were counted and the T cells were identified by FACS analysis of the CD3<sup>+</sup> subpopulation. Statistical significance was calculated using the unpaired Student's t-test and values are depicted as mean ± SEM; (n.s.), p ≥ 0.05; \*, p < 0.05; and \*\*\*, p < 0.001; \*\*\*\*, p < 0.0001.

### 3.1.4 BNPs efficiently ameliorate EAE in mice

Having proven the anti-inflammatory properties of BNPs both *in vitro* and *in vivo*, we investigated their therapeutic potential in the context of EAE. The disease was induced in C57BL/6 wt mice by immunization with 50 µg of MOG<sub>35-55</sub>. This form of EAE is characterized by a chronic progressive disease course that peaks at around day 14-16 post-immunization with hind limb paralysis (score 6-7), followed by partial resolution of the symptoms. C57BL/6 mice received daily doses of PBS, 10 mg/kg Dex, ENPs or 10 mg/kg BNPs on three consecutive days, starting on the day when the first clinical signs appeared (score 2-3). In order to exclude a potential difference in therapeutic efficacy between Dex and BMZ, which is contained in the nanoparticles, an additional group was treated with free BMZ. The disease curves representing the progression of clinical symptoms of EAE showed that all three GC treatment protocols (Dex, BNPs and BMZ) were equally potent in ameliorating EAE (**Figure 3.6 A**). Noteworthy, ENPs did not influence EAE, confirming that the vehicle had no effect in the observed phenotypes.

In order to determine the range of clinical efficacy, the amount of BNPs was titrated in the treatment of EAE. While 5 mg/kg BNPs were still able to ameliorate clinical symptoms, this was no longer the case for 2 mg/kg. (**Figure 3.6 B**). Thus, these data show the potent therapeutic effect of BNPs at 10 mg/kg, and confirm a comparable efficacy to free GCs when they are applied at similar doses.



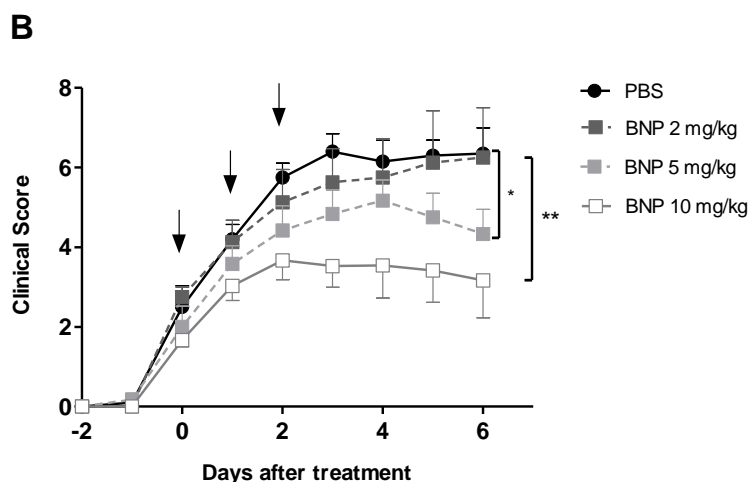


**Figure 3.6 | The therapeutic efficacy of BNPs in the treatment of EAE is similar to free GCs.** EAE was induced by active immunization on C57BL/6 wt mice with 50  $\mu$ g MOG<sub>35-55</sub> in CFA according to our standard protocol (see 2.3.1). **(A)** Having reached a disability score of 2-3, the mice received three consecutive daily i.p. injections of PBS (n=5), 10 mg/kg Dex (n=5), 10 mg/kg BMZ (n=5), ENPs (n=9) or 10 mg/kg BNPs (n=6) (black arrows). The severity of the disease was scored daily and is depicted on a scale from 0 to 10. Day 0 represents the day of the first treatment in each individual mouse. **(B)** To titrate the amount of BNPs, different doses were administered i.p.: 2 mg/kg (n=4), 5 mg/kg (n=6) and 10 mg/kg (n=18). Treatment with PBS served as a control (n=10). Statistical analysis of the scoring curve was performed using the Mann-Whitney test. Values are depicted as mean  $\pm$  SEM; (n.s.),  $p \geq 0.05$ ; \*,  $p < 0.05$ ; \*\*,  $p < 0.01$ .

The EAE model not only mimics the clinical symptoms of ascending paralysis, but also the demyelinating pathology typical for MS at the spinal cord level. This feature can be used as an independent readout of the efficacy of GC therapy. Hence, the extent of demyelination was determined in the spinal cord of mice treated with BNPs or ENPs (as control) three days after starting the therapy (**Figure 3.7**). Although no statistically significant difference was observed, there was a tendency towards reduced demyelination in mice treated with BNPs based on the LFB-PAS staining of the spinal cord sections. This supports our previous conclusions that BNPs are suitable for the treatment of EAE.

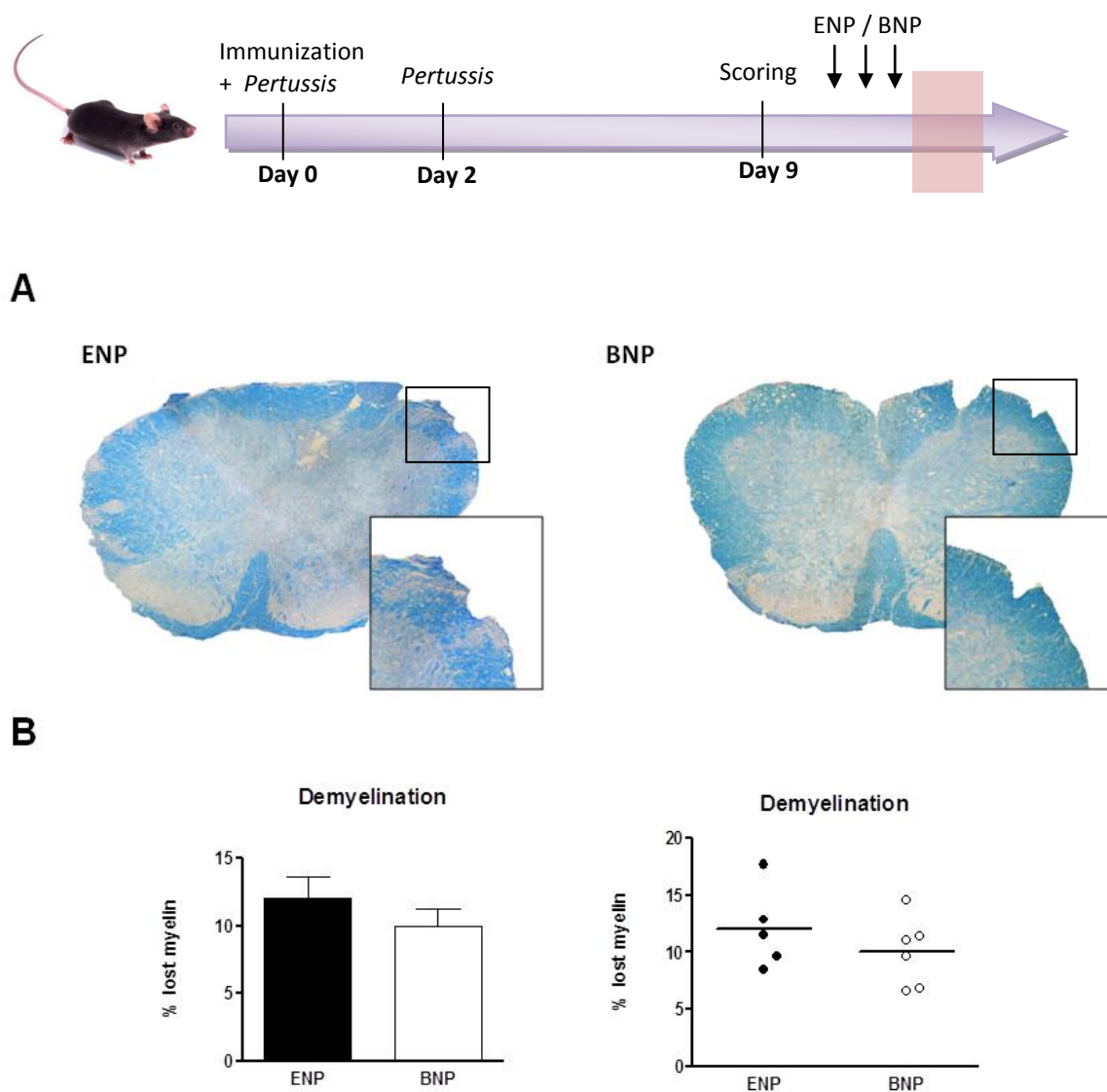
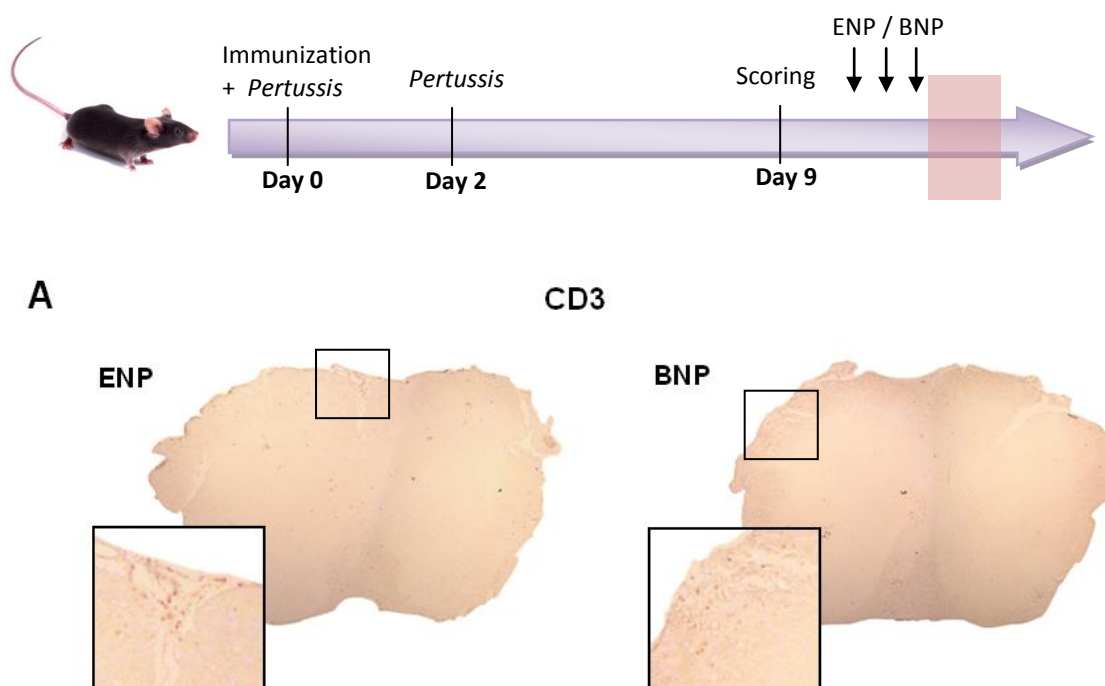


**Figure 3.7 | BNPs improve myelin pathology during EAE.** C57BL/6 wt mice suffering from EAE were treated three times with BNPs on consecutive days once they had reached a clinical score of 2-3 (n=6). Control mice received the same volume of ENPs (n=5). One day after the third injection, the mice were sacrificed and perfused with 4% PFA. Spinal cords were isolated, embedded in paraffin, 3  $\mu$ m sections prepared, and subjected to LFB-PAS staining **(A)**. Quantitative analysis of the demyelinated areas was made using the ImageJ 1.46r Software **(B)**. Values are depicted as mean  $\pm$  SEM.

### 3.1.5 Myeloid cells are essential targets of BNPs in EAE therapy

In the past years, several publications showed that T cells are major targets of GCs in the treatment of EAE (Wüst et al. 2008; Schweingruber et al. 2014). Nevertheless, alternative formulations might alter the mechanism of action of a drug, and previous data from our group revealed that liposomal encapsulation conferred an alternative cell-type specificity to GCs (Schweingruber et al. 2011). So far BNPs appeared to have a preference for myeloid cells over T cells. Therefore, we wanted to find out which cell type was the target of these nanoparticles in the context of EAE therapy.

First, we performed immunohistochemical characterization of the CNS infiltrates in immunized mice treated with ENPs or BNPs. The histological study did not reveal changes in T cell infiltration into the spinal cord after BNP treatment, however, the area occupied by macrophages was significantly reduced in the group of mice treated with BNPs as compared to the control mice receiving ENPs (**Figure 3.8**). These results provide first evidence that nanoparticles act via myeloid cells in the therapy of EAE, as hypothesized.



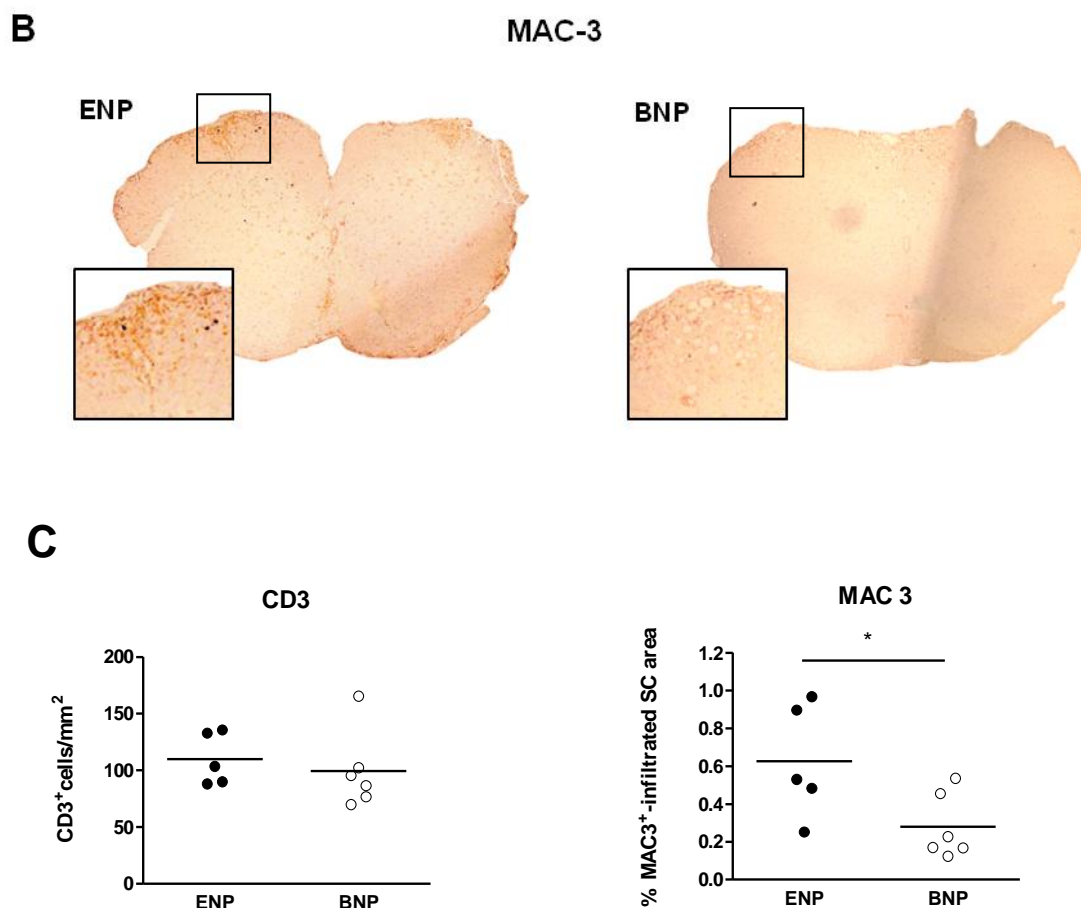


**Figure 3.8 | BNPs reduce macrophage infiltration during EAE therapy.** C57BL/6 wt mice suffering from EAE were treated three times on consecutive days with BNPs once they reached a clinical score of 2-3 (n=6). Control mice received the same amount of ENPs (n=5). One day after the last injection, the mice were sacrificed and perfused with 4% PFA. Spinal cords were isolated, embedded in paraffin, and 3  $\mu$ m sections were stained with monoclonal Abs against CD3 **(A)** or MAC3 **(B)**. Counting of CD3<sup>+</sup> cells and quantification of macrophage infiltration were performed with the ImageJ 1.46r software **(C)**. Statistical significance was calculated using the unpaired Student's t-test and values are depicted as mean  $\pm$  SEM; \*, p < 0.05.

In the previous *in vitro* and *in vivo* experiments it had been found that the presence of the GR was necessary for the immunomodulatory effects of the BNPs, regardless of the cell type (see **Figure 3.4**, **Figure 3.5**). Based on this observation we hypothesized that the therapeutic effect of the BNPs should be abrogated when the GR is deleted from any cell type being essential for the therapeutic efficacy of this treatment.



To address this issue, EAE was induced in several cell type-specific GR knock-out mice.  $GR^{lck}$  mice lack the GR specifically in T cells;  $GR^{lysM}$  are GR-deficient in myeloid cells;  $GR^{lck/lysM}$  have a GR deletion simultaneously in T cells and macrophages; and  $GR^{SLCO1C1}$  carry an inducible GR knock-out construct in endothelial cells of the BBB.  $GR^{fl}$  littermates serve as controls in each case. Once the mice reached a clinical score of 2-3, they were treated with 10 mg/kg BNPs or the same amount of the empty vehicle according to our standard protocol (see **Figure 3.6**). The deletion of the GR in T cells did not affect the capacity of the BNPs to improve EAE, suggesting that they were not essential targets in this context (**Figure 3.9 A**). In contrast,  $GR^{lysM}$  mice not only presented with a more severe disease course, but were also completely refractory to the treatment with BNPs (**Figure 3.9 B**). In line with these findings, the double knock-out mice neither responded to BNP treatment (**Figure 3.9 C**). Finally,  $GR^{SLCO1C1}$  mice responded to the therapy with BNPs, confirming that modulation of brain endothelial cells was dispensable for the beneficial effect of the GC-nanoparticles (**Figure 3.9 D**).

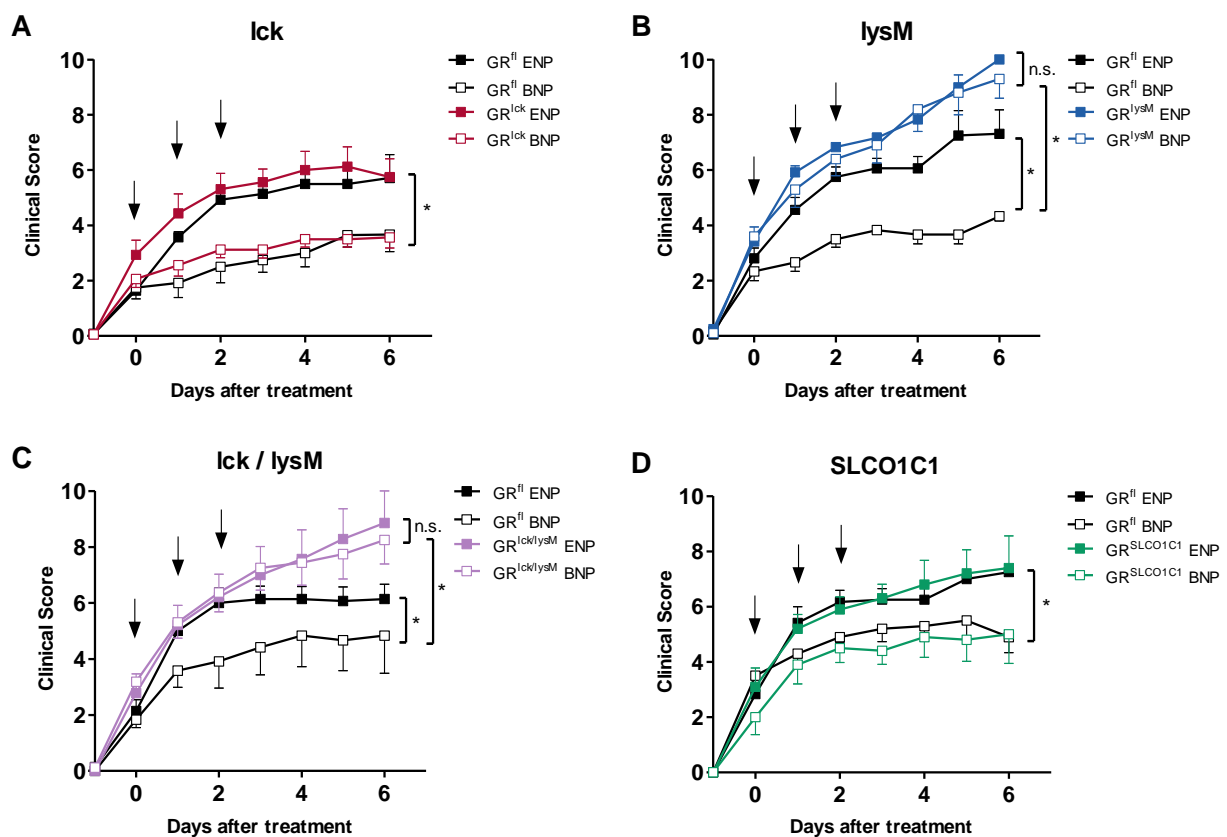


**Figure 3.9 | Myeloid cells are essential targets of BNPs in the treatment of EAE.** EAE was induced by active immunization with MOG<sub>35-55</sub> in four different GR knock out mouse strains: **(A)** GR<sup>lck</sup> (n= 7,6,8,8), **(B)** GR<sup>lysM</sup> (n= 8,3,6,5), **(C)** GR<sup>lck/lysM</sup> (n=7,6,7,8) and **(D)** GR<sup>SLO1C1</sup> (n=6,5,5,5). GR<sup>fl</sup> littermates were used as controls in each experiment. 10 mg/kg BNPs and a similar amount of ENPs were applied i.p. once per day for three consecutive days starting once individual mice reached a clinical score of 2-3. The disease severity was evaluated daily for 6 days after the beginning of the treatment. Statistical analysis of the scoring curves was performed using the Mann-Whitney test; values are depicted as mean ± SEM; (n.s.), p ≥ 0.05; \*, p <0.05.

These data clearly demonstrate that BNPs act mainly via modulation of myeloid cells in the treatment of EAE, whereas T cells and brain endothelial cells play only a minor role for their therapeutic efficacy.

### 3.1.6 BNPs and Dex act synergistically in the treatment of EAE

This study so far demonstrated that the use of the ZrO<sub>2</sub> nanoparticles directed GCs to the myeloid compartment, while conventional therapies using free GCs mainly target T cells. Since both cell types participate in EAE progression, a combination of both delivery methods might cause a synergy via targeting distinct cell types, thereby potentiating the anti-inflammatory properties of GCs even at lower drug concentrations.

In order to explore this possibility, C57BL/6 wt mice suffering from EAE were treated with suboptimal doses of Dex or BNPs, and an additional group received a combination of both with the total amount of GCs being equal to the individual treatments. As observed previously (see **Figure 3.6 B**), a suboptimal dose of BNPs did not achieve therapeutic efficacy. However, mice injected with suboptimal doses of both BNPs and Dex presented with a slightly, but significantly, milder EAE than the mice treated with Dex alone. This supports our hypothesis regarding a synergy between BNPs and free Dex.

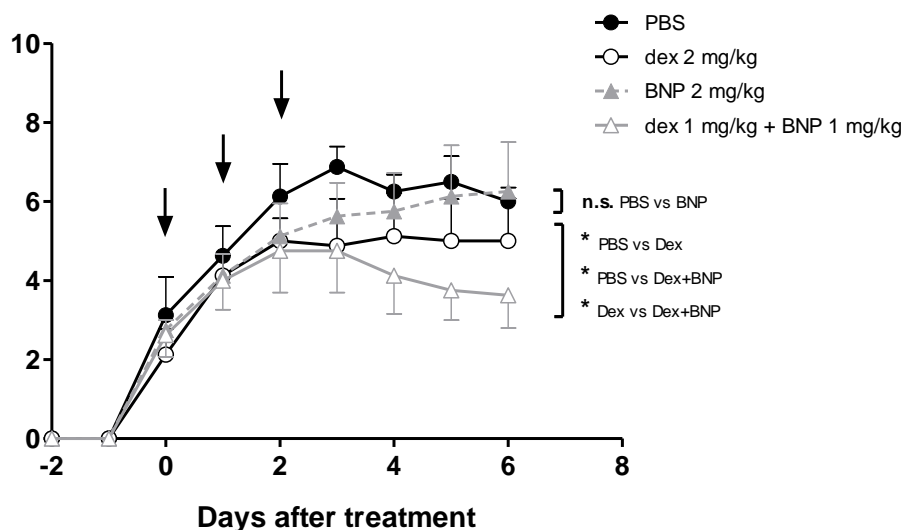


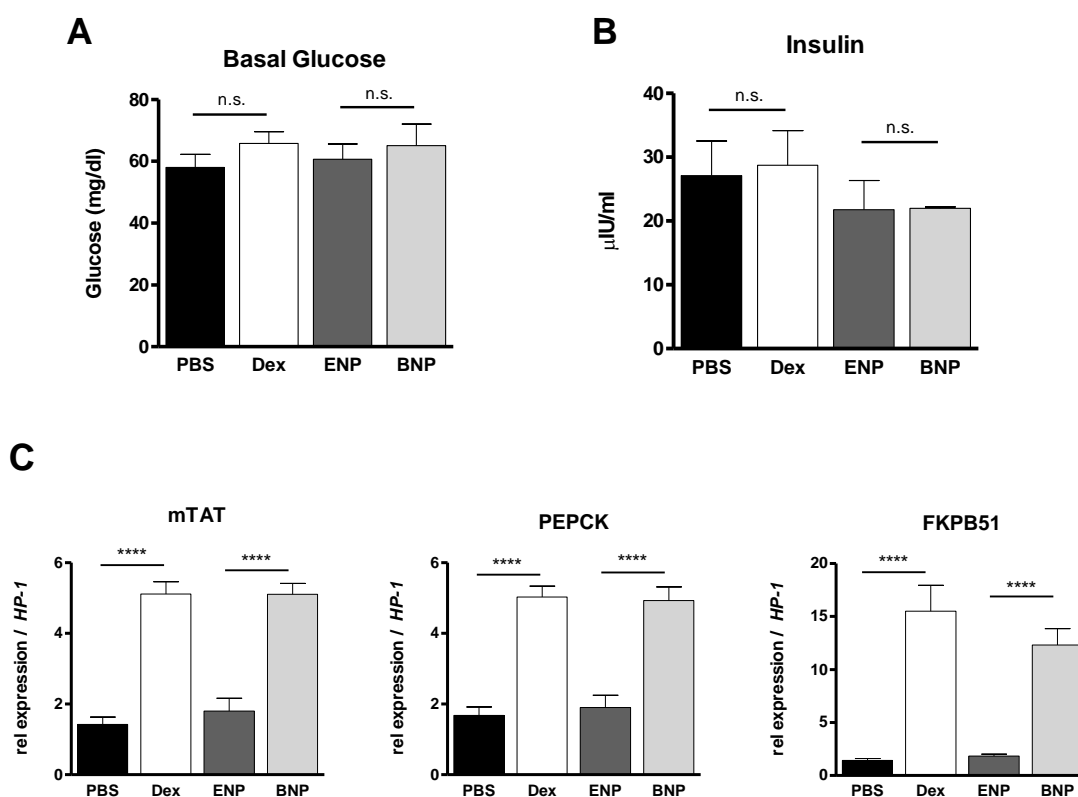
**Figure 3.10 | Combined treatment with BNPs and Dex synergistically improves EAE.** EAE was induced by active immunization on C57BL/6 wt mice with 50  $\mu$ g MOG<sub>35-55</sub>. When mice reached a disability score >1, three consecutive daily injections of PBS (n=4), 2 mg/kg Dex (n=4), 2 mg/kg BNPs (n=4) or 1 mg/kg Dex + 1 mg/kg BNPs (n=4) were applied i.p. (black arrows). Statistical analysis of the scoring curves was performed using the Mann-Whitney test. Values are depicted as mean  $\pm$  SEM; (n.s.),  $p \geq 0.05$ ; \*,  $p < 0.05$ .

### 3.1.7 BNPs partially circumvent GC-associated side-effects

A negative aspect of GC therapies is the frequent occurrence of adverse side effects. (Moghadam-Kia and Werth 2010; Weinstein 2012; Ciriaco et al. 2013; Hunter et al. 2014; Hwang and Weiss 2014). This problem derives from the ubiquitous expression of the GR (Rhen and Cidlowski 2005), that makes GCs important players in numerous homeostatic and metabolic processes. By targeting GCs to the myeloid compartment, we aimed to overcome, at least partially, these side effects. Therefore experiments were set up to determine the effect of BNPs in the context of undesired GC activities.

### 3.1.7.1 Glucose metabolism

To find out whether the use BNP<sub>s</sub> circumvented GC-associated hyperglycemia we treated healthy C57BL/6 wt mice on four consecutive days with 10 mg/kg Dex, 10 mg/kg BNP<sub>s</sub>, or their respective vehicles. One day after the last injection, glucose and insulin levels, as well as the expression of typical gluconeogenic enzymes in the liver were measured after O/N fasting. The increase in blood glucose levels was minimal, presumably due to the moderate dose of the drug (**Figure 3.11 A**). Consistent with the little increase in glucose, insulin concentrations in the serum were unaltered (**Figure 3.11 B**). Surprisingly, the nanoparticles appeared to lower insulin levels, regardless of whether they contained BMZ or not. The reason and relevance of this effect is not known. Regarding gluconeogenesis, the expression levels of the three analyzed hepatic enzymes were significantly increased by Dex and BNP<sub>s</sub> (**Figure 3.11 C**).



---

**Figure 3.11 | Short treatment with BNPs affects glucose metabolism similarly to Dex.** C57BL/6 wt mice were treated i.p. with PBS (n= 12), 10 mg/kg Dex (n=13), ENPs (n=10) or 10 mg/kg BNPs (n=10) once per day for four consecutive days. Subsequently, the food pellets were removed O/N. In the morning (9 AM), glucose levels were measured in blood obtained via tail puncture **(A)**. Afterwards, the mice received an additional injection of the corresponding drug, and 2.5 h later blood serum and liver samples were collected. Insulin levels were determined in serum samples by ELISA **(B)**. The liver samples were used to extract RNA which, after reverse transcription, was used to analyze the expression levels of gluconeogenic enzymes by qRT-PCR. Expression of the housekeeping gene HP-1 was used as reference **(C)**. Values were analyzed using the unpaired Student's t-test and are depicted as mean  $\pm$  SEM; \*\*\*\*,  $p < 0.0001$ .

Since hyperglycemia could hardly be observed, even after application of free GCs, no definite conclusions about the properties of BNPs in this respect could be drawn at this point. To address this, further experiments with modified experimental protocols will be performed in the future.

### 3.1.7.2 Muscle wasting

Another complication observed after GC therapy is skeletal muscle atrophy. To investigate this effect of BNPs, changes in muscle mass were measured in mice treated with Dex or BNPs for four days. On the day after the last injection, the hind limb muscles of the mice were removed, weighted and the values were normalized to the total body weight. Despite the short duration of the corticoid therapy, a slight but non-significant decrease in *tibialis anterior* and *gastrocnemius* mass was found in the Dex-treated mice, and to a minor extent also in BNP-treated animals **(Figure 3.12)**. As for glucose and insulin levels, the GC dose used in this experimental setup appears to be too low to induce meaningful metabolic side-effects in mice.

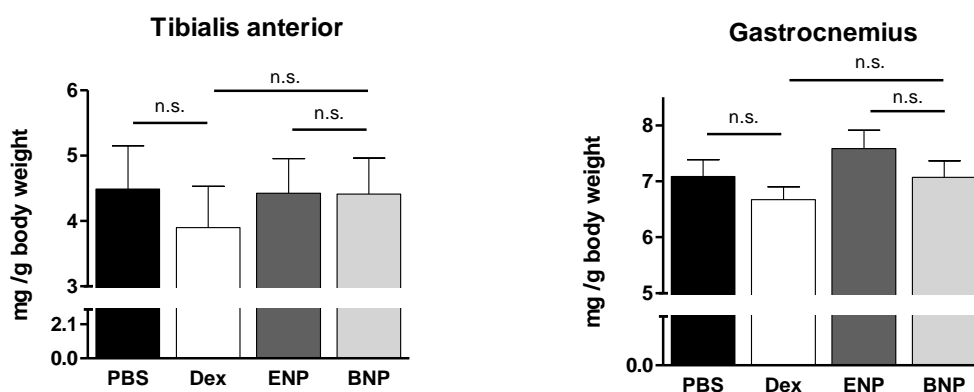


**Figure 3.12 | Short treatment with BNP hardly affects muscle wasting.** C57BL/6 wt mice were treated i.p. with PBS (n=10), 10 mg/kg Dex (n=10), ENPs (n=10) and 10 mg/kg BNPs (n=10) once per day for four consecutive days. The mice were weighted and sacrificed on the day after the last treatment. Skin was removed from the hind limbs to expose the muscle, and *tibialis anterior* and *gastrocnemius* were dissected. The weight of the muscles was determined and referred to the total body weight in each individual mouse. Values were analyzed using the unpaired Student's t-test and are depicted as mean  $\pm$  SEM; (n.s.),  $p \geq 0.05$ .

### 3.1.7.3 Stomach emptying

It has been demonstrated that GC treatment alters NO metabolism in the stomach, slowing down gastric motility (Reichardt et al. 2014). As a consequence, stomach emptying is impaired resulting in an increased weight of the filled stomach. To address this issue, mice were treated with PBS, 10 mg/kg Dex, ENPs or 10 mg/kg BNPs and the weight of the stomach was determined. In both groups receiving GCs, a small but non-significant increase in stomach weight was observed (**Figure 3.13**). This preliminary data indicates that BNP therapy might impair stomach emptying in a similar manner as free Dex and therefore the use of the nanoparticles might not circumvent this GC-associated side-effect.

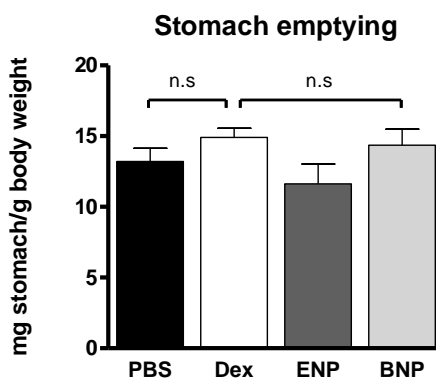


**Figure 3.13 | Short treatment with BNPs and Dex has a mild effect on gastric emptying.** C57BL/6 wt mice were treated i.p. with PBS (n=5), 10 mg/kg Dex (n=5), ENPs (n=5) and 10 mg/kg BNPs (n=5) once per day for four consecutive days. One day after the last treatment the mice were weighted and sacrificed. The full stomach was dissected, weighted and the obtained values were normalized to the total body weight in each individual mouse. Values were analyzed using the unpaired Student's t-test and are depicted as mean  $\pm$  SEM; (n.s.),  $p \geq 0.05$ .

#### 3.1.7.4 Bone re-sorption

An important side effect of GC therapy is the decrease in bone mineral density. To evaluate whether BNPs improved this symptom or not, osteocalcin was used as a surrogate marker of GC-induced osteoporosis, since it is quickly reduced after GC application (Leclerc et al. 2005). The concentrations of osteocalcin in the serum of mice treated with PBS, 10 mg/kg Dex, ENPs or 10 mg/kg BNPs for four consecutive days were determined by ELISA. With this treatment protocol, no significant changes in osteocalcin levels could be detected between any of the experimental groups.

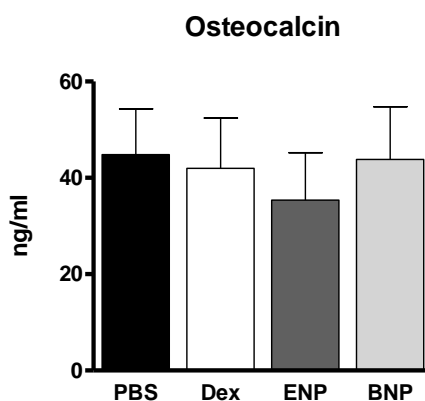


**Figure 3.14 | Short treatment with BNPs does not affect the osteoporosis marker osteocalcin.** Blood was obtained via heart puncture from C57BL/6 wt mice receiving a 4-day treatment with PBS (n=10), 10 mg/kg Dex (n=10), ENPs or 10 mg/kg BNPs (n=10). Serum was separated in a STT Microtainer™ tubes by centrifugation. The levels of osteocalcin were determined on the serum samples by ELISA. Values were analyzed using the unpaired Student's t-test and are depicted as mean  $\pm$  SEM; (n.s.),  $p \geq 0.05$ .

Collectively, our data indicates that the experimental protocol used in the analysis of GC-associated side symptoms needs to be optimized in order to obtain reliable information about the potential of the BNPs to avoid the appearance of unwanted effects.

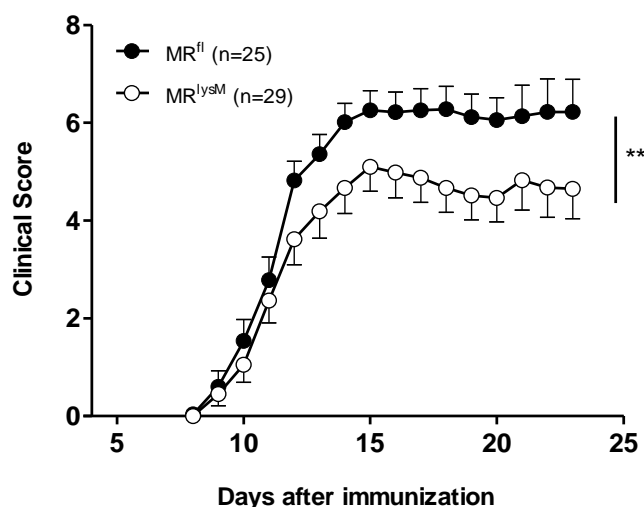


## 3.2 Role of the MR in myeloid cells in EAE

The previous results of this thesis confirmed the crucial role of myeloid cells for the response to GCs in EAE, and showed that this modulation is mediated by the GR. However, the GR is not the only receptor sensitive to GCs in this cell compartment. The MR is also expressed in myeloid cells and is known to promote a pro-inflammatory state in mouse peritoneal macrophages after GC binding (Usher et al. 2010). Hence, we assumed that the deletion of the MR in myeloid cells might potentiate the anti-inflammatory activities of GCs via the GR. Therefore, the aim of the second part of this thesis was to characterize the CNS autoimmune responses in MR<sup>lysM</sup> mice, a knock-out mouse strain harboring a MR deficiency specifically in the myeloid compartment.

### 3.2.1 MR<sup>lysM</sup> mice develop a milder EAE disease

This project is based on the previous work of Li and Schweingruber, two former colleagues of the Reichardt's group, who performed extensive *in vitro* analyses of macrophages derived from MR<sup>lysM</sup> mice. MR-deficient macrophages expressed lower levels of pro-inflammatory genes compared to cells from MR<sup>fl</sup> controls (Li 2013). In line with these results, their capacity to secrete TNF $\alpha$  and NO was diminished as well. Analysis of EAE in MR<sup>lysM</sup> mice showed a milder disease course (**Figure 3.15**), which was reproducible in our current experiments. Furthermore, both peripheral and CNS-infiltrating macrophages from the affected mice adopted a M2 phenotype, confirming a correlation between EAE severity and myeloid cell phenotype (Li 2013).

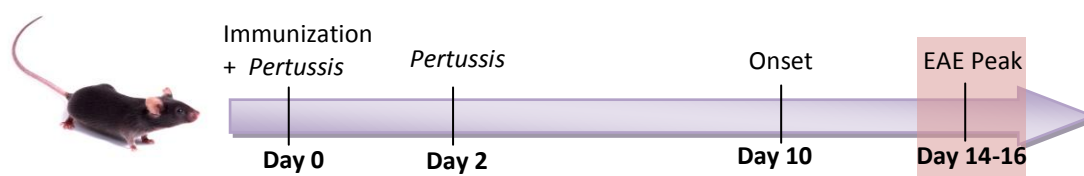
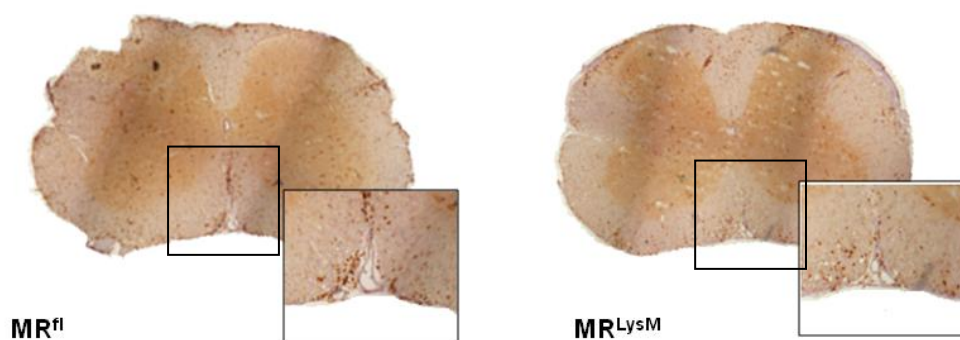
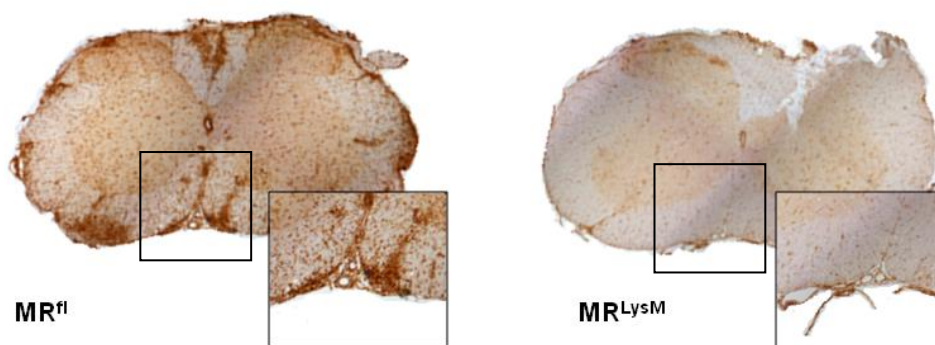


**Figure 3.15 | MR<sup>lysM</sup> mice develop a milder EAE phenotype.** EAE was induced in MR<sup>fl</sup> and MR<sup>lysM</sup> mice by active immunization with 50  $\mu$ g of MOG<sub>35-55</sub> emulsified in CFA. Mice were weighted and scored daily from day 9 post-immunization on. **(A)** Cumulative disease curve as determined in experiments performed by Li and Schweingruber (Li 2013). Statistical analysis was performed using the Mann-Whitney test; values are depicted as mean  $\pm$  SEM; \*\*,  $p < 0.01$ .

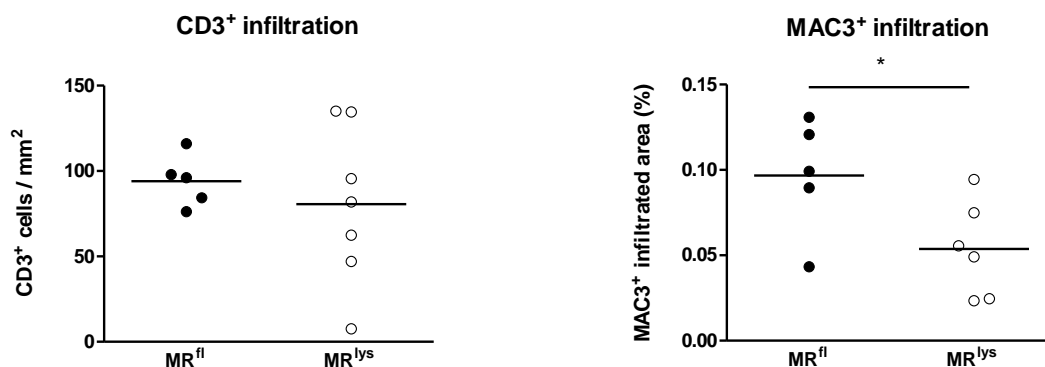
The aim of this part of my thesis was to continue and complete the characterization of EAE in MR<sup>lysM</sup> mice. Since the clinical signs of disability in EAE generally mirror neuronal pathology, we aimed to corroborate the milder disease course observed in the MR<sup>lysM</sup> group via histological analysis of the spinal cord in those mice. These experiments were performed in collaboration with Li and Schweingruber, and the preliminary histological data was already included in the thesis of Li (Li 2013).

First, CNS infiltration by immune cells was determined. Once T cells have been primed by antigen-specific APCs in the periphery, they proliferate and acquire effector functions. Several days later, they migrate to the CNS to encounter their cognate antigen again and become re-stimulated, therefore infiltration of antigen-specific T cells is considered a major hallmark of EAE pathogenesis (Schweingruber et al. 2014). The histological analysis of MR<sup>lysM</sup> mice revealed that, in spite of the milder disease course in the MR<sup>lysM</sup> mice, infiltration by CD3<sup>+</sup> cells into the spinal cord was largely similar in both genotypes (**Figure 3.16 A**). Besides

T cell migration, a massive infiltration of monocytes is observed at the onset of EAE and during MS relapses (Huitinga et al. 1990). Once in the CNS, these monocytes differentiate into macrophages that process and present myelin antigens, thereby contributing to the secretion of cytokines and other soluble mediators which cause oligodendroglial death and neuronal damage. Since MR-deletion might affect different features of monocytes/macrophages including migration, the presence of monocytes and macrophages in the CNS was also investigated by IHC using an anti-MAC3 Ab. Indeed, the infiltration of the spinal cord by MAC3<sup>+</sup> cells in MR<sup>LysM</sup> mice was significantly lower compared to the MR<sup>fl</sup> control animals (**Figure 3.16 B**).

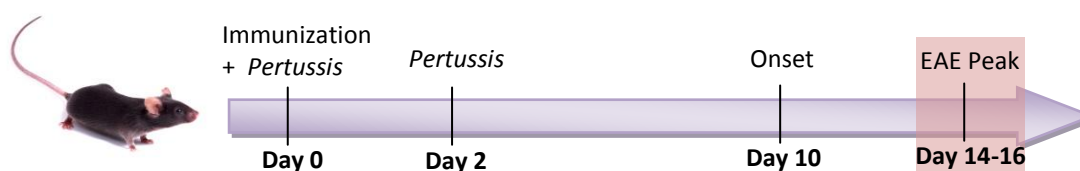
**A****B**

C



**Figure 3.16 | Macrophage infiltration into the spinal cord is reduced in MR<sup>lysM</sup> mice during EAE.** MR<sup>fl</sup> (n=5) and MR<sup>lysM</sup> (n=7-6) mice were immunized according to our standard protocol (see 2.3.1) and spinal cords were isolated and fixed in PFA at the peak of the disease (in collaboration with Li and Schweingruber). After paraffin embedding, 3  $\mu$ m sections were cut and mounted on microscopic slides. IHC staining was performed with Abs against CD3 (A) and MAC3 (B). The number of CD3<sup>+</sup> cells per mm<sup>3</sup> of total spinal cord area and the area infiltrated by MAC3<sup>+</sup> cells in relation to the total white matter area were determined with the help of the ImageJ 1.46r software (C). Values were analyzed using the unpaired Student's t-test and are depicted as mean  $\pm$  SEM; \*, p < 0.05.

Additionally, the extent of neurodegeneration in these mice was evaluated. To this end, histological analysis of demyelination and axonal loss were performed on spinal cord sections from MR<sup>fl</sup> and MR<sup>lysM</sup> mice at the peak of EAE disease. In agreement with the milder EAE score, the average number and size of demyelinated lesions was significantly reduced in the myeloid-specific knock-out mice. Furthermore, axonal density in MR<sup>lysM</sup> mice was partially preserved (Figure 3.17).



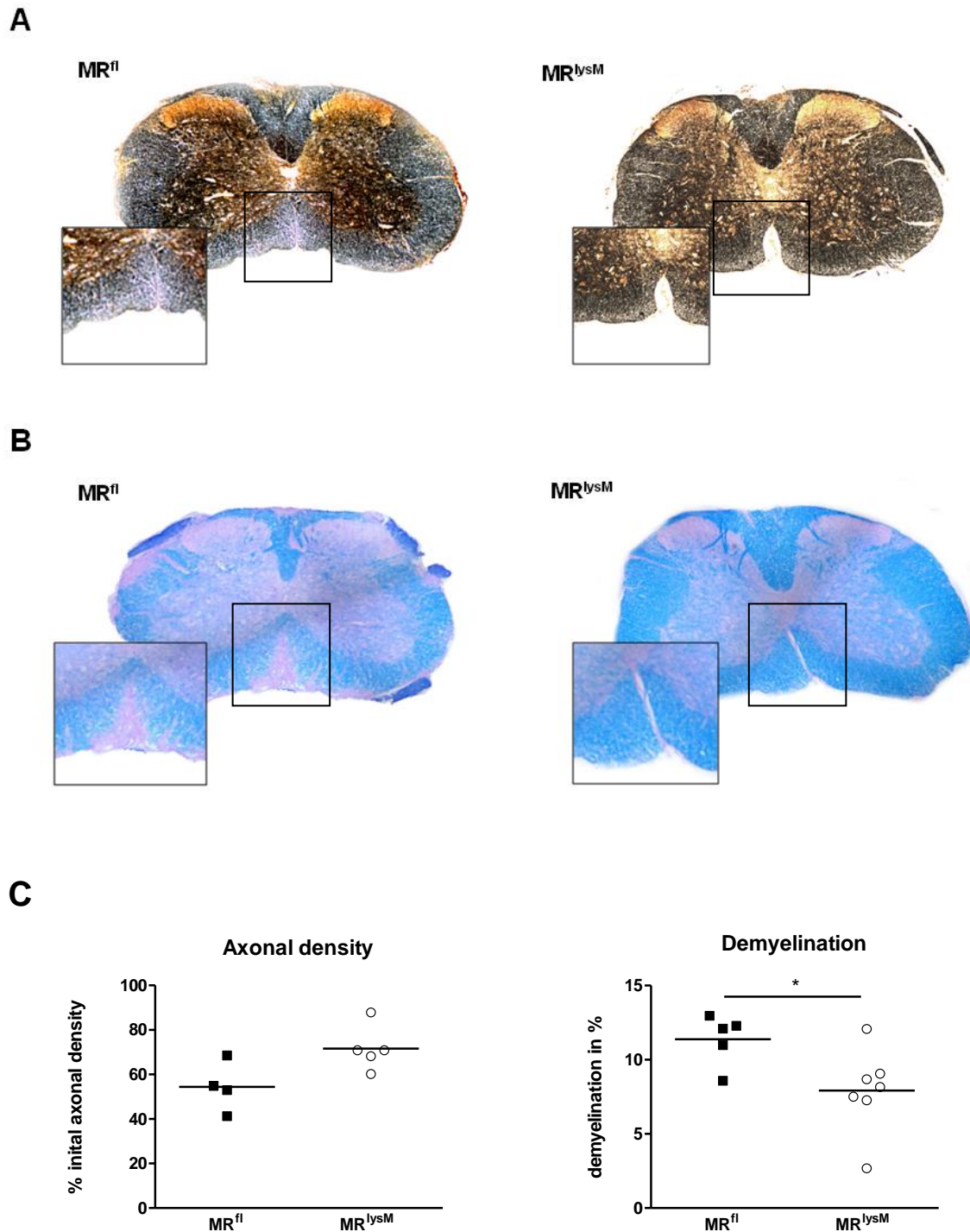


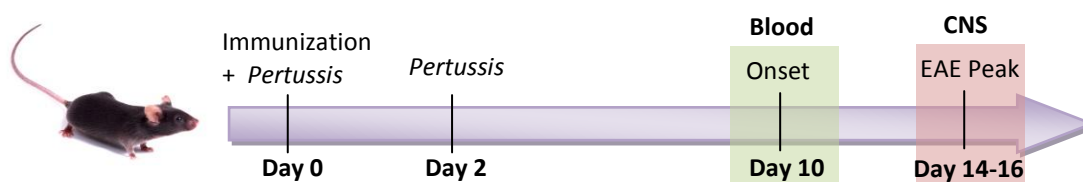
**Figure 3.17 | Demyelination and axonal damage in MR<sup>lysM</sup> mice during EAE are not as severe as in MR<sup>fl</sup> mice.** MR<sup>fl</sup> (n=5-4) and MR<sup>lysM</sup> (n=7-5) mice were immunized according to our standard protocol (see 2.3.1) and spinal cords were isolated and fixed in PFA at the peak of the disease (in collaboration with Li and Schweingruber). After paraffin embedding, 3  $\mu$ m sections were cut and mounted on microscopic slides. Bielschowsky silver staining was performed to visualize axonal fibers (**A**), and myelin was stained according to the LFB/PAS protocol (**B**). Quantification of the axonal densities and the percentage of myelin lost were carried

out with the ImageJ 1.46r software (C). Values were analyzed with the unpaired Student's t-test and are depicted as mean  $\pm$  SEM; \*,  $p < 0.05$ .

Taken together, deletion of the MR in myeloid cells markedly ameliorates EAE in terms of clinical symptoms, monocyte infiltration into the spinal cord and demyelination.

### 3.2.2 MR deletion alters the activation state of circulating and CNS-infiltrating monocytes

In search of mechanisms that could explain the reduced presence of monocytes and macrophages in the CNS of MR-deficient mice, the activation state of peripheral and CNS-infiltrating monocytes was analyzed at the onset and peak of EAE. Blood circulating monocytes were defined as  $CD11b^+ Ly6G^-$  cells, whereas in the CNS they were distinguished from other resident myeloid cells on the basis of their  $CD11b^+ CD45^{high}$  phenotype. The numbers of inflammatory monocytes, which can be distinguished from resting ones due to an increased expression of Ly6C on their surface, were determined by FACS analysis using a monoclonal Ab against Ly6C (Figure 3.18). Based on this systematic we observed that the percentage of inflammatory monocytes in blood and spinal cord was significantly reduced in mutant mice. Thus, a reduction in the number of activated monocytes could be one of factors contributing to the ameliorated EAE observed in  $MR^{lysM}$  mice.



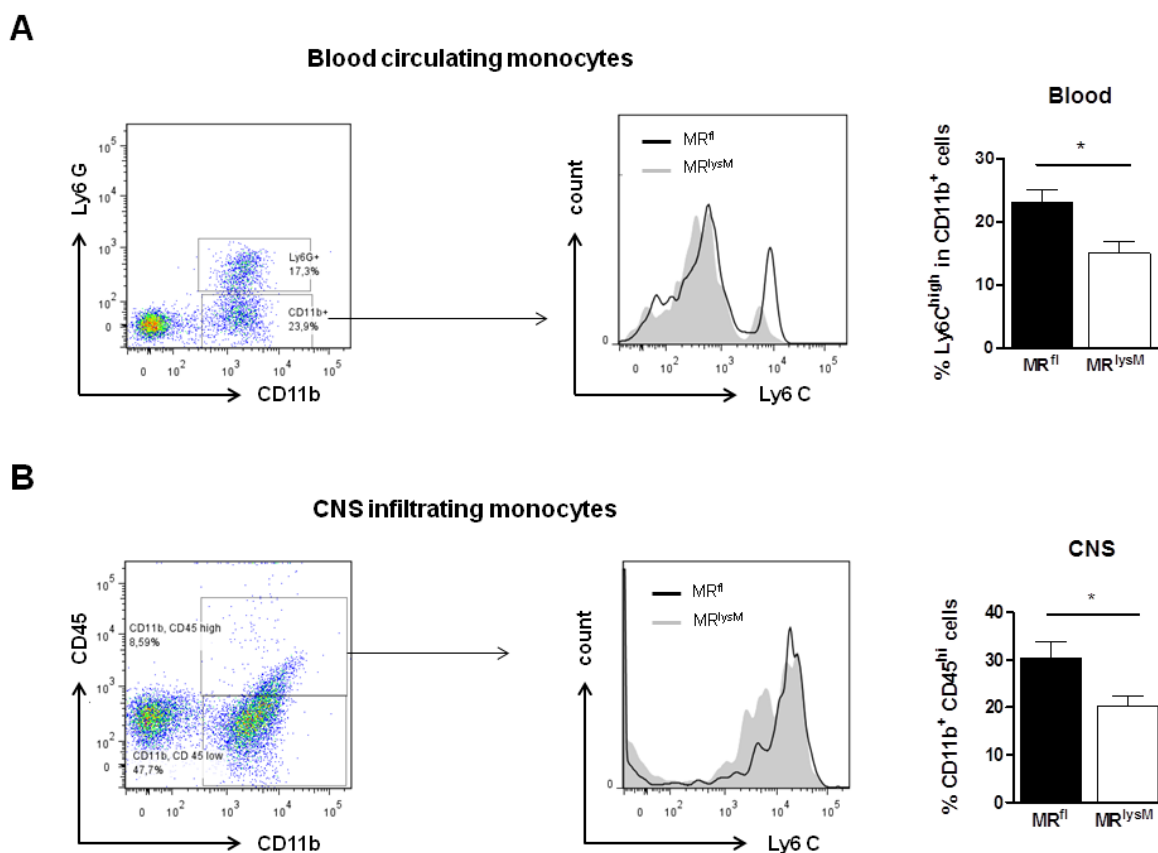
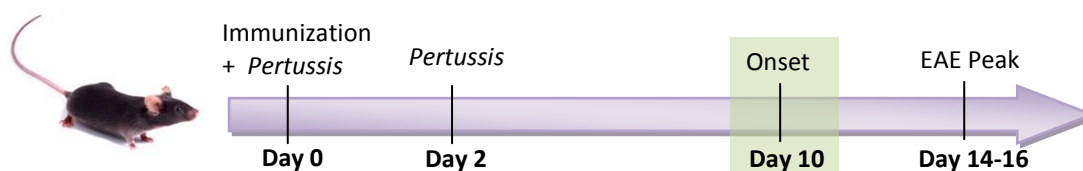


**Figure 3.18 | The percentage of inflammatory monocytes in blood and spinal cord of  $MR^{lysm}$  mice is reduced during EAE.** EAE was induced according to our standard protocol (see 2.3.1) in  $MR^{fl}$  and  $MR^{lysm}$  mice. **(A)** At day 10 after immunization, the mice were sacrificed and blood was collected in Alsevers solution to avoid clotting (n=6,4). The cells were stained with Abs against CD11b, Ly6C and Ly6G, treated with Optilyse to remove erythrocytes and analyzed 2 h later by FACS. Inflammatory monocytes were defined according to the systematic of Perlmann and colleagues (Rose et al. 2012).  $Ly6G^+$  cells were excluded from the  $CD11b^+$  population, and then inflammatory monocytes were distinguished from resting monocytes based on their higher Ly6C expression. **(B)** Spinal cords from the mice with ongoing EAE were obtained at the peak of the disease (day 14-16), and homogenized to separate mononuclear cells on a Percoll gradient (n=16,15). The cells were stained with Abs against CD11b and CD45.2 to differentiate monocytes/macrophages from microglia (Prinz et al. 2011). Subsequently, the monocytes were subdivided into inflammatory and resting ones on the basis of the Ly6C expression levels. **(C)** The quantification of the data was performed with GraphPad Prism. Values were analyzed using the unpaired Student's t-test and are depicted as mean  $\pm$  SEM; \*,  $p < 0.05$ .

### 3.2.3 Monocytes and neutrophils in secondary lymphoid organs are not affected by the MR deletion

Up to this point, we have found that the MR deletion affected circulating monocytes and infiltrating monocyte/macrophages during EAE. However we had no information about the activated state of macrophages in peripheral lymphoid organs, where they fulfill an important task shaping the environment for T cell priming and differentiation. Therefore, using the same FACS gating strategy as for blood samples (**Figure 3.18 A**), monocyte activation was analyzed in the spleen and the lymph nodes of MR<sup>lysM</sup> mice at disease onset. In these organs we could not find changes between knock-out and control mice in the proportion of Ly6C<sup>high</sup> monocytes (**Figure 3.19 A**).

It has to be taken into account that in MR<sup>lysM</sup> mice the cre recombinase does not only delete floxed genes in 83-98% of macrophages, but also in nearly 100% of neutrophils (Clausen et al. 1999). Neutrophils are a major component of the spinal cord infiltrates in C57BL/6 mice, especially in the early phases of the disease (Soulika et al. 2009; Wu et al. 2010). Hence, to exclude any potential alterations in this cell compartment, the proportion of CD11b<sup>+</sup> cells expressing Ly6G was determined in immunized mice at the onset of the disease. The FACS data revealed that the number of Ly6G<sup>+</sup> cells was similar for both genotypes (**Figure 3.19 B**). We therefore believe that it is very unlikely that neutrophils contribute to the EAE phenotype observed in MR<sup>lysM</sup> mice.





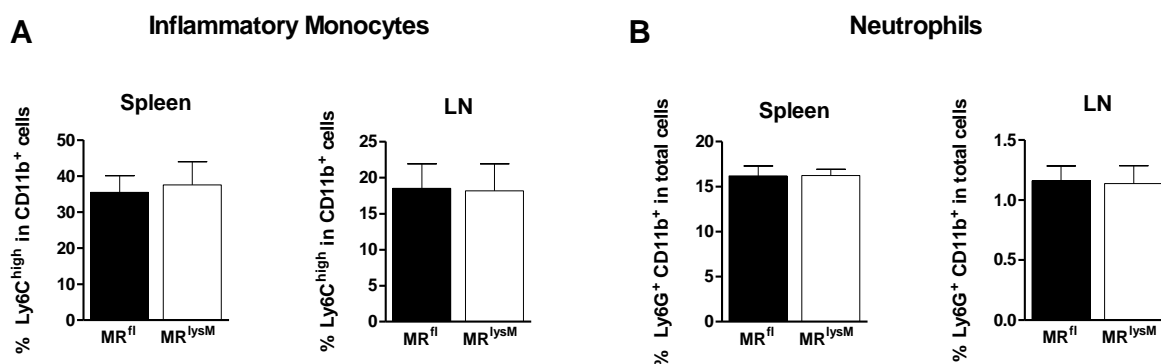


**Figure 3.19 | Inflammatory monocytes and neutrophils are unaffected in secondary lymphoid organs of MR<sup>lysM</sup> mice during EAE.** Spleens and lymph nodes from MR<sup>fl</sup> (n=9) and MR<sup>lysM</sup> (n=7) mice were analyzed at day 10 after EAE induction (see 2.3.1). Single-cell suspensions were obtained and stained with monoclonal Abs against CD11b, Ly6G and Ly6C. The percentages of CD11b<sup>+</sup> Ly6C<sup>high</sup> cells, corresponding to inflammatory monocytes **(A)**, and CD11b<sup>+</sup>/ Ly6G<sup>+</sup> cells, corresponding to neutrophils **(B)**, were determined by FACS. Values were analyzed using the unpaired Student's t-test and are depicted as mean ± SEM.

### 3.2.4 T cell interactions with MR<sup>lysM</sup> macrophages

It is generally accepted that MS and EAE are T cell-driven diseases. In the MR<sup>lysM</sup> mouse model T cells neither express Cre nor the MR, thus there should not be any direct effect of the MR deficiency on T cells. Nevertheless, macrophages present antigens and secrete cytokines that influence T cell differentiation, participating both in the activation of T cells in the periphery and their re-activation in the CNS. Therefore, MR deletion from myeloid cells might impact EAE indirectly via this mechanism as well. To test this hypothesis the interaction between T cells and MR<sup>lysM</sup> myeloid cells was investigated.

### 3.2.4.1 The cytokine secretion profile is altered in MR-deficient BMDMs

Soluble factors released by macrophages strongly influence T cell differentiation. Hence, we analyzed selected cytokines secreted by BMDMs obtained from MR<sup>fl</sup> and MR<sup>lysM</sup> mice. Following stimulation with IFN $\gamma$  and LPS, the cytokine profile of the activated MR<sup>lysM</sup> BMDMs was shifted towards the M2 phenotype (**Figure 3.20**). More specifically, mutant BMDMs secreted less TNF $\alpha$  and IL-6, considered to be pro-inflammatory, but higher amounts of the regulatory cytokine IL-10. In the absence of IFN $\gamma$ /LPS stimulation, all three cytokines were barely detectable in the supernatant (data not shown).

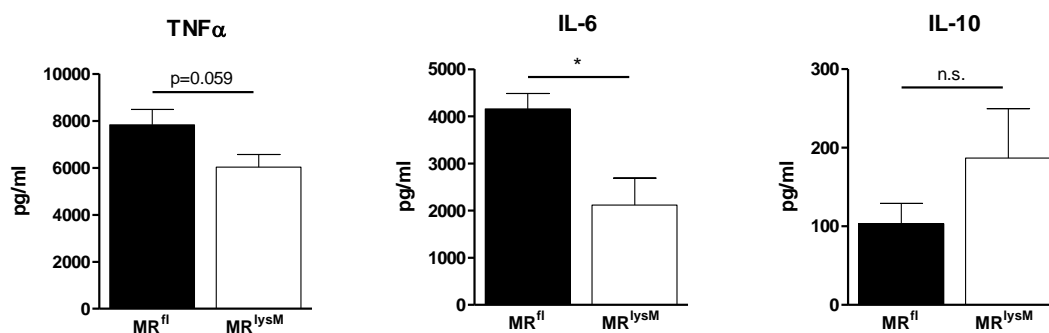


**Figure 3.20 | MR-deficient BMDMs secrete less M1 cytokines, whereas M2 cytokine release is increased.** BMDMs were generated from MR<sup>fl</sup> (n=6) and MR<sup>lysM</sup> (n=6) mice and seeded in 96-well plates at a concentration of  $1 \cdot 10^5$  cells/well. Then, they were stimulated for 24 h with 20 ng/ml LPS and 50 ng/ml IFN $\gamma$ . The concentration of TNF $\alpha$ , IL-6 and IL-10 in the supernatant was determined by CBA. Values were analyzed using the unpaired Student's t-test and are depicted as mean  $\pm$  SEM; n.s.,  $p \geq 0.05$ ; \*,  $p < 0.05$ .

### 3.2.4.1 MR<sup>lysM</sup> macrophages are potent APCs *in vitro*

It is known that macrophages can act as APCs in different situations. Since the phenotypic changes observed in the MR-deficient BMDMs might alter their capacity to present antigens to T cells and to activate them, this feature was evaluated *in vitro*. MR<sup>fl</sup> and MR<sup>lysM</sup> BMDMs were co-cultured with 2D2 T cells in the presence of MOG<sub>35-55</sub> and the proliferation rate of the T cells was determined by FACS. BMDMs efficiently stimulated T cell proliferation regardless of the genotype (**Figure 3.21 B**).

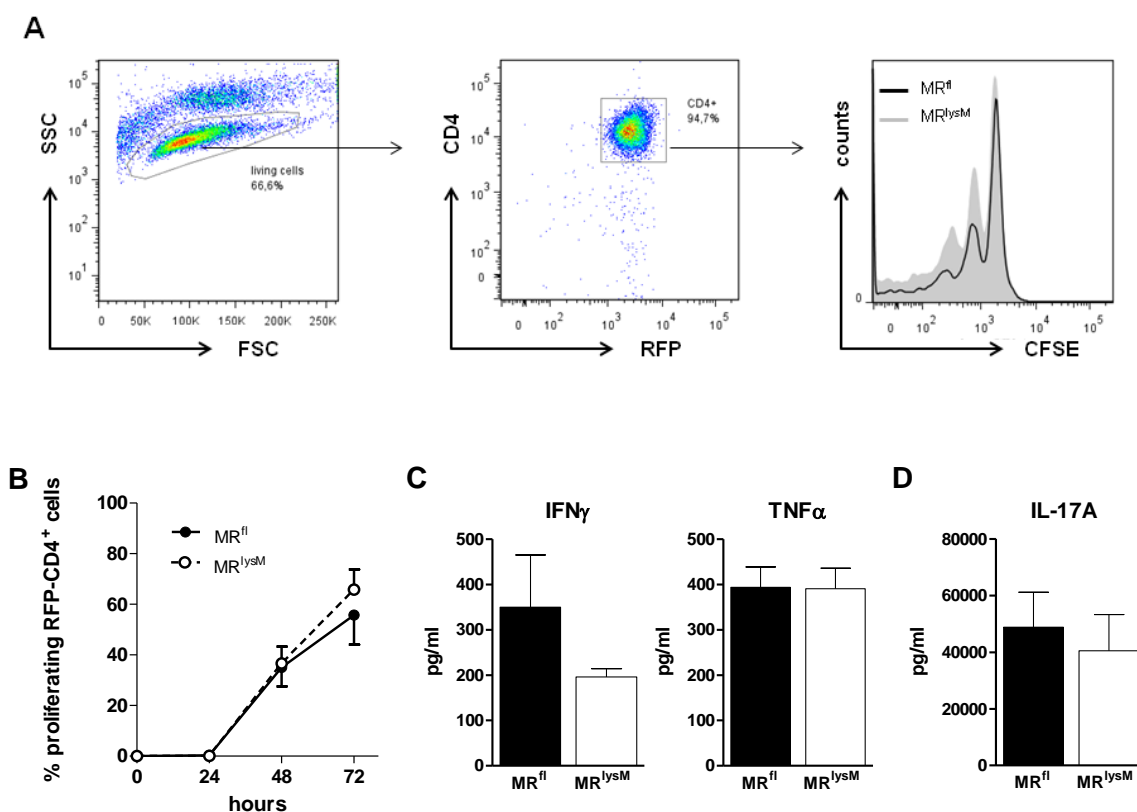


**Figure 3.21 | MR<sup>lysM</sup> BMDMs stimulate MOG<sub>35-55</sub>-specific stimulation of 2D2 T cell proliferation *in vitro*.** BMDMs were generated from MR<sup>fl</sup> (n=6) and MR<sup>lysM</sup> (n=6) mice. **(A,B)** 1·10<sup>5</sup> BMDMs/well were plated in triplicates and the same numbers of CFSE-labeled T cells purified from 2D2 RFP mice were added together with 20 μg/ml MOG<sub>35-55</sub>. Non-adherent cells were collected after 24 h, 48 h and 72 h, stained with an anti-CD4 Ab and analyzed by FACS. Cell proliferation was determined based on the sequential dilution of the CFSE staining after gating on the CD4<sup>+</sup> RFP<sup>+</sup> cell population. **(C)** After 72 h, the supernatants were collected and analyzed by CBA to determine the levels of selected cytokines. **(D)** 1·10<sup>5</sup> BMDMs generated from the bone marrow of MR<sup>fl</sup> (n=11) and MR<sup>lysM</sup> (n=11) mice were plated in 96 well plates and 1·10<sup>5</sup> Th17 2D2 cells (*kindly provided by Judith Strauß, IMSF Göttingen*) were added to the cultures. 72 h later the supernatants were collected and IL-17A concentrations were determined by ELISA. Values were analyzed using the unpaired Student's t-test and are depicted as mean ± SEM.

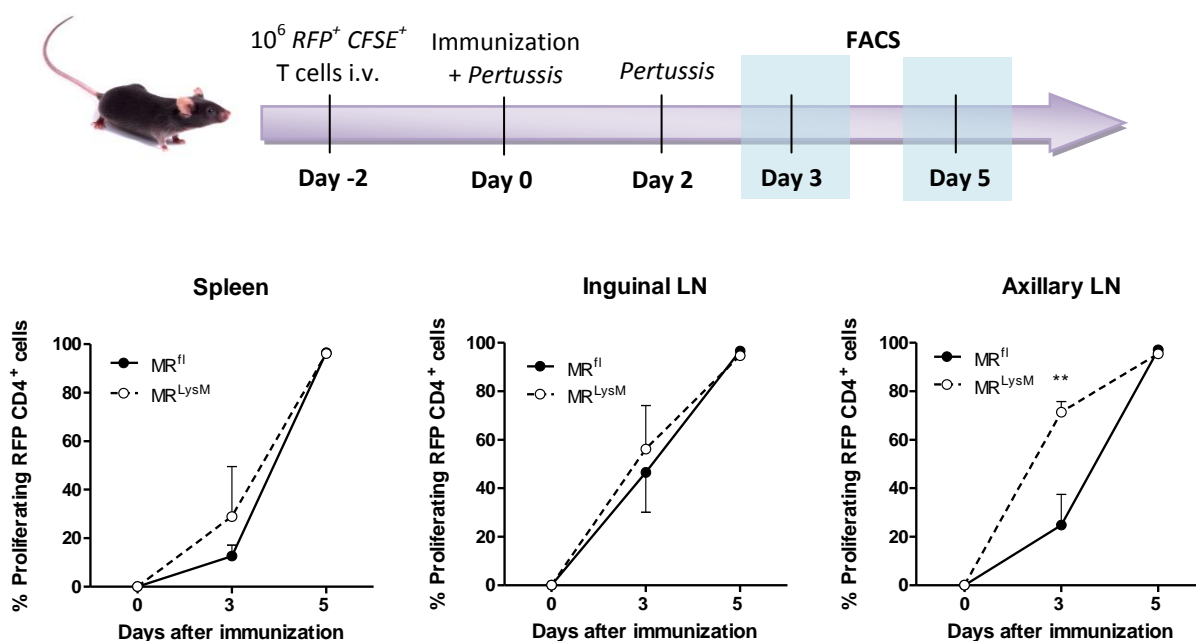
Since the changes in the cytokines produced by the MR<sup>lysM</sup> BMDMs might have an effect on T cell activation, the cytokine secretion of different BMDM/2D2 T cell co-cultures was additionally analyzed by CBA. IFN<sub>γ</sub> release was slightly lower when MR-deficient BMDMs

were used, whereas TNF $\alpha$  secretion was similar in both genotypes (**Figure 3.21 C**). IL-17A was hardly detected in the culture medium, therefore we chose another experimental setting to analyze this cytokine. Th17 polarized 2D2 effector T cells were co-cultured with BMDMs from the MR<sup>lysM</sup> and MR<sup>fl</sup> to test whether IL-17 levels were altered after re-stimulation with MOG<sub>35-55</sub>. In this setting, IL-17 production induced by MR-deficient BMDMs was comparable to the control situation (**Figure 3.21 D**).

### 3.2.5 The role of T cells in the pathogenesis of EAE in MR<sup>lysM</sup> mice

#### 3.2.5.1 MR-deficiency does not impair MOG-specific T cell priming *in vivo*

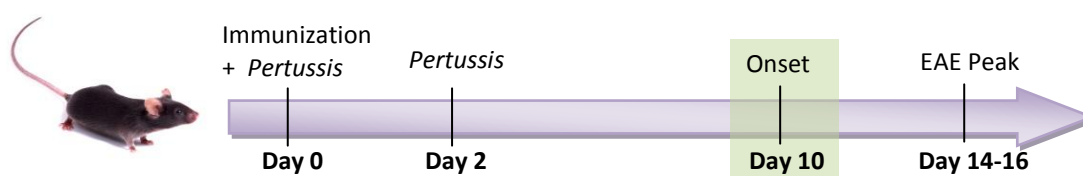
Having tested T cell priming by MR<sup>lysM</sup> macrophages *in vitro* we took a closer look at the *in vivo* situation and analyzed the priming of adoptively transferred 2D2 T cells in MR<sup>lysM</sup> mice after immunization. In line with the *in vitro* experiments, no major changes in T cell proliferation were observed in the spleen and the inguinal lymph nodes, although, for unknown reasons, T cells proliferated somewhat faster in the axillary lymph nodes of the mutant mice compared to the MR<sup>fl</sup> littermates (**Figure 3.22**).



**Figure 3.22 | T cell priming in MR<sup>lysM</sup> mice in the early phases of EAE is unaffected.** MOG-specific T cells were purified from RFP<sup>+</sup> 2D2 mice and subsequently labeled with CFSE.  $1 \cdot 10^6$  of these T cells were i.v. injected into MR<sup>fl</sup> (n=3) and MR<sup>lysM</sup> (n=3) mice. Two days later EAE was induced by active immunization with MOG<sub>35-55</sub>. 3 and 5 days after immunization, spleens, draining (inguinal) lymph nodes and non-draining (axillary) lymph nodes were analyzed by FACS to determine the proliferation rate of the injected RFP<sup>+</sup> 2D2 T cells. Values were analyzed using the unpaired Student's t-test and are depicted as mean  $\pm$  SEM; \*\*, p < 0.01.

### 3.2.5.2 Secretion of Th1 and Th17 cytokines during EAE is impaired in MR<sup>lysM</sup> mice

Up to this point it appeared that T cell priming and migration to the CNS were not relevant for the attenuation of EAE in MR<sup>lysM</sup> mice. However, MR-deficiency in myeloid cells might alter the phenotype of effector T cells. Therefore, the capacity of antigen-specific peripheral T cells to produce pro-inflammatory cytokines was studied. Total splenocytes and lymph node cells from immunized mice were isolated briefly before the onset of EAE and re-stimulated with MOG<sub>35-55</sub> *in vitro*. Subsequently, secretion of Th1 and Th17 cytokines was determined by ELISA as a measure of T cell effector functions. The results showed that antigen-specific effector T cells from MR<sup>lysM</sup> did not secrete pro-inflammatory cytokines as efficiently as the ones from MR<sup>fl</sup> mice. Importantly, secretion was impaired for IL-17A, IFN $\gamma$ , TNF $\alpha$  and GM-CSF, the main pro-inflammatory cytokines involved in the pathogenesis of EAE (Figure 3.23).



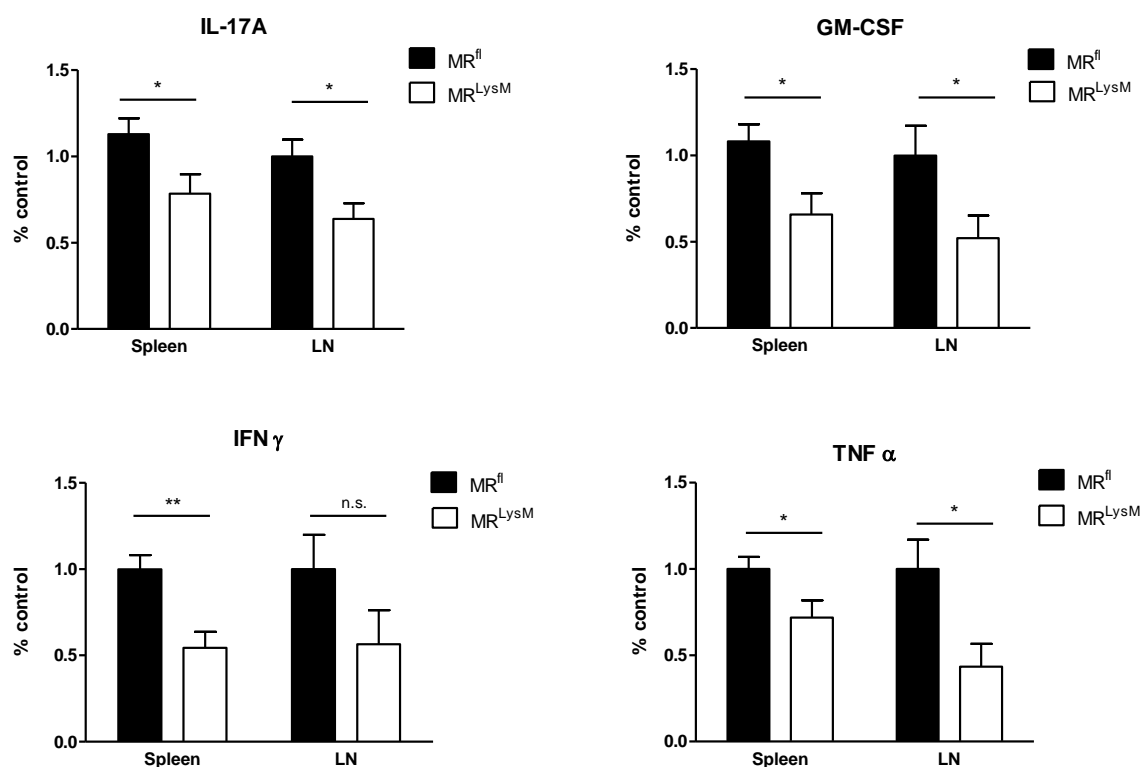


**Figure 3.23 | Secretion of pro-inflammatory cytokines by effector T cells is reduced in the secondary lymphoid organs of MR<sup>lysM</sup> mice before the onset of EAE.** MR<sup>fl</sup> and MR<sup>lysM</sup> mice were immunized with MOG<sub>35-55</sub> (see 2.3.1) and spleens and lymph nodes were removed at the onset of the disease (day 10 after immunization). Single cell suspensions were prepared and  $3 \cdot 10^5$  lymph node cells or  $6 \cdot 10^5$  splenocytes were re-stimulated *in vitro* by adding 20  $\mu\text{g}/\text{ml}$  of MOG<sub>35-55</sub> for 72 h (4 independent experiments). The supernatants were analyzed by ELISA to quantify the amounts of IL-17A (n=8,10), GM-CSF (n=9,9), IFN $\gamma$  (n=10,9) and TNF $\alpha$  (n=8,7). The mean value of the MR<sup>fl</sup> control group in each individual experiment was set to 1 and the values obtained from MR<sup>lysM</sup> mice were normalized to the controls. Values were analyzed using the unpaired Student's t test and are depicted as mean  $\pm$  SEM; (n.s.),  $p \geq 0.05$ ; \*,  $p < 0.05$ ; \*\*,  $p < 0.01$ .

### 3.2.5.3 MR deficiency in myeloid cells leads to increased numbers of peripheral Treg cells

Treg cells play an important role in the control of autoimmune responses such as EAE (Kohm et al. 2003), although their exact mechanisms have been a matter of debate for many years (Zhang et al. 2004; McGeachy et al. 2005; Tischner et al. 2006; O'Connor et al. 2007; Korn et al. 2007b). Furthermore, a close relationship between M2 macrophages and the increased

appearance of Treg cells in the context of CNS inflammation has been proposed (Keating et al. 2009; Zhang et al. 2009). Therefore, and in view of the reduced cytokine expression by peripheral encephalitogenic T cells, we decided to analyze the frequency of Treg cells in spleen and lymph nodes briefly before the onset of the disease. In line with the previously observed polarization of macrophages to the M2 phenotype, we also found higher numbers of Treg cells in the spleen and the lymph nodes of  $MR^{lySM}$  mice compared to  $MR^{fl}$  controls (**Figure 3.24 B**). This was true not only for immunized mice, but also for naïve ones, and reached significance in the spleen. In addition, the spinal cord was analyzed at the peak of the disease. However, in this case the frequency of Treg cells among all infiltrating  $CD4^+$  T cells was similar in  $MR^{fl}$  and  $MR^{lySM}$  mice (**Figure 3.24 C**).

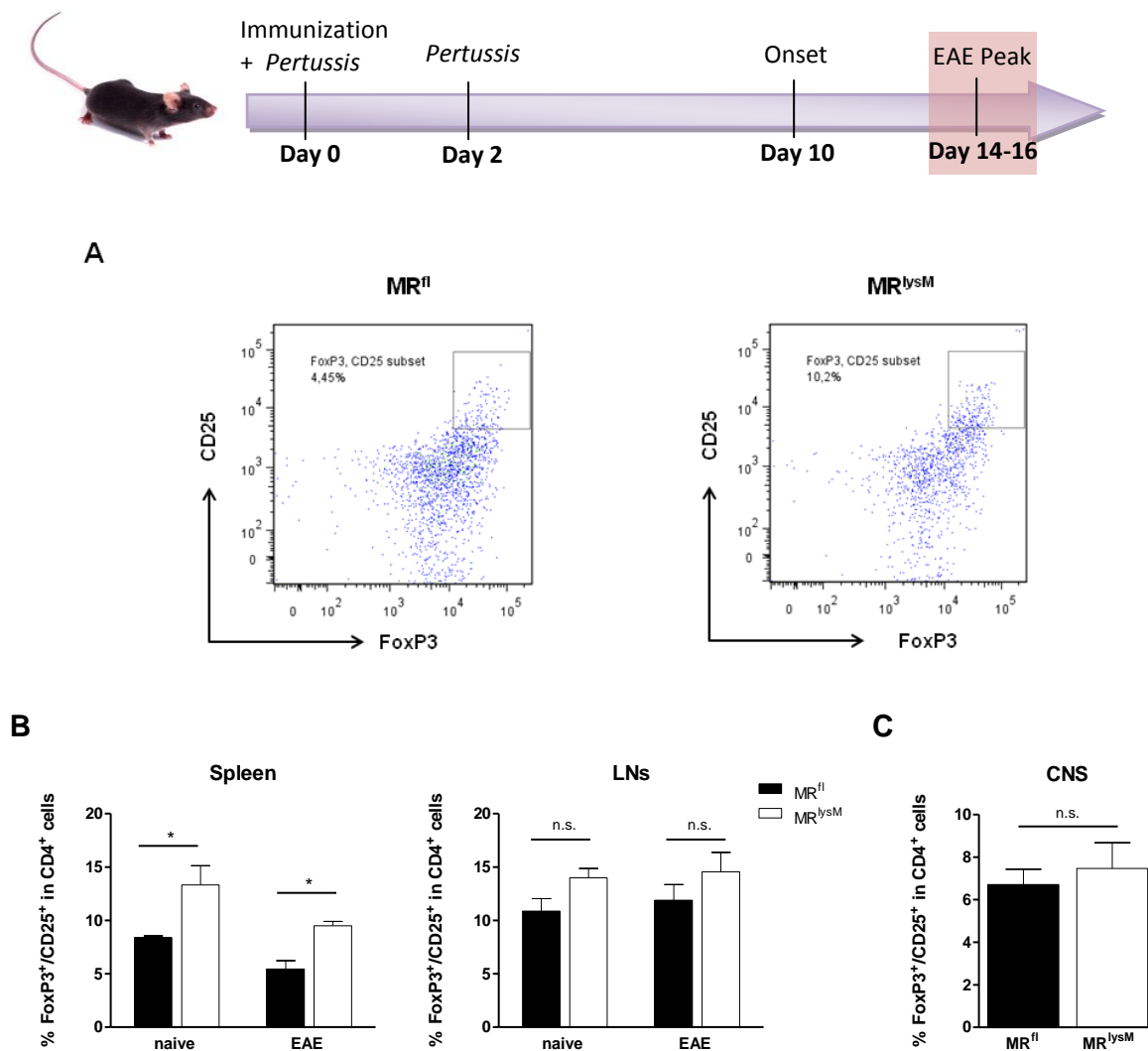


**Figure 3.24 | The frequency of Treg cells in peripheral lymphoid organs is increased in MR<sup>lysM</sup> mice.** (A,B) Single-cell suspensions from spleens and lymph nodes of MR<sup>fl</sup> and MR<sup>lysM</sup> mice were obtained either under healthy conditions (n=4, 4) or at day 10 after EAE induction (n= 3, 3). (C) To analyze the percentage of Treg cells in the CNS, spinal cords from MR<sup>fl</sup> (n=11) and MR<sup>lysM</sup> (n=12) mice at the peak of EAE were homogenized and mononuclear cells were separated via Percoll gradient. The cells were first stained with Abs against CD4 and CD25 and then permeabilized to allow access of the anti-FoxP3 Ab to its target antigen. Total living cells were first gated on the CD4<sup>+</sup> cell population, among which the CD25<sup>+</sup> FoxP3<sup>+</sup> cells were defined as Treg cells. Values were analyzed using the unpaired Student's t-test and are depicted as mean ± SEM; (n.s.), p ≥ 0.05; \*, p <0.05.

Taken together, the M2 polarized macrophages in MR<sup>lysM</sup> mice appear to foster the generation of Treg cells in peripheral lymphoid organs. These cells act locally rather than migrating to the spinal cord. Furthermore, MR-deficient myeloid cells within the CNS are also not able to induce Treg cells locally.

### 3.2.6 The phenotype of microglia during EAE is altered in MR<sup>lysM</sup> mice

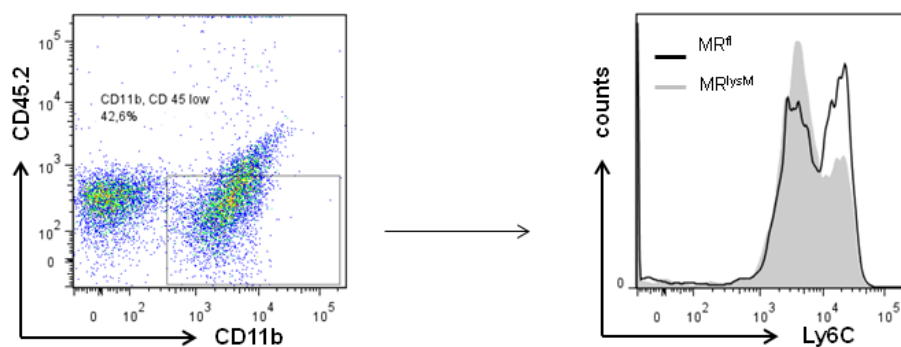
The myeloid compartment is composed of both circulating and resident cells, with the latter ones being mostly derived from common myeloid precursors that migrate to the different tissues during the early development. Within the CNS microglia represents the population of myeloid cells that are in charge of responding to inflammatory insults, and of surveillance and homeostasis in the absence of inflammation. Microglial cells share many features with peripheral resident macrophages, including their response to GCs. Several earlier *in vitro* studies revealed that GCs inhibit microglia proliferation (Ganter et al. 1992), NO production (Jun et al. 1994) and cytokine release (Chao et al. 1992). Moreover, microglia also expresses the GR as well as the MR, and it has been suggested that the two receptors might mediate opposite effects of GCs (Tanaka et al. 1997). It is noteworthy that previous studies had confirmed that LysM<sup>Cre</sup> transgenic mice were a suitable tool to disrupt genes in microglial cells (Schweingruber et al. 2011). Therefore, we aimed to investigate whether the deletion of the MR in microglia had any influence on their properties and whether these potential changes might contribute to the ameliorated disease in MR<sup>lysM</sup> mice.



Mononuclear cells were eluted from the spinal cord of  $MR^{lysM}$  and  $MR^{fl}$  mice at the peak of EAE and analyzed by FACS. The activation state of microglial cells, defined as  $CD11b^+CD45.2^{low}$ , can be distinguished by FACS analysis on the basis of Ly6C surface levels. The frequency of reactive microglia, characterized by higher Ly6C surface levels, was reduced in MR-deficient animals as compared to controls (**Figure 3.25 B**). This indicates that the activation of microglial cells was impaired in the absence of the MR, which might contribute to the amelioration of the disease in the mutant mice.



A



B

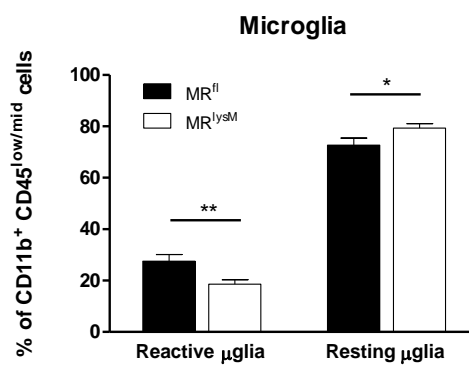


**Figure 3.25 | The frequency of reactive microglia in the spinal cord of MR<sup>lysM</sup> mice is reduced.** Spinal cords from MR<sup>fl</sup> (n=20) and MR<sup>lysM</sup> (n=21) mice were removed at the peak of EAE, homogenized and the mononuclear cells were separated using a Percoll gradient. The cells were incubated with Abs against CD11b, CD45.2 and Ly6C and analyzed by FACS. Following the gating strategy published by Prinz et al., microglial cells were distinguished from infiltrating myeloid cells by their lower expression levels of CD45.2, and reactive microglial cells were identified by their high Ly6C expression levels. Values were analyzed using the unpaired Student's t-test and are depicted as mean  $\pm$  SEM; \*, p <0.05; \*\*, p <0.01.

## 4 DISCUSSION

### 4.1 EAE therapy with betamethasone nanoparticles

The popularity of nanoparticles for diagnostic and therapeutic applications is gaining ground over the years, and this is reflected by the increasing number of publications dealing with this topic. In MS research, the use of nanoparticles has several advantages compared to conventional methods. Magnetic nanoparticles improve the contrast and the image resolution in MRI studies, and allow the tracking of phagocytic cells in the affected brain areas of rats suffering from EAE (Merodio et al. 2000; Rausch et al. 2004; Mikita et al. 2011; Hunger et al. 2014). Furthermore, the benefits of nanocarriers for the delivery of therapeutic drugs have also been studied. For instance, encapsulation in PEG-liposomes increases the circulation time of the contained drug and promotes accumulation in inflamed target organs. An increased brain bioavailability of the antioxidant tempamine was reported in mice suffering from EAE when they were treated with nanoliposomes (Kizelsztejn et al. 2009). Moreover, since phagocytic immune cells engulfing the nanoparticles function as APCs, different nano-carriers have been tested to deliver tolerogenic peptides together with adjuvant molecules to establish T cell tolerance (Büyüktimkin et al. 2012; Yuan et al. 2014; Hunter et al. 2014b). In this project, we exploited the advantages of these delivery systems to improve the properties of GCs. Liposomal formulations of GCs have already been used before in different animal models of autoimmunity with promising results (Metselaar et al. 2003; Schmidt et al. 2003; Linker et al. 2008; Schweingruber et al. 2011). However, this doctoral thesis evaluates for the first time the therapeutic potential of an innovative nanomaterial which combines inorganic carrier molecules with the therapeutic organic compound in its crystallized structure (Heck et al. 2015). The *in vitro* and *in vivo* experiments presented here showed that the used IOH-NPs, composed of ZrO<sub>2</sub> and BMZ-phosphate, efficiently delivered the GC resulting in the consequent immunomodulation. Moreover, the present study revealed that myeloid cells were specific targets during the treatment of EAE.

#### 4.1.1 BNPs are anti-inflammatory in different immune cell types, albeit with different efficacy

Among the plethora of effects that GCs exert on the immune system (see 1.3.2), induction of T cell apoptosis and alternative polarization of macrophages are well characterized and have been proposed as mechanisms involved in the immunomodulation by GCs (Tuckermann et al. 2005; Varga et al. 2008). Therefore, these two cellular events were analyzed and served as parameters to assess the efficacy of the BNPs. Previous unpublished data of our group indicated that, when used at similar concentrations as Dex *in vitro*, the effect of BNPs was comparable to the free GC. Both GC formulations led to a similar reduction of pro-inflammatory molecules in macrophages, and induced T cell apoptosis to the same extent. With the present study I corroborated these results and additionally confirmed that these effects were mediated by the GR, as shown by the abrogation of GC modulation in the absence of the receptor (**Figure 3.5**). Furthermore, the consequences of nanoparticle administration *in vivo* were evaluated. 10 mg/kg of i.p.-injected BNPs decreased the expression of MHC class II and the co-stimulatory molecule CD86 on the surface of macrophages isolated from the peritoneum. Moreover, these macrophages were not able to respond to LPS/INF $\gamma$  stimulation to the same extent as macrophages from mice receiving only vehicle (**Figure 3.2**). In line with the *in vitro* experiments, the phenotype of peritoneal macrophages isolated from mice receiving BNPs did not differ from the one of mice treated with free Dex. However, the analysis of T cell apoptosis *in vivo* revealed differences between both treatments. While Dex efficiently reduced T cell numbers already 24 h after injection, BNPs barely affected T cell survival 72 h later (**Figure 3.3**). This was a first sign of the specificity of the nanoparticles, the efficacy of which appeared to change depending on the cell type *in vivo* but not *in vitro*. This is not surprising considering that, due to their size between 40-90 nm, BNPs are expected to be pinocytosed by macrophages and inflammatory monocytes rather than by T cells (Weissleder et al. 2014). Evidence for this is provided by the fact that in cell cultures of splenocytes, lymph node cells or peritoneal lavages, CD11b<sup>+</sup> cells appeared to incorporate higher amounts of BNPs than T cells or B cells (**Figure 3.1**). In line with this finding, previous data from our group had revealed that the pro-apoptotic effect of the BNPs on T cells *in vitro* is attenuated at lower BNP concentrations, a tendency that was

not observed with free GCs. This indicates that at high drug concentrations various immune cells are potentially targeted by the BNPs, but at reduced dosage the different cell types compete for the uptake of the nanoparticles, and in that case myeloid cells are the preferred target of BNPs.

#### **4.1.2 Myeloid cells are major targets of BNPs in EAE therapy**

Our group and others had already demonstrated that nanoformulations such as liposomes are suitable vehicles to treat autoimmune diseases with GCs (Metselaar et al. 2003; Schmidt et al. 2003; Linker et al. 2008; Schweingruber et al. 2011). Schweingruber and colleagues showed that liposomes loaded with prednisolone (PL) are more potent than free GCs in reducing paralysis symptoms in mice with EAE, even at a reduced dosage and application frequency (Schweingruber et al. 2011). In the present study, BNP i.p. injection on three consecutive days during disease onset had a significant and sustained effect on EAE progression, diminishing the clinical score by at least 3 points in a scale from 1 to 10 (**Figure 3.6**). Titration of BNPs in subsequent EAE experiments showed that this therapeutic effect was concentration-dependent. Furthermore, when different GCs were applied in parallel, the efficacy of the BNPs was comparable to Dex and BMZ. However, in contrast to PL, BNPs did not appear to have a superior potency. This differential effect between the two nano-compounds is surprising considering that BMZ is almost six times more potent than prednisolone when tested as a free GC (Van Rensburg 2011). Thus, the mechanisms of action employed by liposomes and ZrO<sub>2</sub> nanoparticles might not be the same. Regarding the effect of the inorganic structure of the particles, ENPs neither improved nor worsened the EAE symptoms of the mice, which indicates that BNP therapy is well tolerated, at least in this disease model.

Mirroring MS, demyelination and massive leukocyte infiltration into the spinal cord are major histopathological hallmarks of chronic progressive EAE in C57BL/6 mice (Berard et al. 2010). It is known that GC therapies hamper the entry of immune cells into the CNS via restoration of the BBB (Rosenberg et al. 1996; Pitzalis et al. 2002), re-direction of T cells

(Fischer et al. 2013) and induction of apoptosis in diverse immune cell subsets (Leussink et al. 2001; Tuckermann et al. 2005). The reduced number of immune infiltrates, in combination with the M2-polarizing effect of GCs on both CNS resident and migrating myeloid cells, helps improving the demyelinating pathology. The present study shows that BNP treatment prevented demyelination to some extent and significantly reduced monocyte/macrophage infiltration into the CNS (**Figure 3.7, Figure 3.8**). However, T cell numbers within the spinal cord were unaffected. The decrease in T cell infiltrates after Dex treatment has been reported in the past (Schweingruber et al. 2014), hence our histological data indicates once again that BNPs might not act efficiently on T cells when applied *in vivo*.

It was previously shown in this work that the anti-inflammatory effects of the BNPs required the GR both *in vitro* and *in vivo* (**Figure 3.4, Figure 3.5**). Thus, to elucidate the cellular target of the BNPs in the treatment of EAE, different cell type-specific GR knock-out mice strains were employed. GR<sup>lck</sup> mice, devoid of the GR in T cells, responded to the BNP therapy similarly to GR<sup>fl</sup> controls (**Figure 3.9 A**). In other words, the presence of the GR in T cells was dispensable for the treatment, and therefore this cell type is probably not the major target of the BNPs. The same was the case for GR<sup>SLO1C1</sup> mice, where the GR is absent in endothelial cells of the BBB (**Figure 3.9 D**). It is worth to mention that Dex application in those mice led to similar results as BNP treatment (data not shown). This suggests that the well-known protective role of GCs regarding BBB integrity (Paul and Bolton 1995; Engelhardt 2000) might not be essential for their therapeutic effect during EAE, but rather an indirect consequence of the therapy (as already postulated in Wüst et al. 2008). The third genotype tested was the GR<sup>lysM</sup> mouse strain, where the Cre-mediated excision of the GR affects only myeloid cells. In contrast to the other studied genotypes, these mice were completely refractory to the BNP therapy and presented with a disease progression identical to mutant mice receiving only vehicle (**Figure 3.9 B**). In view of these data, it can be stated that myeloid cells are preferred targets of the BNPs in the treatment of EAE.

Since T cells are known to be major mediators of conventional GCs during EAE (Wüst et al. 2008; Fischer et al. 2013; Schweingruber et al. 2014), we can also conclude from our experiments that BNPs employ a different route of action than free GCs. This change in cell

specificity had already been observed by Schweingruber and colleagues using PL, the liposomal formulation of GCs (Schweingruber et al. 2011). However, PL treatment in GR<sup>lysM</sup> mice led to a mild therapeutic effect, meaning that, in contrast to BNPs, PL had a residual effect in other cell types besides myeloid cells. Considering the undesirable consequences of GCs' off-target effects, the tighter specificity of BNPs might represent an advantage of IOH-NPs over liposomes.

#### **4.1.3 Are BNPs a potential solution to GC-derived side effects?**

Short-time high-dose GCs are a mainstay for the treatment of acute relapses of MS, but whether a sustained GC treatment would decrease the relapse rate or prevent the worsening of brain lesions remains controversial (Zivadinov et al. 2001; Then Bergh et al. 2006; Sorensen et al. 2009; Ravnborg et al. 2010; Ciriaco et al. 2013). The promising therapeutic potential of this approach claims for more clinical studies, but the broad spectrum of GC-associated side effects is an important limiting factor for the use of prolonged high dose pulsed GCs (Moghadam-Kia and Werth 2010; Weinstein 2012; Ciriaco et al. 2013; Hunter et al. 2014; Hwang and Weiss 2014). Responsible for these side effects is the fact that the GR is ubiquitously expressed (Rhen and Cidlowski 2005), and therefore GCs modulate not just immune responses, but also salt-water homeostasis, glucose metabolism, bone re-adsorption and mood variations, among others. In order to circumvent these consequences of GCs several strategies have been tested, for instance dissociating ligands that act only via the trans-repressing mechanism of the GR (Wüst et al. 2009). However, none of these compounds could be translated into a successful therapy with clinical use so far. In this doctoral thesis we propose the targeting of GC therapy to the myeloid cell compartment as a means to solve this issue.

As a first approach, the occurrence of side effects was analyzed in the context of the experimental protocol used for the EAE experiments, consisting in short-time daily i.p. injection of a moderate dose of GCs (10 mg/kg). A small increase in fasting glucose levels was observed in both Dex- and BNP-treated animals compared to their respective controls,

although this increase was not significant (**Figure 3.11 A**). Furthermore, a marked induction of hepatic enzymes involved in gluconeogenesis was observed shortly after Dex or BNP injection (**Figure 3.11 C**), indicating that both Dex and BNPs act similarly on hepatocytes increasing the production of glucose. However, it could also be expected that Kupfer cells, the phagocytic liver-resident macrophages, incorporated a considerable proportion of the injected nanoparticles. Then, hypothetically, BMZ loaded in the BNPs might polarize Kupfer cells to a M2-like state, reported to prevent insulin resistance (Odegaard et al. 2008; Huang et al. 2010), thereby counteracting the elevated blood glucose levels. This and other possible compensatory mechanism should be evaluated in the future with different experimental conditions. Similarly to the results observed regarding glucose levels, no considerable changes in stomach weight occurred (**Figure 3.13**). For the analysis of GC-derived osteoporosis, serum levels of the hormone osteocalcin were measured. Osteocalcin is a promising cognate marker, since it is strongly reduced shortly after GC application and has been shown to be a link between GC-induced bone remodeling and energy metabolism (Brennan-Speranza and Conigrave 2015). However, no differences in osteocalcin were found in the serum of mice treated with Dex or BNPs (**Figure 3.14**). The last side effect analyzed was muscle wasting. We found that mice receiving Dex presented with a slightly reduced muscle weight, whereas in the BNP-treated ones the difference was hardly perceptible (**Figure 3.12**). In any case, none of those values were statistically significant, and probably a longer duration of the GC treatment will be needed to identify changes in muscle mass.

Collectively, the analysis of short-term BNPs side effects did not provide clear information, since not even the free GC induced significant changes in the studied parameters. Published data from our group and others showed strong metabolic effects derived from prolonged Dex treatment (Waddell et al. 2008; Reichardt et al. 2014). Therefore further experiments will be performed with longer GC exposure periods or higher concentrations. Only applying this alternative protocol we will be able to determine whether BNPs are better tolerated than conventional GC therapies.



#### 4.1.4 BNP therapy: open questions and perspectives

The data presented here show that BNPs, in spite of modulating both macrophage phenotype and T cell responses *in vitro*, specifically target the myeloid compartment *in vivo*. This targeted delivery of GCs opens the path to new therapeutic options. One alternative that was tested in this thesis was the combination of free GCs and BNPs in order to obtain an additive effect of both T cell suppression and macrophage M2 polarization. Indeed, the administration of suboptimal doses of Dex and BNPs together showed a superior potency in the treatment of EAE than the same amounts of the individual drugs alone (**Figure 3.10**). Hence, combined therapy with BNPs and free GCs might increase the therapeutic efficacy of the drug allowing the use of reduced dosage, with the consequent advantages regarding side effects and patient compliance.

An important factor for the therapeutic success of the nanoparticles is their biodistribution. Generally, particles with a size of 10-100 nm tend to accumulate in organs where macrophages are present, like spleen, liver, lymph nodes and bone marrow (Weissleder et al. 2014). Moreover, the delivery route via inflammatory monocytes should lead to higher concentrations of the drug at the site of inflammation, meaning that the use of BNPs may achieve not only cell type-specificity, but also direct targeting of the damaged tissue. Evidence of this phenomenon was provided by Metselaar and colleagues, who showed that rats receiving PL recovered from adjuvant-induced experimental arthritis (AIA) thanks to delivery of the GC in the inflamed joint (Metselaar et al. 2003). Also Merodio and colleagues observed CNS localization of albumin nanoparticles in a rat model of EAE, and suggested that macrophages and microglia were involved in this distribution (Merodio et al. 2000). Unfortunately, we were not able to determine whether BNPs specifically targeted the injured spinal cord in the treatment of EAE. The presence of the fluorescent molecule FMN in the BNPs allowed their identification by FACS in different cell subsets in culture, however the attempts to track the particles in different organs after i.p. injection were unsuccessful. Noteworthy, *in vivo* analyses by intra-vital 2-PM after either i.v. or stereotactic injection could not trace the BNPs, meaning that at tolerable doses for the mice the FMN signal of the nanoparticles does not reach the limit of detection. Since ZrO<sub>2</sub> has already been coupled to other fluorescent compounds for cell imaging in the past (Heck et al. 2015), the

biodistribution of the BNPs could be elucidated by means of those alternative nanoparticles in the future.

Questions regarding the BNPs' pharmacokinetics and pharmacodynamics are also important for the success of the therapy. Until now it is unknown whether BNPs bind to albumin or other proteins in the blood, or how long they remain in the circulation before they are cleared from the organism. Something else to take into account is whether the nanoparticles are leaky and release the drug before reaching their target. In the present study, the inefficacy of the BNP treatment in the GR<sup>lysM</sup> knock-out mice indicates that, if there was some hypothetical circulating free BMZ, the amount was so low that no therapeutic effect derived from it. With regard to their behavior intracellularly, it is known that medium size nanoparticles, like BNPs, are taken up via micro-/macro-pinocytosis (Weissleder et al. 2014). In theory, the drug would become active in the cytoplasm by enzymatic or spontaneous hydrolysis. However, how the remaining ZrO<sub>2</sub> is metabolized and/or excreted is still unknown, and potential toxic effects have to be evaluated. According to the results presented here, the apparent promotion of CD8<sup>+</sup> T cell proliferation induced by ENPs in splenocytes (**Figure 3.3**) suggests that the nanoparticles might not be completely innocuous. Several publications report that ZrO<sub>2</sub> particles are hemocompatible and well tolerated by HEK-293 cells and the macrophage cell line RAW-264.7. Moreover, they present low genotoxicity *in vitro* and after oral administration in larvae of *Drosophila melanogaster* (Demir et al. 2013; Karunakaran et al. 2013; Saxena et al. 2013). Nonetheless, other studies described a certain immunogenic potential, and showed that ZrO<sub>2</sub> may increase the expression of TNF $\alpha$ , IL-6 and IL-1 $\beta$  in macrophages (Obando-Pereda et al. 2014). The *in vitro* experiments on BMDMs and peritoneal macrophages included in this thesis are discrepant in that regard. However, previous data showed that in some cases IL-6 and IL-1 $\beta$  expression were slightly increased after ENP exposure in BMDMs (Ring, unpublished data). Hence, it is conceivable that the observed net anti-inflammatory potential of BNPs represents in fact a combination of an even stronger anti-inflammatory effect of BMZ and a mild pro-inflammatory effect of ZrO<sub>2</sub>. If this premise was true, it would also explain why BNPs are not as potent as PL in the treatment of EAE. After all, ENPs did not appear to affect EAE severity, which speaks in favor of the general biocompatibility of BNPs at therapeutic concentrations.

Actually, current studies with BNPs and other variants of IOH-NPs are showing promising results for the analysis and therapy of different autoimmune disorders, such as allergic asthma and acute Graft-versus-Host Disease (Markus et al. 2015; our unpublished data). We therefore believe that this delivery system has the potential to be a successful and better tolerated vehicle for drugs in the future.

## 4.2 The role of the MR in myeloid cells during EAE

The here presented results showing the attenuation of EAE by BNPs provide additional evidence that the different macrophage phenotypes play a crucial role in EAE and MS. But beyond treatment with synthetic GCs, there are other ways to bias macrophage polarization into a deactivating state. A distinctive feature of myeloid cells is that they co-express the GR and the MR, but not 11 $\beta$ -HSD II, a situation that allows GCs to access both nuclear receptors (Funder 1997). Interestingly, despite the structural similarities between the GR and the MR (Funder 1997), their activation by GCs has been shown to induce opposing polarization states on macrophages and microglia (Usher et al. 2010; Chantong et al. 2012). This is particularly important for the response to endogenous GCs in mice. Unlike cortisol (the human endogenous GC), corticosterone binds to the MR with 10-fold higher affinity than to the GR. *In vitro* studies showed that, due to this property, low concentrations of corticosterone had immunostimulatory effects via MR signaling, whereas increased amounts of this GC strongly reduced pro-inflammatory genes acting via the GR (Tanaka et al. 1997; Lim et al. 2007; Chantong et al. 2012). These observations suggest that at physiological GC concentrations a great part of the response of myeloid cells to GCs is mediated by the MR. Therefore, we wondered whether the absence of the MR would potentiate the anti-inflammatory effects of endogenous GCs via the GR. In the second part of this project the phenotype of mice with MR-deficient myeloid cells was studied in the context of CNS autoimmunity using a cell type-specific knock-out mouse strain, the MR<sup>lysM</sup> mice.

#### 4.2.1 MR deficiency in myeloid cells promotes M2-like polarization and causes a milder EAE phenotype

It is well known that classically activated macrophages contribute to EAE pathology by presenting myelin antigens to T cells (Almolda et al. 2011), secreting pro-inflammatory cytokines (Hendriks et al. 2004) and exerting direct neurotoxicity (Reynolds et al. 2007; Shijie et al. 2009). Other groups have also reported that an imbalance of the M1/M2 equilibrium has important consequences for EAE disease progression (Mikita et al. 2011). Therefore, we hypothesized that, since the MR promotes M1 polarization, the deletion of the MR from myeloid cells might alleviate clinical symptoms in mice with EAE. Indeed, when MR<sup>lysM</sup> mice were immunized with MOG<sub>35-55</sub> they developed a milder form of the disease compared to their littermate controls (**Figure 3.15**). In a rat model of relapsing EAE, Mikita and colleagues found that M2 macrophages accumulated in the CNS before relapse resolution, and that administration of *ex vivo* polarized M2 monocytes suppressed EAE symptoms (Mikita et al. 2011). Schweingruber and Li had previously shown that, at the peak of EAE, mononuclear cells isolated from the spinal cord of MR<sup>lysM</sup> mice express higher levels of typical M2-markers, mainly Arg-1, whereas the expression of the M1-gene iNOS is markedly down-regulated (Li 2013). In these mice, the constitutively increased proportion of M2-polarized macrophages, which results from the exclusive GR binding of endogenous corticosterone, appears to stop disease progression earlier than in wt mice, although it is not enough to completely abrogate EAE.

In line with the ameliorated EAE clinical course, the histopathological characteristics of MR<sup>lysM</sup> mice also differed from the ones of MR<sup>fl</sup> controls. Similarly to the above described effects of BNP treatment, spinal cord infiltration by CD3<sup>+</sup> T cells was comparable in both groups, whereas MAC3<sup>+</sup> infiltrates were significantly reduced in the knock-out mice (**Figure 3.16**). It is worth to mention that the nature of those MAC3<sup>+</sup> cells is hard to determine on the histological basis, since this surface marker is shared by infiltrating monocytes/macrophages, PVMs and activated microglia (Giulian and Baker 1986). The FACS analysis of spinal cord mononuclear cells corroborates that, at the peak of EAE, the proportion of reactive microglia is indeed reduced in MR<sup>lysM</sup> mice (**Figure 3.25**).

Furthermore, the percentage of inflammatory monocyte/macrophages infiltrating the spinal cord was reduced as well (**Figure 3.18**). However, with the current data we cannot definitively conclude that there was less macrophage infiltration into the spinal cord. It can only be stated that those myeloid cells within the CNS, which are pro-inflammatory in nature, were less frequent. In accordance with this phenotype, a significantly lower percentage of demyelination and partially preserved axonal density were observed (**Figure 3.17**). Previous data from Li showing decreased NO release and increased phagocytic capacity in MR<sup>lysM</sup> BMDMs support these results (Li 2013). NO has neurotoxic effects (Aboul-Enein et al. 2006; Zindler and Zipp 2010) and M2 macrophages and microglia are known to promote neuronal regeneration via clearance of myelin debris (Neumann et al. 2009). Therefore, a direct connection between the clinical course of EAE and the altered phenotype in the MR-deficient monocyte/macrophages can be drawn. Moreover, we suspect that the reduced proportion of reactive microglia also contributes to the observed phenotype. Microglia, since they originate from myeloid precursors in the yolk sac, have also been reported to be a target of the LysM<sup>Cre</sup> mediated gene deletion in mice (Prinz et al. 2008; Schweingruber et al. 2011). It has been shown that blockade of the MR with the antagonist spironolactone counteracts pro-inflammatory effects induced by aldosterone or corticosterone in a mouse microglia cell line, which confirms a role of the MR in microglia activation as well (Chantong et al. 2012). However, it cannot be assured yet whether the reduction in reactive microglia was due to the MR deficiency or just a secondary effect of the anti-inflammatory CNS milieu. To shed light on this question, *in vitro* experiments with primary microglia cells from MR<sup>lysM</sup> mice should be performed.

#### 4.2.2 MR deletion in myeloid cells alters T cell responses during EAE

The altered polarization state of MR-deficient myeloid cells could partially explain the improved clinical disease course in the MR<sup>lysM</sup> mice, but it was not clear yet whether other cell types contributed to this phenotype. Although the deletion of the MR in MR<sup>lysM</sup> mice is restricted to the myeloid compartment, myeloid cells act in close collaboration with T cells at different stages of EAE progression. It is actually known that T cells are the most important

---

players in the pathomechanisms leading to EAE, therefore potential changes in T cell responses were also investigated.

Some myeloid cells, including macrophages, act as professional APCs, and efficient presentation of myelin epitopes is crucial for EAE. This process is involved in the initial priming of T cells, as well as in the maintenance of the CNS inflammatory response in the chronic phase of the disease. As it was previously shown in this thesis, GCs down-regulate MHC class II and co-stimulatory molecules acting via the GR. Therefore we wondered whether antigen presentation was impaired in MR-deficient macrophages. Co-culture of BMDMs with naïve 2D2 T cells in the presence of MOG<sub>35-55</sub> demonstrated that MR<sup>lysM</sup> BMDMs were able to present antigens and induced T cell proliferation as efficiently as MR<sup>fl</sup> cells (**Figure 3.21**). Next, T cell priming was studied *in vivo* by adoptive transfer of CFSE-labeled 2D2 T cells in MOG<sub>35-55</sub> immunized mice. Three days after immunization part of the adoptively transferred 2D2 T cells were already proliferating in the spleen and the lymph nodes (**Figure 3.22**) However, surprisingly, there was a tendency towards increased T cell proliferation in the MR<sup>lysM</sup> mice, reaching significance in the axillary lymph nodes. Since the *in vitro* experiments on BMDMs indicated that T cell activation by MR<sup>lysM</sup> macrophages was neither impaired nor increased, it could be hypothesized that other cell types rather than macrophages are responsible for the apparently enhanced T cell proliferation *in vivo*. DCs are the major cell type involved in T cell priming during EAE (Greter et al. 2005). However, it is not known whether they express significant levels of MR and furthermore, LysM<sup>Cre</sup> transgenic mice do not appear to target any type of DC with high efficiency (Prinz et al. 2008). Therefore, the question why the proliferation rate in the axillary lymph nodes was increased remains to be answered. In any case, the presumed differences in T cell priming did not lead to changes in T cell infiltration between MR<sup>lysM</sup> and control mice. Hence we believe that this effect was of minor importance for the observed EAE alleviation.

During EAE, macrophages have also the task of shaping T cells responses by providing a specific cytokine environment. This study showed that *in vitro* BMDM activation induced the release of inflammatory cytokines such as IL-6 and TNF $\alpha$ , however this induction was milder in BMDMs from MR<sup>lysM</sup> mice. On the contrary, IL-10 secretion by MR<sup>lysM</sup> BMDMs was

increased compared to the controls (**Figure 3.20**). Thus, we wondered whether the altered cytokine profile in macrophages would lead to changes in the T cell activation pattern. Co-culture of 2D2 T cells with MR<sup>lysM</sup> BMDMs led to a reduced secretion of IFN $\gamma$  by T cells, whereas TNF $\alpha$  release, in contrast, was unaffected (**Figure 3.21**). Levels of other T cell cytokines such as IL-4, IL-17, IL-2 and IL-10 were barely detectable. These data suggest that, although T cell priming and T cell migration appeared to be unaltered, the activated state of the primed T cells might be milder once they reach the CNS. Previous data from Li, however, refute this hypothesis. In his experiments the expression levels of IL-17A and IFN $\gamma$  in the spinal cord of MR<sup>lysM</sup> mice was comparable to the one in MR<sup>fl</sup> mice (Li 2013). In the present work, we did find changes in the functionality of T cells during EAE, but they were restricted to the periphery. *Ex vivo* re-stimulation of splenocytes and lymph node cells revealed that T cells from the knock-out mice secreted less pro-inflammatory cytokines than the controls shortly before disease onset (**Figure 3.23**). IFN $\gamma$ , TNF $\alpha$  and IL-17A levels were significantly reduced, indicating that Th1 and Th17 responses might be impaired in the MR<sup>lysM</sup> mice. Importantly, GM-CSF, the only T cell cytokine known to be essential for EAE development (Codarri et al. 2011; El-Behi et al. 2011), was also significantly lower in both the spleen and the lymph nodes of MR<sup>lysM</sup> mice. One of the roles of GM-CSF is promoting the release of myeloid progenitors from the bone marrow, therefore the reduction of this cytokine might account for the lower percentages of circulating inflammatory monocytes found in MR<sup>lysM</sup> mice (**Figure 3.18**), and might explain the presumably reduced monocyte infiltration into the spinal cord.

Having demonstrated that peripheral T cells of MR<sup>lysM</sup> mice produced lower amounts of pro-inflammatory cytokines during EAE, we analyzed whether MR-deficient myeloid cells were directly inducing this phenotype on T cells. *In vitro* re-stimulation of MOG-specific Th17 cells co-cultured with MR<sup>lysM</sup> BMDMs did not affect the protein levels of IL-17A in the culture medium (**Figure 3.21**). Furthermore, no changes in the proportion of inflammatory monocytes or granulocyte numbers were observed in the spleens and lymph nodes of the MR<sup>lysM</sup> mice (**Figure 3.19**). Altogether, these data exclude a direct connection between the knock-out myeloid cells and the altered T cell functionality in the periphery. One of the major mechanisms of T cell suppression is mediated by Treg cells. Hence, this cell

compartment was additionally analyzed. An elevated percentage of Treg cells was found in the spleen and lymph nodes of MOG<sub>35-55</sub>-immunized MR<sup>lysM</sup> mice shortly before EAE onset (**Figure 3.24**). Interestingly, this increased Treg cell population was also found in healthy mice before immunization. Furthermore, it appeared that these peripheral Treg cells did not migrate to the CNS, indicating that their suppressive function might not be antigen-specific. Evidence of this is the comparable proportion of Treg cells in the spinal cords of MR<sup>fl</sup> and MR<sup>lysM</sup> mice, in line with the unaltered T cell infiltration and cytokine secretion observed in the CNS. All in all, these results point to Treg cells as secondary mediators of the milder EAE phenotype in the MR<sup>lysM</sup> mice.

#### 4.2.3 MR deletion in myeloid cells partially restores peripheral tolerance

Summing-up, the presented data suggest that the improved EAE clinical symptoms observed in the MR<sup>lysM</sup> mice are the result of two distinct regulatory mechanisms that, moreover, are separately compartmentalized. On the one hand, myeloid-targeted deletion of the MR promotes a deactivating state in microglia and monocytes/macrophages infiltrating the spinal cord. These M2 polarized myeloid cells establish a milder pro-inflammatory milieu within the CNS that prevents tissue damage and supports myelin regeneration. On the other hand, Treg cells act together with M2-monocytes in the periphery restraining effector T cell responses in secondary lymphoid organs, which also contribute to the overall reduced inflammatory response.

This synchronized intervention of M2-like macrophages and Treg cells has been extensively reported in different contexts. Hu and colleagues showed that adoptive transfer of CD4<sup>+</sup> CD25<sup>+</sup> Treg cells reduced the pro-inflammatory state of peritoneal macrophages, down-regulating MHC class II molecules and CD86 expression, increasing phagocytosis and IL-10 expression and altering the Arg1/iNOS balance (Hu et al. 2012). The macrophage phenotype described by Hu and colleagues, noteworthy, strongly resembles to the one induced by GCs. Conversely, human anti-inflammatory monocytes have been also shown to induce CD25<sup>+</sup> FoxP3<sup>+</sup> Treg cells with a potent suppressive activity (Savage et al. 2008). The same authors



proposed the production of ROS by macrophages as the link between these monocytes and the increased Treg induction (Kraaij et al. 2010). In agreement with the results of this thesis, GC-induced M2-like macrophages have also been reported to promote the generation of Treg cells. In a rat model of experimental autoimmune neuritis, Zhang and colleagues showed that Compound A, a GR agonist that just acts via the trans-repression mechanism, induced M2-like macrophages *in vivo* and *in vitro*. Furthermore, treatment with Compound A reduced disease severity and increased the numbers of Treg cells in the lymph nodes, where Th1 and Th2 cytokines were strongly suppressed (Zhang et al. 2009). Another study closely related to ours demonstrated that repetitive stimulation of naive splenic T cells with monocytes that had been matured in the presence of Dex yielded higher proportions of FoxP3<sup>+</sup> Treg cells *in vitro* (Varga et al. 2014). Moreover, when these GC-induced monocytes were injected in mice with severe colitis the clinical symptoms rapidly improved, and clusters of FoxP3<sup>+</sup> cells were found in the damaged colon. In line with Varga and colleagues, the MR<sup>lysM</sup> model, via deletion of the MR from myeloid cells, achieves a sustained M2-like polarization throughout the lifetime of the mouse, which would be equivalent to the repetitive stimulation of naïve T cells to increase the proportion of Treg cells. Unfortunately, Varga and colleagues could not identify the mechanism used by the GC-induced monocytes to induced Treg differentiation, and neither could we yet.

In a way, this effect could be interpreted as a reinforcement of the peripheral tolerance throughout lifetime. As example supporting this notion, a recent report proposed that during pregnancy, fetal tolerance was partly induced by generation of M2-macrophages and Treg cells via soluble factor secreted by the placenta (Svensson-Arvelund et al. 2015). This study highlights the importance of this combined regulatory mechanism, linking innate and adaptive immunity, to prevent potentially harmful immune responses, such as MS and other autoimmune disorders. The data presented in this thesis, moreover, provides evidences of the participation of GCs in the establishment of tolerance via myeloid cells, and opens new paths for alternative therapeutic strategies based on this principle.

### 4.3 Conclusions

For many years T cells have been considered the major therapeutic targets of GC treatment in neuroinflammatory diseases. However, the experimental data presented in this doctoral thesis show that when GC modulation is restricted to myeloid cells it is also able to change the course of the model disease EAE. This supports the already existing literature that postulate an important role of monocytes/macrophages in the therapy of autoimmune disorders with GCs (Metselaar et al. 2003; Mikita et al. 2011; Schweingruber et al. 2011; Varga et al. 2014). In view of the successful therapeutic effect of the myeloid-targeted therapy and the tight cell specificity of the system, BNPs were proposed as an alternative to overcome GC-associated side effects, but the obtained data did not provide conclusive information in this respect yet.

Furthermore, this study contributes to the understanding of the distinct participation of the GR and the MR in CNS autoimmunity. GR deletion from myeloid cells aggravated the clinical symptoms of EAE and rendered the mice resistant to the BNP therapy, whereas MR ablation in MR<sup>lysM</sup> mice had a beneficial effect in terms of disease severity. Additional unpublished data from our group indicates that systemic application of an MR antagonist also ameliorates EAE disease progression, although not to the same extent as the myeloid-specific knock-out. In our view, combining both experimental approaches, namely the delivery of the MR antagonist via nanoparticles, might increase the effective concentration of the drug in myeloid cells improving its efficacy. This and other potential variants of the strategies described in this thesis should be further investigated in the future.

Last but not least, we identified an involvement of M2-polarized monocytes/macrophages, and indirectly of endogenous GCs, in the establishment of peripheral tolerance. Under this new perspective, the above described low-dose pulsed GC protocols gain relevance. Sustained exposure of myeloid cells to GCs, either by synthetic GC application or targeted blockade of the MR, might assist the peripheral regulatory mechanisms in charge of maintaining tolerance; this could lead to a reduced relapse rate or improved recovery in MS patients, as it did in the mouse model of chronic-progressive EAE employed for this study.

---

## 5 References

- Aboul-Enein F, Weiser P, Höftberger R, Lassmann H, Bradl M (2006): Transient axonal injury in the absence of demyelination: a correlate of clinical disease in acute experimental autoimmune encephalomyelitis. *Acta Neuropathol (Berl)* 111, 539–547
- Abromson-Leeman S, Bronson RT, Dorf ME (2009): Encephalitogenic T cells that stably express both T-bet and ROR gamma t consistently produce IFNgamma but have a spectrum of IL-17 profiles. *J Neuroimmunol* 215, 10–24
- Adorini L, Guéry JC, Trembleau S (1996): Manipulation of the Th1/Th2 cell balance: an approach to treat human autoimmune diseases? *Autoimmunity* 23, 53–68
- Ajami B, Bennett JL, Krieger C, McNagny KM, Rossi FMV (2011): Infiltrating monocytes trigger EAE progression, but do not contribute to the resident microglia pool. *Nat Neurosci* 14, 1142–1149
- Alberts DS, Muggia FM, Carmichael J, Winer EP, Jahanzeb M, Venook AP, Skubitz KM, Rivera E, Sparano JA, DiBella NJ, et al. (2004): Efficacy and safety of liposomal anthracyclines in phase I/II clinical trials. *Semin Oncol* 31, 53–90
- Almawi WY, Beyhum HN, Rahme AA, Rieder MJ (1996): Regulation of cytokine and cytokine receptor expression by glucocorticoids. *J Leukoc Biol* 60, 563–572
- Almolda B, Gonzalez B, Castellano B (2011): Antigen presentation in EAE: role of microglia, macrophages and dendritic cells. *Front Biosci Landmark Ed* 16, 1157–1171
- Ando DG, Clayton J, Kono D, Urban JL, Sercarz EE (1989): Encephalitogenic T cells in the B10.PL model of experimental allergic encephalomyelitis (EAE) are of the Th-1 lymphokine subtype. *Cell Immunol* 124, 132–143
- Babbe H, Roers A, Waisman A, Lassmann H, Goebels N, Hohlfeld R, Friese M, Schröder R, Deckert M, Schmidt S, et al. (2000): Clonal expansions of CD8(+) T cells dominate the T cell infiltrate in active multiple sclerosis lesions as shown by micromanipulation and single cell polymerase chain reaction. *J Exp Med* 192, 393–404
- Barker CF, Billingham RE (1972): Analysis of local anatomic factors that influence the survival times of pure epidermal and full-thickness skin homografts in guinea pigs. *Ann Surg* 176, 597–604
- Barnett MH, Prineas JW (2004): Relapsing and remitting multiple sclerosis: pathology of the newly forming lesion. *Ann Neurol* 55, 458–468
- Bartholome B, Spies CM, Gaber T, Schuchmann S, Berki T, Kunkel D, Bienert M, Radbruch A, Burmester G-R, Lauster R, et al. (2004): Membrane glucocorticoid receptors (mGCR) are expressed in normal human peripheral blood mononuclear cells and up-regulated after in vitro stimulation and in patients with rheumatoid arthritis. *FASEB J Off Publ Fed Am Soc Exp Biol* 18, 70–80

- Batchelor PE, Liberatore GT, Wong JY, Porritt MJ, Frerichs F, Donnan GA, Howells DW (1999): Activated macrophages and microglia induce dopaminergic sprouting in the injured striatum and express brain-derived neurotrophic factor and glial cell line-derived neurotrophic factor. *J Neurosci Off J Soc Neurosci* 19, 1708–1716
- Batoulis H, Recks MS, Addicks K, Kuerten S (2011): Experimental autoimmune encephalomyelitis – achievements and prospective advances. *APMIS* 119, 819–830
- Baumann S, Dostert A, Novac N, Bauer A, Schmid W, Fas SC, Krueger A, Heinzel T, Kirchhoff S, Schütz G, Krammer PH (2005): Glucocorticoids inhibit activation-induced cell death (AICD) via direct DNA-dependent repression of the CD95 ligand gene by a glucocorticoid receptor dimer. *Blood* 106, 617–625
- Becher B, Durell BG, Noelle RJ (2002): Experimental autoimmune encephalitis and inflammation in the absence of interleukin-12. *J Clin Invest* 110, 493–497
- Becher B, Durell BG, Noelle RJ (2003): IL-23 produced by CNS-resident cells controls T cell encephalitogenicity during the effector phase of experimental autoimmune encephalomyelitis. *J Clin Invest* 112, 1186–1191
- Beck RW, Cleary PA, Trobe JD, Kaufman DI, Kupersmith MJ, Paty DW, Brown CH (1993): The effect of corticosteroids for acute optic neuritis on the subsequent development of multiple sclerosis. The Optic Neuritis Study Group. *N Engl J Med* 329, 1764–1769
- Bene NC, Alcaide P, Wortis HH, Jaffe IZ (2014): Mineralocorticoid receptors in immune cells: Emerging role in cardiovascular disease. *Steroids* 0, 38-45
- Ben-Nun A, Wekerle H, Cohen IR (1981): The rapid isolation of clonable antigen-specific T lymphocyte lines capable of mediating autoimmune encephalomyelitis. *Eur J Immunol* 11, 195–199
- Berard JL, Wolak K, Fournier S, David S (2010): Characterization of relapsing-remitting and chronic forms of experimental autoimmune encephalomyelitis in C57BL/6 mice. *Glia* 58, 434–445
- Berger S, Wolfer DP, Selbach O, Alter H, Erdmann G, Reichardt HM, Chepkova AN, Welzl H, Haas HL, Lipp H-P, Schütz G (2006): Loss of the limbic mineralocorticoid receptor impairs behavioral plasticity. *Proc Natl Acad Sci U S A* 103, 195–200
- Bettelli E (2007): Building different mouse models for human MS. *Ann N Y Acad Sci* 1103, 11–18
- Bettelli E, Pagany M, Weiner HL, Linington C, Sobel RA, Kuchroo VK (2003): Myelin Oligodendrocyte Glycoprotein-specific T Cell Receptor Transgenic Mice Develop Spontaneous Autoimmune Optic Neuritis. *J Exp Med* 197, 1073–1081
- Blotta MH, DeKruyff RH, Umetsu DT (1997): Corticosteroids inhibit IL-12 production in human monocytes and enhance their capacity to induce IL-4 synthesis in CD4+ lymphocytes. *J Immunol Baltim Md 1950* 158, 5589–5595
- Boster A, Edan G, Frohman E, Javed A, Stuve O, Tselis A, Weiner H, Weinstock-Guttman B, Khan O, Multiple Sclerosis Clinical Research Center, Department of Neurology, Wayne State University School of Medicine (2008): Intense immunosuppression in patients with rapidly worsening multiple sclerosis: treatment guidelines for the clinician. *Lancet Neurol* 7, 173–183

- Braun TP, Marks DL (2015): The regulation of muscle mass by endogenous glucocorticoids. *Front Physiol* 6
- Brennan-Speranza TC, Conigrave AD (2015): Osteocalcin: an osteoblast-derived polypeptide hormone that modulates whole body energy metabolism. *Calcif Tissue Int* 96, 1–10
- Brown JWL, Coles AJ (2013): Alemtuzumab: evidence for its potential in relapsing-remitting multiple sclerosis. *Drug Des Devel Ther* 7, 131–138
- Büyüktimkin B, Wang Q, Kiptoo P, Stewart JM, Berkland C, Siahaan TJ (2012): Vaccine-like controlled-release delivery of an immunomodulating peptide to treat experimental autoimmune encephalomyelitis. *Mol Pharm* 9, 979–985
- Carlson T, Kroenke M, Rao P, Lane TE, Segal B (2008): The Th17-ELR+ CXC chemokine pathway is essential for the development of central nervous system autoimmune disease. *J Exp Med* 205, 811–823
- Carson MJ, Doose JM, Melchior B, Schmid CD, Ploix CC (2006): CNS immune privilege: hiding in plain sight. *Immunol Rev* 213, 48–65
- Carswell R (1838): *Pathological anatomy: illustrations of the elementary forms of disease*. Longman, Orme, Brown, Green and Longman (London)
- Chandler VL, Maler BA, Yamamoto KR (1983): DNA sequences bound specifically by glucocorticoid receptor in vitro render a heterologous promoter hormone responsive in vivo. *Cell* 33, 489–499
- Chantong B, Kratschmar DV, Nashev LG, Balazs Z, Odermatt A (2012): Mineralocorticoid and glucocorticoid receptors differentially regulate NF-kappaB activity and pro-inflammatory cytokine production in murine BV-2 microglial cells. *J Neuroinflammation* 9, 260
- Chao CC, Hu S, Close K, Choi CS, Molitor TW, Novick WJ, Peterson PK (1992): Cytokine release from microglia: differential inhibition by pentoxifylline and dexamethasone. *J Infect Dis* 166, 847–853
- Chen X, Winkler-Pickett RT, Carbonetti NH, Ortaldo JR, Oppenheim JJ, Howard OMZ (2006): Pertussis toxin as an adjuvant suppresses the number and function of CD4+CD25+ T regulatory cells. *Eur J Immunol* 36, 671–680
- Chu CQ, Wittmer S, Dalton DK (2000): Failure to suppress the expansion of the activated CD4 T cell population in interferon gamma-deficient mice leads to exacerbation of experimental autoimmune encephalomyelitis. *J Exp Med* 192, 123–128
- Ciriaco M, Ventrice P, Russo G, Scicchitano M, Mazzitello G, Scicchitano F, Russo E (2013): Corticosteroid-related central nervous system side effects. *J Pharmacol Pharmacother* 4, S94–S98
- Clausen BE, Burkhardt C, Reith W, Renkawitz R, Förster I (1999): Conditional gene targeting in macrophages and granulocytes using LysMcre mice. *Transgenic Res* 8, 265–277

- Codarri L, Gyölvézi G, Tosevski V, Hesske L, Fontana A, Magnenat L, Suter T, Becher B (2011): ROR $\gamma$ t drives production of the cytokine GM-CSF in helper T cells, which is essential for the effector phase of autoimmune neuroinflammation. *Nat Immunol* 12, 560–567
- Coghlan MJ, Jacobson PB, Lane B, Nakane M, Lin CW, Elmore SW, Kym PR, Luly JR, Carter GW, Turner R, et al. (2003): A novel antiinflammatory maintains glucocorticoid efficacy with reduced side effects. *Mol Endocrinol Baltim Md* 17, 860–869
- Compston A, Coles A (2002): Multiple sclerosis. *The Lancet* 359, 1221–1231
- Cua DJ, Sherlock J, Chen Y, Murphy CA, Joyce B, Seymour B, Lucian L, To W, Kwan S, Churakova T, et al. (2003): Interleukin-23 rather than interleukin-12 is the critical cytokine for autoimmune inflammation of the brain. *Nature* 421, 744–748
- D'Adamio F, Zollo O, Moraca R, Ayroldi E, Bruscoli S, Bartoli A, Cannarile L, Migliorati G, Riccardi C (1997): A new dexamethasone-induced gene of the leucine zipper family protects T lymphocytes from TCR/CD3-activated cell death. *Immunity* 7, 803–812
- Demir E, Burgucu D, Turna F, Aksakal S, Kaya B (2013): Determination of TiO<sub>2</sub>, ZrO<sub>2</sub>, and Al<sub>2</sub>O<sub>3</sub> nanoparticles on genotoxic responses in human peripheral blood lymphocytes and cultured embryonic kidney cells. *J Toxicol Environ Health A* 76, 990–1002
- Dinkel K, Dhabhar FS, Sapolsky RM (2004): Neurotoxic effects of polymorphonuclear granulocytes on hippocampal primary cultures. *Proc Natl Acad Sci U S A* 101, 331–336
- Duffy SS, Lees JG, Moalem-Taylor G (2014): The Contribution of Immune and Glial Cell Types in Experimental Autoimmune Encephalomyelitis and Multiple Sclerosis. *Mult Scler Int* 2014
- El-Behi M, Ciric B, Dai H, Yan Y, Cullimore M, Safavi F, Zhang G-X, Dittel BN, Rostami A (2011): The encephalitogenicity of T(H)17 cells is dependent on IL-1- and IL-23-induced production of the cytokine GM-CSF. *Nat Immunol* 12, 568–575
- Elkabes S, DiCicco-Bloom EM, Black IB (1996): Brain microglia/macrophages express neurotrophins that selectively regulate microglial proliferation and function. *J Neurosci Off J Soc Neurosci* 16, 2508–2521
- Engelhardt B (2000): Role of glucocorticoids on T cell recruitment across the blood-brain barrier. *Z Für Rheumatol* 59 Suppl 2, II/18-21
- Ehrlich P, Morgenroth J (1957): On Hemolysins: second communication. In *The Collected papers of Paul Erlich*, vol.2. Immunol and Cancer Research, Ed. Himmelweit 165-172
- Ferber IA, Brocke S, Taylor-Edwards C, Ridgway W, Dinisco C, Steinman L, Dalton D, Fathman CG (1996): Mice with a disrupted IFN-gamma gene are susceptible to the induction of experimental autoimmune encephalomyelitis (EAE). *J Immunol Baltim Md* 1950 156, 5–7
- Fernández-Menéndez S, Fernández-Morán M, Fernández-Vega I, Pérez-Álvarez A, Villafani-Echazú J (2016): Epstein–Barr virus and multiple sclerosis. From evidence to therapeutic strategies. *J Neurol Sci* 361, 213–219

- Filippini G, Brusaferrri F, Sibley WA, Citterio A, Ciucci G, Midgard R, Candelise L (2000): Corticosteroids or ACTH for acute exacerbations in multiple sclerosis. *Cochrane Database Syst Rev* CD001331
- Fischer HJ, Schweingruber N, Lühder F, Reichardt HM (2013): The potential role of T cell migration and chemotaxis as targets of glucocorticoids in multiple sclerosis and experimental autoimmune encephalomyelitis. *Mol Cell Endocrinol* 380, 99–107
- Folgueras AR, Fueyo A, García-Suárez O, Cox J, Astudillo A, Tortorella P, Campestre C, Gutiérrez-Fernández A, Fanjul-Fernández M, Pennington CJ, et al. (2008): Collagenase-2 deficiency or inhibition impairs experimental autoimmune encephalomyelitis in mice. *J Biol Chem* 283, 9465–9474
- Ford ML, Evavold BD (2005): Specificity, magnitude, and kinetics of MOG-specific CD8+ T cell responses during experimental autoimmune encephalomyelitis. *Eur J Immunol* 35, 76–85
- Freund J, Stern ER, Pisani TM (1947): Isoallergic encephalomyelitis and radiculitis in guinea pigs after one injection of brain and Mycobacteria in water-in-oil emulsion. *J Immunol Baltim Md* 1950 57, 179–194
- Funder JW (1993): Mineralocorticoids, glucocorticoids, receptors and response elements. *Science* 259, 1132–1133
- Funder JW (1997): Glucocorticoid and mineralocorticoid receptors: biology and clinical relevance. *Annu Rev Med* 48, 231–240
- van Furth R, Cohn ZA, Hirsch JG, Humphrey JH, Spector WG, Langevoort HL (1972): The mononuclear phagocyte system: a new classification of macrophages, monocytes, and their precursor cells. *Bull World Health Organ* 46, 845–852
- Ganter S, Northoff H, Männel D, Gebicke-Härter PJ (1992): Growth control of cultured microglia. *J Neurosci Res* 33, 218–230
- Gascoyne DM, Kypta RM, Vivanco M d M (2003): Glucocorticoids inhibit apoptosis during fibrosarcoma development by transcriptionally activating Bcl-xL. *J Biol Chem* 278, 18022–18029
- Gayo A, Mozo L, Suárez A, Tuñon A, Lahoz C, Gutiérrez C (1998): Glucocorticoids increase IL-10 expression in multiple sclerosis patients with acute relapse. *J Neuroimmunol* 85, 122–130
- Geissmann F, Jung S, Littman DR (2003): Blood monocytes consist of two principal subsets with distinct migratory properties. *Immunity* 19, 71–82
- Giulian D, Baker TJ (1986): Characterization of ameboid microglia isolated from developing mammalian brain. *J Neurosci Off J Soc Neurosci* 6, 2163–2178
- Gold R, Kappos L, Arnold DL, Bar-Or A, Giovannoni G, Selmaj K, Tornatore C, Sweetser MT, Yang M, Sheikh SI, et al. (2012): Placebo-controlled phase 3 study of oral BG-12 for relapsing multiple sclerosis. *N Engl J Med* 367, 1098–1107
- Goodin DS (2014): Glucocorticoid treatment of multiple sclerosis. *Handb Clin Neurol* 122, 455–464

- Goodkin DE, Kinkel RP, Weinstock-Guttman B, VanderBrug-Medendorp S, Secic M, Gogol D, Perryman JE, Uccelli MM, Neilley L (1998): A phase II study of i.v. methylprednisolone in secondary-progressive multiple sclerosis. *Neurology* 51, 239–245
- Gordon AN, Fleagle JT, Guthrie D, Parkin DE, Gore ME, Lacave AJ (2001): Recurrent epithelial ovarian carcinoma: a randomized phase III study of pegylated liposomal doxorubicin versus topotecan. *J Clin Oncol Off J Am Soc Clin Oncol* 19, 3312–3322
- Gran B, Zhang G-X, Yu S, Li J, Chen X-H, Ventura ES, Kamoun M, Rostami A (2002): IL-12p35-deficient mice are susceptible to experimental autoimmune encephalomyelitis: evidence for redundancy in the IL-12 system in the induction of central nervous system autoimmune demyelination. *J Immunol Baltim Md 1950* 169, 7104–7110
- Greter M, Heppner FL, Lemos MP, Odermatt BM, Goebels N, Laufer T, Noelle RJ, Becher B (2005): Dendritic cells permit immune invasion of the CNS in an animal model of multiple sclerosis. *Nat Med* 11, 328–334
- Groux H, O’Garra A, Bigler M, Rouleau M, Antonenko S, de Vries JE, Roncarolo MG (1997): A CD4+ T-cell subset inhibits antigen-specific T-cell responses and prevents colitis. *Nature* 389, 737–742
- Haak S, Croxford AL, Kreyborg K, Heppner FL, Pouly S, Becher B, Waisman A (2009): IL-17A and IL-17F do not contribute vitally to autoimmune neuro-inflammation in mice. *J Clin Invest* 119, 61–69
- Haas J, Hug A, Viehöver A, Fritzsching B, Falk CS, Filser A, Vetter T, Milkova L, Korporal M, Fritz B, et al. (2005): Reduced suppressive effect of CD4+CD25<sup>high</sup> regulatory T cells on the T cell immune response against myelin oligodendrocyte glycoprotein in patients with multiple sclerosis. *Eur J Immunol* 35, 3343–3352
- Hafner DA, Compston A, Sawcer S, Lander ES, Daly MJ, De Jager PL, de Bakker PIW, Gabriel SB, Mirel DB, Ivinson AJ, et al. (2007): Risk alleles for multiple sclerosis identified by a genomewide study. *N Engl J Med* 357, 851–862
- Harris MG, Hulseberg P, Ling C, Karman J, Clarkson BD, Harding JS, Zhang M, Sandor A, Christensen K, Nagy A, et al. (2014): Immune privilege of the CNS is not the consequence of limited antigen sampling. *Sci Rep* 4, 4422
- Hauser SL, Goodwin DS: Multiple sclerosis and other demyelinating diseases; in: *Harrison’s Principles of Internal Medicine*, Band 2, 17th edition; McGraw-Hill Medical, New York, NY, USA 2008, 2611–2621
- Heck JG, Napp J, Simonato S, Möllmer J, Lange M, Reichardt HM, Staudt R, Alves F, Feldmann C (2015): Multifunctional Phosphate-Based Inorganic–Organic Hybrid Nanoparticles. *J Am Chem Soc* 137, 7329–7336
- Hedström AK, Olsson T, Alfredsson L (2015): Smoking is a major preventable risk factor for multiple sclerosis. *Mult Scler J* 1352458515609794
- Hench PS, Kendall EC, Slocumb CH, Polley HF (1950): Cortisone, its effects on rheumatoid arthritis, rheumatic fever, and certain other conditions. *Merck Rep* 59, 9–14



- Hendriks JJA, Alblas J, van der Pol SMA, van Tol EAF, Dijkstra CD, de Vries HE (2004): Flavonoids influence monocytic GTPase activity and are protective in experimental allergic encephalitis. *J Exp Med* 200, 1667–1672
- Hertenberg D, Lehmann-Horn K, Kinzel S, Husterer V, Cravens PD, Kieseier BC, Hemmer B, Brück W, Zamvil SS, Stüve O, Weber MS (2013): Developmental maturation of innate immune cell function correlates with susceptibility to central nervous system autoimmunity. *Eur J Immunol* 43, 2078–2088
- Hirota K, Duarte JH, Veldhoen M, Hornsby E, Li Y, Cua DJ, Ahlfors H, Wilhelm C, Tolaini M, Menzel U, et al. (2011): Fate mapping of IL-17-producing T cells in inflammatory responses. *Nat Immunol* 12, 255–263
- Hodge S, Hodge G, Flower R, Han P (1999): Methyl-prednisolone up-regulates monocyte interleukin-10 production in stimulated whole blood. *Scand J Immunol* 49, 548–553
- Hou W, Wu Y, Sun S, Shi M, Sun Y, Yang C, Pei G, Gu Y, Zhong C, Sun B (2003): Pertussis toxin enhances Th1 responses by stimulation of dendritic cells. *J Immunol Baltim Md 1950* 170, 1728–1736
- Hu X, Liu G, Hou Y, Shi J, Zhu L, Jin D, Peng J, Zhao Y (2012): Induction of M2-like macrophages in recipient NOD-scid mice by allogeneic donor CD4(+)CD25(+) regulatory T cells. *Cell Mol Immunol* 9, 464–472
- Huang W, Metlakunta A, Dedousis N, Zhang P, Sipula I, Dube JJ, Scott DK, O’Doherty RM (2010): Depletion of liver Kupffer cells prevents the development of diet-induced hepatic steatosis and insulin resistance. *Diabetes* 59, 347–357
- Hucke S, Eschborn M, Liebmann M, Herold M, Freise N, Engbers A, Ehling P, Meuth SG, Roth J, Kuhlmann T, et al. (2016): Sodium chloride promotes pro-inflammatory macrophage polarization thereby aggravating CNS autoimmunity. *J Autoimmun* 67, 90–101
- Huitinga I, van Rooijen N, de Groot CJ, Uitdehaag BM, Dijkstra CD (1990): Suppression of experimental allergic encephalomyelitis in Lewis rats after elimination of macrophages. *J Exp Med* 172, 1025–1033
- Hume DA (2015): The Many Alternative Faces of Macrophage Activation. *Front Immunol* 6, 370
- Hunger M, Budinger E, Zhong K, Angenstein F (2014): Visualization of acute focal lesions in rats with experimental autoimmune encephalomyelitis by magnetic nanoparticles, comparing different MRI sequences including phase imaging. *J Magn Reson Imaging* 39, 1126–1135
- Hunter RW, Ivy JR, Bailey MA (2014a): Glucocorticoids and renal Na<sup>+</sup> transport: implications for hypertension and salt sensitivity. *J Physiol* 592, 1731–1744
- Hunter Z, McCarthy DP, Yap WT, Harp CT, Getts DR, Shea LD, Miller SD (2014b): A biodegradable nanoparticle platform for the induction of antigen-specific immune tolerance for treatment of autoimmune disease. *ACS Nano* 8, 2148–2160
- Huppert J, Closhen D, Croxford A, White R, Kulig P, Pietrowski E, Bechmann I, Becher B, Luhmann HJ, Waisman A, Kuhlmann CRW (2010): Cellular mechanisms of IL-17-induced blood-brain barrier disruption. *FASEB J Off Publ Fed Am Soc Exp Biol* 24, 1023–1034

- Hutchison KA, Dittmar KD, Stancato LF, Pratt WB (1996): Ability of various members of the hsp70 family of chaperones to promote assembly of the glucocorticoid receptor into a functional heterocomplex with hsp90. *J Steroid Biochem Mol Biol* 58, 251–258
- Hwang JL, Weiss RE (2014): Steroid-induced diabetes: a clinical and molecular approach to understanding and treatment. *Diabetes Metab Res Rev* 30, 96–102
- Iliff JJ, Goldman SA, Nedergaard M (2015): Implications of the discovery of brain lymphatic pathways. *Lancet Neurol* 14, 977–979
- Imrich H, Harzer K (2001): On the role of peripheral macrophages during active experimental allergic encephalomyelitis (EAE). *J Neural Transm Vienna Austria* 1996 108, 379–395
- Johnson KP, Brooks BR, Cohen JA, Ford CC, Goldstein J, Lisak RP, Myers LW, Panitch HS, Rose JW, Schiffer RB (1995): Copolymer 1 reduces relapse rate and improves disability in relapsing-remitting multiple sclerosis: results of a phase III multicenter, double-blind placebo-controlled trial. The Copolymer 1 Multiple Sclerosis Study Group. *Neurology* 45, 1268–1276
- Jun CD, Hoon-Ryu null, Um JY, Kim TY, Kim JM, Kang SS, Kim HM, Chung HT (1994): Involvement of protein kinase C in the inhibition of nitric oxide production from murine microglial cells by glucocorticoid. *Biochem Biophys Res Commun* 199, 633–638
- Kappos L, Radue E-W, O'Connor P, Polman C, Hohlfeld R, Calabresi P, Selmaj K, Agoropoulou C, Leyk M, Zhang-Auberson L, et al. (2010): A placebo-controlled trial of oral fingolimod in relapsing multiple sclerosis. *N Engl J Med* 362, 387–401
- Karunakaran G, Suriyaprabha R, Manivasakan P, Yuvakkumar R, Rajendran V, Kannan N (2013): Screening of in vitro cytotoxicity, antioxidant potential and bioactivity of nano- and micro-ZrO<sub>2</sub> and -TiO<sub>2</sub> particles. *Ecotoxicol Environ Saf* 93, 191–197
- Kashiwamura Y, Sano Y, Abe M, Shimizu F, Haruki H, Maeda T, Kawai M, Kanda T (2011): Hydrocortisone enhances the function of the blood-nerve barrier through the up-regulation of claudin-5. *Neurochem Res* 36, 849–855
- Kassiotis G, Pasparakis M, Kollias G, Probert L (1999): TNF accelerates the onset but does not alter the incidence and severity of myelin basic protein-induced experimental autoimmune encephalomyelitis. *Eur J Immunol* 29, 774–780
- Keating P, O'Sullivan D, Tierney JB, Kenwright D, Miromoeini S, Mawasse L, Brombacher F, La Flamme AC (2009): Protection from EAE by IL-4R $\alpha$ (-/-) macrophages depends upon T regulatory cell involvement. *Immunol Cell Biol* 87, 534–545
- Kerfoot SM, Long EM, Hickey MJ, Andonegui G, Lapointe BM, Zanardo RCO, Bonder C, James WG, Robbins SM, Kuberski P (2004): TLR4 contributes to disease-inducing mechanisms resulting in central nervous system autoimmune disease. *J Immunol Baltim Md* 1950 173, 7070–7077
- Kiefer R, Kreutzberg GW (1991): Effects of dexamethasone on microglial activation in vivo: selective downregulation of major histocompatibility complex class II expression in regenerating facial nucleus. *J Neuroimmunol* 34, 99–108
- Kierdorf K, Prinz M (2013): Factors regulating microglia activation. *Front Cell Neurosci* 7, 44

- Kizelsztejn P, Ovadia H, Garbuzenko O, Sigal A, Barenholz Y (2009): Pegylated nanoliposomes remote-loaded with the antioxidant tempamine ameliorate experimental autoimmune encephalomyelitis. *J Neuroimmunol* 213, 20–25
- Kleiman A, Hübner S, Rodriguez Parkitna JM, Neumann A, Hofer S, Weigand MA, Bauer M, Schmid W, Schütz G, Libert C, et al. (2012): Glucocorticoid receptor dimerization is required for survival in septic shock via suppression of interleukin-1 in macrophages. *FASEB J Off Publ Fed Am Soc Exp Biol* 26, 722–729
- Kleinewietfeld M, Manzel A, Titze J, Kvakana H, Yosef N, Linker RA, Müller DN, Hafler DA (2013): Sodium Chloride Drives Autoimmune Disease by the Induction of Pathogenic Th17 Cells. *Nature* 496, 518–522
- Koenen HJPM, Smeets RL, Vink PM, van Rijssen E, Boots AMH, Joosten I (2008): Human CD25<sup>high</sup>Foxp3<sup>pos</sup> regulatory T cells differentiate into IL-17-producing cells. *Blood* 112, 2340–2352
- Koh DR, Fung-Leung WP, Ho A, Gray D, Acha-Orbea H, Mak TW (1992): Less mortality but more relapses in experimental allergic encephalomyelitis in CD8<sup>-/-</sup> mice. *Science* 256, 1210–1213
- Kohm AP, Carpentier PA, Miller SD (2003): Regulation of experimental autoimmune encephalomyelitis (EAE) by CD4<sup>+</sup>CD25<sup>+</sup> regulatory T cells. *Novartis Found Symp* 252, 45-52-54, 106–114
- Komiyama Y, Nakae S, Matsuki T, Nambu A, Ishigame H, Kakuta S, Sudo K, Iwakura Y (2006): IL-17 plays an important role in the development of experimental autoimmune encephalomyelitis. *J Immunol Baltim Md 1950* 177, 566–573
- Korn T, Oukka M, Kuchroo V, Bettelli E (2007a): Th17 cells: effector T cells with inflammatory properties. *Semin Immunol* 19, 362–371
- Korn T, Anderson AC, Bettelli E, Oukka M (2007b): The dynamics of effector T cells and Foxp3<sup>+</sup> regulatory T cells in the promotion and regulation of autoimmune encephalitis. *J Neuroimmunol* 191, 51–60
- Korn T, Bettelli E, Oukka M, Kuchroo VK (2009): IL-17 and Th17 Cells. *Annu Rev Immunol* 27, 485–517
- Körner H, Riminton DS, Strickland DH, Lemckert FA, Pollard JD, Sedgwick JD (1997): Critical points of tumor necrosis factor action in central nervous system autoimmune inflammation defined by gene targeting. *J Exp Med* 186, 1585–1590
- Kotter MR, Li W, Franklin RJM (2006): Myelin impairs CNS remyelination by inhibiting oligodendrocyte precursor cell differentiation. *J Neurosci* 26(1), 328-332
- Kraaij MD, Savage ND, van der Kooij SW, Koekoek K, Wang J, van den Berg JM, Ottenhoff THM, Kuijpers TW, Holmdahl R, van Kooten C, Gelderman KA (2010): Induction of regulatory T cells by macrophages is dependent on production of reactive oxygen species. *Proc Natl Acad Sci U S A* 107, 17686–17691

- Krakowski M, Owens T (1996): Interferon-gamma confers resistance to experimental allergic encephalomyelitis. *Eur J Immunol* 26, 1641–1646
- Kroenke MA, Segal BM (2011): IL-23 modulated myelin-specific T cells induce EAE via an IFN $\gamma$  driven, IL-17 independent pathway. *Brain Behav Immun* 25, 932–937
- Kuo T, McQueen A, Chen T-C, Wang J-C (2015): Regulation of Glucose Homeostasis by Glucocorticoids. *Adv Exp Med Biol* 872, 99–126
- Kurschus FC, Croxford AL, Heinen AP, Wörtge S, Ielo D, Waisman A (2010): Genetic proof for the transient nature of the Th17 phenotype. *Eur J Immunol* 40, 3336–3346
- Lafaille JJ, Keere FV, Hsu AL, Baron JL, Haas W, Raine CS, Tonegawa S (1997): Myelin basic protein-specific T helper 2 (Th2) cells cause experimental autoimmune encephalomyelitis in immunodeficient hosts rather than protect them from the disease. *J Exp Med* 186, 307–312
- Langrish CL, Chen Y, Blumenschein WM, Mattson J, Basham B, Sedgwick JD, McClanahan T, Kastelein RA, Cua DJ (2005): IL-23 drives a pathogenic T cell population that induces autoimmune inflammation. *J Exp Med* 201, 233–240
- Lassmann H, Brück W, Lucchinetti CF (2007): The Immunopathology of Multiple Sclerosis: An Overview. *Brain Pathol* 17, 210–218
- Leclerc N, Noh T, Khokhar A, Smith E, Frenkel B (2005): Glucocorticoids inhibit osteocalcin transcription in osteoblasts by suppressing Egr2/Krox20-binding enhancer. *Arthritis Rheum* 52, 929–939
- Leray E, Moreau T, Fromont A, Edan G (2016): Epidemiology of multiple sclerosis. *Rev Neurol (Paris)* 172, 3–13
- Leussink VI, Jung S, Merschedorf U, Toyka KV, Gold R (2001): High-dose methylprednisolone therapy in multiple sclerosis induces apoptosis in peripheral blood leukocytes. *Arch Neurol* 58, 91–97
- Li X (2013): Myeloid cell-specific ablation of the mineralocorticoid receptor attenuates experimental autoimmune encephalomyelitis. <http://hdl.handle.net/11858/00-1735-0000-000D-FB53-E>
- Lim H-Y, Müller N, Herold MJ, van den Brandt J, Reichardt HM (2007): Glucocorticoids exert opposing effects on macrophage function dependent on their concentration. *Immunology* 122, 47–53
- Linker RA, Weller C, Lühder F, Mohr A, Schmidt J, Knauth M, Metselaar JM, Gold R (2008): Liposomal glucocorticosteroids in treatment of chronic autoimmune demyelination: long-term protective effects and enhanced efficacy of methylprednisolone formulations. *Exp Neurol* 211, 397–406
- Litchfield S, Nagy Z (2001): New temperature modification makes the Bielschowsky silver stain reproducible. *Acta Neuropathol (Berl)* 101, 17–21
- Litzenburger T, Fässler R, Bauer J, Lassmann H, Linington C, Wekerle H, Iglesias A (1998): B lymphocytes producing demyelinating autoantibodies: development and function in gene-targeted transgenic mice. *J Exp Med* 188, 169–180

- Liu Y, Teige I, Birnir B, Issazadeh-Navikas S (2006): Neuron-mediated generation of regulatory T cells from encephalitogenic T cells suppresses EAE. *Nat Med* 12, 518–525
- Louw A, Swart P, de Kock SS, van der Merwe KJ (1997): Mechanism for the stabilization in vivo of the aziridine precursor --(4-acetoxyphenyl)-2-chloro-N-methyl-ethylammonium chloride by serum proteins. *Biochem Pharmacol* 53, 189–197
- Lublin FD, Maurer PH, Berry RG, Tippett D (1981): Delayed, relapsing experimental allergic encephalomyelitis in mice. *J Immunol Baltim Md 1950* 126, 819–822
- Lucchinetti C, Brück W, Parisi J, Scheithauer B, Rodriguez M, Lassmann H (2000): Heterogeneity of multiple sclerosis lesions: implications for the pathogenesis of demyelination. *Ann Neurol* 47, 707–717
- Luche H, Weber O, Nageswara Rao T, Blum C, Fehling HJ (2007): Faithful activation of an extra-bright red fluorescent protein in „knock-in“ Cre-reporter mice ideally suited for lineage tracing studies. *Eur J Immunol* 37, 43–53
- Mantovani A, Sica A, Sozzani S, Allavena P, Vecchi A, Locati M (2004): The chemokine system in diverse forms of macrophage activation and polarization. *Trends Immunol* 25, 677–686
- Markus MA, Napp J, Behnke T, Mitkovski M, Monecke S, Dullin C, Kilfeather S, Dressel R, Resch-Genger U, Alves F (2015): Tracking of Inhaled Near-Infrared Fluorescent Nanoparticles in Lungs of SKH-1 Mice with Allergic Airway Inflammation. *ACS Nano* 9, 11642–11657
- Martinez FO, Gordon S (2014): The M1 and M2 paradigm of macrophage activation: time for reassessment. *F1000Prime Rep* 6, 13
- Matsushima GK, Morell P (2001): The neurotoxicant, cuprizone, as a model to study demyelination and remyelination in the central nervous system. *Brain Pathol Zurich Switz* 11, 107–116
- McColl SR, Staykova MA, Wozniak A, Fordham S, Bruce J, Willenborg DO (1998): Treatment with anti-granulocyte antibodies inhibits the effector phase of experimental autoimmune encephalomyelitis. *J Immunol Baltim Md 1950* 161, 6421–6426
- McDonald WI, Compston A, Edan G, Goodkin D, Hartung HP, Lublin FD, McFarland HF, Paty DW, Polman CH, Reingold SC, et al. (2001): Recommended diagnostic criteria for multiple sclerosis: guidelines from the International Panel on the diagnosis of multiple sclerosis. *Ann Neurol* 50, 121–127
- McGeachy MJ, Stephens LA, Anderton SM (2005): Natural recovery and protection from autoimmune encephalomyelitis: contribution of CD4+CD25+ regulatory cells within the central nervous system. *J Immunol Baltim Md 1950* 175, 3025–3032
- Medawar PB (1948): Immunity to Homologous Grafted Skin. III. The Fate of Skin Homographs Transplanted to the Brain, to Subcutaneous Tissue, and to the Anterior Chamber of the Eye. *Br J Exp Pathol* 29, 58–69
- Merodio M, Irache JM, Eclancher F, Mirshahi M, Villarroya H (2000): Distribution of albumin nanoparticles in animals induced with the experimental allergic encephalomyelitis. *J Drug Target* 8, 289–303

- Metselaar JM, Wauben MHM, Wagenaar-Hilbers JPA, Boerman OC, Storm G (2003): Complete remission of experimental arthritis by joint targeting of glucocorticoids with long-circulating liposomes. *Arthritis Rheum* 48, 2059–2066
- Mikita J, Dubourdieu-Cassagno N, Deloire MS, Vekris A, Biran M, Raffard G, Brochet B, Cannon M-H, Franconi J-M, Boiziau C, Petry KG (2011): Altered M1/M2 activation patterns of monocytes in severe relapsing experimental rat model of multiple sclerosis. Amelioration of clinical status by M2 activated monocyte administration. *Mult Scler J* 17, 2–15
- Mildner A, Mack M, Schmidt H, Brück W, Djukic M, Zabel MD, Hille A, Priller J, Prinz M (2009): CCR2+Ly-6Chi monocytes are crucial for the effector phase of autoimmunity in the central nervous system. *Brain J Neurol* 132, 2487–2500
- Miller DM, Weinstock-Guttman B, Béthoux F, Lee JC, Beck G, Block V, Durelli L, LaMantia L, Barnes D, Sellebjerg F, Rudick RA (2000): A meta-analysis of methylprednisolone in recovery from multiple sclerosis exacerbations. *Mult Scler Houndmills Basingstoke Engl* 6, 267–273
- Miller H, Newell DJ, Ridley A (1961): Multiple sclerosis. Trials of maintenance treatment with prednisolone and soluble aspirin. *Lancet Lond Engl* 1, 127–129
- Milligan NM, Newcombe R, Compston DA (1987): A double-blind controlled trial of high dose methylprednisolone in patients with multiple sclerosis: 1. Clinical effects. *J Neurol Neurosurg Psychiatry* 50, 511–516
- Mimura LAN, Chiuso-Minicucci F, Fraga-Silva TFC, Zorzella-Pezavento S. G, Franca TG., Ishikawa LLW, Penitenti M, Ikoma MRV, Sartori A (2016): Association of myelin peptide with vitamin D prevents autoimmune encephalomyelitis development. *Neuroscience* 317, 130–140
- Moghadam-Kia S, Werth VP (2010): Prevention and treatment of systemic glucocorticoid side effects. *Int J Dermatol* 49, 239–248
- Mosmann TR, Cherwinski H, Bond MW, Giedlin MA, Coffman RL (1986): Two types of murine helper T cell clone. I. Definition according to profiles of lymphokine activities and secreted proteins. *J Immunol Baltim Md 1950* 136, 2348–2357
- Mosser DM, Edwards JP (2008): Exploring the full spectrum of macrophage activation. *Nat Rev Immunol* 8, 958–969
- Murphy AC, Lalor SJ, Lynch MA, Mills KHG (2010): Infiltration of Th1 and Th17 cells and activation of microglia in the CNS during the course of experimental autoimmune encephalomyelitis. *Brain Behav Immun* 24, 641–651
- Neumann H, Kotter MR, Franklin RJM (2009): Debris clearance by microglia: an essential link between degeneration and regeneration. *Brain J Neurol* 132, 288–295
- Obando-Pereda GA, Fischer L, Stach-Machado DR (2014): Titanium and zirconia particle-induced pro-inflammatory gene expression in cultured macrophages and osteolysis, inflammatory hyperalgesia and edema in vivo. *Life Sci* 97, 96–106
- O'Connor RA, Malpass KH, Anderton SM (2007): The inflamed central nervous system drives the activation and rapid proliferation of Foxp3+ regulatory T cells. *J Immunol Baltim Md 1950* 179, 958–966

- Odegaard JI, Ricardo-Gonzalez RR, Red Eagle A, Vats D, Morel CR, Goforth MH, Subramanian V, Mukundan L, Ferrante AW, Chawla A (2008): Alternative M2 activation of Kupffer cells by PPARdelta ameliorates obesity-induced insulin resistance. *Cell Metab* 7, 496–507
- Oppmann B, Lesley R, Blom B, Timans JC, Xu Y, Hunte B, Vega F, Yu N, Wang J, Singh K, et al. (2000): Novel p19 protein engages IL-12p40 to form a cytokine, IL-23, with biological activities similar as well as distinct from IL-12. *Immunity* 13, 715–725
- Panitch HS, Hirsch RL, Schindler J, Johnson KP (1987): Treatment of multiple sclerosis with gamma interferon: exacerbations associated with activation of the immune system. *Neurology* 37, 1097–1102
- Papadopoulou A, Kappos L, Sprenger T (2012): Teriflunomide for oral therapy in multiple sclerosis. *Expert Rev Clin Pharmacol* 5, 617–628
- Paty DW, Li DK (1993): Interferon beta-1b is effective in relapsing-remitting multiple sclerosis. II. MRI analysis results of a multicenter, randomized, double-blind, placebo-controlled trial. UBC MS/MRI Study Group and the IFNB Multiple Sclerosis Study Group. *Neurology* 43, 662–667
- Paul C, Bolton C (1995): Inhibition of blood-brain barrier disruption in experimental allergic encephalomyelitis by short-term therapy with dexamethasone or cyclosporin A. *Int J Immunopharmacol* 17, 497–503
- Pitt B, Zannad F, Remme WJ, Cody R, Castaigne A, Perez A, Palensky J, Wittes J (1999): The effect of spironolactone on morbidity and mortality in patients with severe heart failure. Randomized Aldactone Evaluation Study Investigators. *N Engl J Med* 341, 709–717
- Pitzalis C, Pipitone N, Perretti M (2002): Regulation of leukocyte-endothelial interactions by glucocorticoids. *Ann N Y Acad Sci* 966, 108–118
- Polman CH, O'Connor PW, Havrdova E, Hutchinson M, Kappos L, Miller DH, Phillips JT, Lublin FD, Giovannoni G, Wajgt A, et al. (2006): A randomized, placebo-controlled trial of natalizumab for relapsing multiple sclerosis. *N Engl J Med* 354, 899–910
- Prinz M, Schmidt H, Mildner A, Knobloch K-P, Hanisch U-K, Raasch J, Merkler D, Detje C, Gutcher I, Mages J, et al. (2008): Distinct and nonredundant in vivo functions of IFNAR on myeloid cells limit autoimmunity in the central nervous system. *Immunity* 28, 675–686
- Prinz M, Priller J, Sisodia SS, Ransohoff RM (2011): Heterogeneity of CNS myeloid cells and their roles in neurodegeneration. *Nat Neurosci* 14, 1227–1235
- Procaccini C, De Rosa V, Pucino V, Formisano L, Matarese G (2015): Animal models of Multiple Sclerosis. *Eur J Pharmacol* 759, 182–191
- Rauch A, Seitz S, Baschant U, Schilling AF, Illing A, Stride B, Kirilov M, Mandic V, Takacz A, Schmidt-Ullrich R, et al. (2010): Glucocorticoids suppress bone formation by attenuating osteoblast differentiation via the monomeric glucocorticoid receptor. *Cell Metab* 11, 517–531
- Rausch M, Hiestand P, Foster CA, Baumann DR, Cannet C, Rudin M (2004): Predictability of FTY720 efficacy in experimental autoimmune encephalomyelitis by in vivo macrophage tracking: Clinical implications for ultrasmall superparamagnetic iron oxide-enhanced magnetic resonance imaging. *J Magn Reson Imaging* 20, 16–24

- Ravnborg M, Sørensen PS, Andersson M, Celius EG, Jongen PJ, Elovaara I, Bartholomé E, Constantinescu CS, Beer K, Garde E, Sperling B (2010): Methylprednisolone in combination with interferon beta-1a for relapsing-remitting multiple sclerosis (MECOMBIN study): a multicentre, double-blind, randomised, placebo-controlled, parallel-group trial. *Lancet Neurol* 9, 672–680
- Reichardt HM, Kaestner KH, Tuckermann J, Kretz O, Wessely O, Bock R, Gass P, Schmid W, Herrlich P, Angel P, Schütz G (1998): DNA binding of the glucocorticoid receptor is not essential for survival. *Cell* 93, 531–541
- Reichardt SD, Föller M, Rexhepaj R, Pathare G, Minnich K, Tuckermann JP, Lang F, Reichardt HM (2012): Glucocorticoids enhance intestinal glucose uptake via the dimerized glucocorticoid receptor in enterocytes. *Endocrinology* 153, 1783–1794
- Reichardt SD, Weinhage T, Rotte A, Föller M, Oppermann M, Lühder F, Tuckermann JP, Lang F, van den Brandt J, Reichardt HM (2014): Glucocorticoids induce gastroparesis in mice through depletion of l-arginine. *Endocrinology* 155, 3899–3908
- Renno T, Zeine R, Girard JM, Gillani S, Dodelet V, Owens T (1994): Selective enrichment of Th1 CD45RBlow CD4+ T cells in autoimmune infiltrates in experimental allergic encephalomyelitis. *Int Immunol* 6, 347–354
- Renoux C (2011): Natural history of multiple sclerosis: long-term prognostic factors. *Neurol Clin* 29, 293–308
- van Rensburg K (2011): A guide to prescribing corticosteroids. *SA Pharm J* 78, 32–38
- Reynolds A, Laurie C, Mosley RL, Gendelman HE (2007): Oxidative stress and the pathogenesis of neurodegenerative disorders. *Int Rev Neurobiol* 82, 297–325
- Rhen T, Cidlowski JA (2005): Antiinflammatory Action of Glucocorticoids — New Mechanisms for Old Drugs. *N Engl J Med* 353, 1711–1723
- Rickard AJ, Morgan J, Tesch G, Funder JW, Fuller PJ, Young MJ (2009): Deletion of mineralocorticoid receptors from macrophages protects against deoxycorticosterone/salt-induced cardiac fibrosis and increased blood pressure. *Hypertension* 54, 537–543
- Ridder DA, Lang M-F, Salinin S, Röderer J-P, Struss M, Maser-Gluth C, Schwaninger M (2011): TAK1 in brain endothelial cells mediates fever and lethargy. *J Exp Med* 208, 2615–2623
- Rivers TM, Sprunt DH, Berry GP (1933): Observations on attempts to produce acute disseminated encephalomyelitis in monkeys. *J Exp Med* 58, 39–53
- Rose S, Misharin A, Perlman H (2012): A novel Ly6C/Ly6G-based strategy to analyze the mouse splenic myeloid compartment. *Cytom Part J Int Soc Anal Cytol* 81, 343–350
- Rosenberg GA, Dencoff JE, Correa N, Reiners M, Ford CC (1996): Effect of steroids on CSF matrix metalloproteinases in multiple sclerosis: relation to blood-brain barrier injury. *Neurology* 46, 1626–1632
- Rószter T (2015): Understanding the Mysterious M2 Macrophage through Activation Markers and Effector Mechanisms. *Mediators Inflamm* 2015, 816460



- Sadovnick AD (1993): Familial recurrence risks and inheritance of multiple sclerosis. *Curr Opin Neurol Neurosurg* 6, 189–194
- Sakaguchi S, Yamaguchi T, Nomura T, Ono M (2008): Regulatory T cells and immune tolerance. *Cell* 133, 775–787
- Sakai DD, Helms S, Carlstedt-Duke J, Gustafsson JA, Rottman FM, Yamamoto KR (1988): Hormone-mediated repression: a negative glucocorticoid response element from the bovine prolactin gene. *Genes Dev* 2, 1144–1154
- Savage NDL, de Boer T, Walburg KV, Joosten SA, van Meijgaarden K, Geluk A, Ottenhoff THM (2008): Human anti-inflammatory macrophages induce Foxp3+ GITR+ CD25+ regulatory T cells, which suppress via membrane-bound TGFbeta-1. *J Immunol Baltim Md 1950* 181, 2220–2226
- Sawcer S, Hellenthal G, Pirinen M, Spencer CCA, Patsopoulos NA, Moutsianas L, Dilthey A, Su Z, Freeman C, Hunt SE, et al. (2011): Genetic risk and a primary role for cell-mediated immune mechanisms in multiple sclerosis. *Nature* 476, 214–219
- Saxena V, Diaz A, Clearfield A, Batteas JD, Hussain MD (2013): Zirconium phosphate nanoplatelets: a biocompatible nanomaterial for drug delivery to cancer. *Nanoscale* 5, 2328–2336
- Schakman O, Kalista S, Barbé C, Loumaye A, Thissen JP (2013): Glucocorticoid-induced skeletal muscle atrophy. *Int J Biochem Cell Biol* 45, 2163–2172
- Schmidt J, Metselaar JM, Gold R (2003): Intravenous liposomal prednisolone downregulates in situ TNF-alpha production by T-cells in experimental autoimmune encephalomyelitis. *J Histochem Cytochem Off J Histochem Soc* 51, 1241–1244
- Schweingruber N, Haine A, Tiede K, Karabinskaya A, van den Brandt J, Wüst S, Metselaar JM, Gold R, Tuckermann JP, Reichardt HM, Lühder F (2011): Liposomal encapsulation of glucocorticoids alters their mode of action in the treatment of experimental autoimmune encephalomyelitis. *J Immunol Baltim Md 1950* 187, 4310–4318
- Schweingruber N, Fischer HJ, Fischer L, van den Brandt J, Karabinskaya A, Labi V, Villunger A, Kretzschmar B, Huppke P, Simons M, et al. (2014): Chemokine-mediated redirection of T cells constitutes a critical mechanism of glucocorticoid therapy in autoimmune CNS responses. *Acta Neuropathol (Berl)* 127, 713–729
- Shijie J, Takeuchi H, Yawata I, Harada Y, Sonobe Y, Doi Y, Liang J, Hua L, Yasuoka S, Zhou Y, et al. (2009): Blockade of glutamate release from microglia attenuates experimental autoimmune encephalomyelitis in mice. *Tohoku J Exp Med* 217, 87–92
- Skurkovich S, Boiko A, Beliaeva I, Buglak A, Alekseeva T, Smirnova N, Kulakova O, Tchechonin V, Gurova O, Deomina T, et al. (2001): Randomized study of antibodies to IFN-gamma and TNF-alpha in secondary progressive multiple sclerosis. *Mult Scler Houndmills Basingstoke Engl* 7, 277–284
- Smith AJ, Liu Y, Peng H, Beers R, Racke MK, Lovett-Racke AE (2011): Comparison of a classical Th1 bacteria versus a Th17 bacteria as adjuvant in the induction of experimental autoimmune encephalomyelitis. *J Neuroimmunol* 237, 33–38

- Sorensen PS, Mellgren SI, Svenningsson A, Elovaara I, Frederiksen JL, Beiske AG, Myhr K-M, Søgaaard LV, Olsen IC, Sandberg-Wollheim M (2009): NORdic trial of oral Methylprednisolone as add-on therapy to Interferon beta-1a for treatment of relapsing-remitting Multiple Sclerosis (NORMIMS study): a randomised, placebo-controlled trial. *Lancet Neurol* 8, 519–529
- Soulika AM, Lee E, McCauley E, Miers L, Bannerman P, Pleasure D (2009): Initiation and progression of axonopathy in experimental autoimmune encephalomyelitis. *J Neurosci Off J Soc Neurosci* 29, 14965–14979
- Steinbach K, Piedavent M, Bauer S, Neumann JT, Friese MA (2013): Neutrophils amplify autoimmune central nervous system infiltrates by maturing local APCs. *J Immunol Baltim Md 1950* 191, 4531–4539
- Steinbuch M, Youket TE, Cohen S (2004): Oral glucocorticoid use is associated with an increased risk of fracture. *Osteoporos Int J Establ Result Coop Eur Found Osteoporos Natl Osteoporos Found USA* 15, 323–328
- Strehl C, Gaber T, Löwenberg M, Hommes DW, Verhaar AP, Schellmann S, Hahne M, Fangradt M, Wagegg M, Hoff P, et al. (2011): Origin and functional activity of the membrane-bound glucocorticoid receptor. *Arthritis Rheum* 63, 3779–3788
- Stromnes IM, Cerretti LM, Liggitt D, Harris RA, Goverman JM (2008): Differential regulation of central nervous system autoimmunity by T(H)1 and T(H)17 cells. *Nat Med* 14, 337–342
- Strömstedt PE, Poellinger L, Gustafsson JA, Carlstedt-Duke J (1991): The glucocorticoid receptor binds to a sequence overlapping the TATA box of the human osteocalcin promoter: a potential mechanism for negative regulation. *Mol Cell Biol* 11, 3379–3383
- Svensson-Arvelund J, Mehta RB, Lindau R, Mirrasekhian E, Rodriguez-Martinez H, Berg G, Lash GE, Jenmalm MC, Ernerudh J (2015): The human fetal placenta promotes tolerance against the semiallogeneic fetus by inducing regulatory T cells and homeostatic M2 macrophages. *J Immunol Baltim Md 1950* 194, 1534–1544
- Tabansky I, Messina MD, Bangeranye C, Goldstein J, Blitz-Shabbir KM, Machado S, Jeganathan V, Wright P, Najjar S, Cao Y, et al. (2015): Advancing drug delivery systems for the treatment of multiple sclerosis. *Immunol Res* 63, 58–69
- Tahover E, Patil YP, Gabizon AA (2015): Emerging delivery systems to reduce doxorubicin cardiotoxicity and improve therapeutic index: focus on liposomes. *Anticancer Drugs* 26, 241–258
- Tanaka J, Fujita H, Matsuda S, Toku K, Sakanaka M, Maeda N (1997): Glucocorticoid- and mineralocorticoid receptors in microglial cells: The two receptors mediate differential effects of corticosteroids. *Glia* 20, 23–37
- Then Bergh F, Kümpfel T, Schumann E, Held U, Schwan M, Blazevic M, Wismüller A, Holsboer F, Yassouridis A, Uhr M, et al. (2006): Monthly intravenous methylprednisolone in relapsing-remitting multiple sclerosis - reduction of enhancing lesions, T2 lesion volume and plasma prolactin concentrations. *BMC Neurol* 6, 19
- Thornton AM, Shevach EM (2000): Suppressor effector function of CD4+CD25+ immunoregulatory T cells is antigen nonspecific. *J Immunol Baltim Md 1950* 164, 183–190

- Tischner D, Weishaupt A, van den Brandt J, Müller N, Beyersdorf N, Ip CW, Toyka KV, Hünig T, Gold R, Kerkau T, Reichardt HM (2006): Polyclonal expansion of regulatory T cells interferes with effector cell migration in a model of multiple sclerosis. *Brain J Neurol* 129, 2635–2647
- Toft-Hansen H, Nuttall RK, Edwards DR, Owens T (2004): Key metalloproteinases are expressed by specific cell types in experimental autoimmune encephalomyelitis. *J Immunol Baltim Md* 1950 173, 5209–5218
- Tourtellotte WW, Haerer AF (1965): Use of an oral corticosteroid in the treatment of multiple sclerosis; a double-blind study. *Arch Neurol* 12, 536–545
- Traboulsee AL, Bernales CQ, Ross JP, Lee JD, Sadovnick AD, Vilariño-Güell C (2014): Genetic variants in IL2RA and IL7R affect multiple sclerosis disease risk and progression. *Neurogenetics* 15, 165–169
- Tran EH, Hoekstra K, van Rooijen N, Dijkstra CD, Owens T (1998): Immune invasion of the central nervous system parenchyma and experimental allergic encephalomyelitis, but not leukocyte extravasation from blood, are prevented in macrophage-depleted mice. *J Immunol Baltim Md* 1950 161, 3767–3775
- Tronche F, Kellendonk C, Kretz O, Gass P, Anlag K, Orban PC, Bock R, Klein R, Schütz G (1999): Disruption of the glucocorticoid receptor gene in the nervous system results in reduced anxiety. *Nat Genet* 23, 99–103
- Tsunoda I, Libbey JE, Kobayashi-Warren M, Fujinami RS (2006): IFN- $\gamma$  production and astrocyte recognition by autoreactive T cells induced by Theiler's virus infection: Role of viral strains and capsid proteins. *J Neuroimmunol* 172, 85–93
- Tuckermann JP, Kleiman A, McPherson KG, Reichardt HM (2005): Molecular mechanisms of glucocorticoids in the control of inflammation and lymphocyte apoptosis. *Crit Rev Clin Lab Sci* 42, 71–104
- Tuohy VK, Lu Z, Sobel RA, Laursen RA, Lees MB (1989): Identification of an encephalitogenic determinant of myelin proteolipid protein for SJL mice. *J Immunol Baltim Md* 1950 142, 1523–1527
- Usher MG, Duan SZ, Ivaschenko CY, Frieler RA, Berger S, Schütz G, Lumeng CN, Mortensen RM (2010): Myeloid mineralocorticoid receptor controls macrophage polarization and cardiovascular hypertrophy and remodeling in mice. *J Clin Invest* 120, 3350–3364
- Varga G, Ehrchen J, Tsianakas A, Tenbrock K, Rattenholl A, Seeliger S, Mack M, Roth J, Sunderkoetter C (2008): Glucocorticoids induce an activated, anti-inflammatory monocyte subset in mice that resembles myeloid-derived suppressor cells. *J Leukoc Biol* 84, 644–650
- Varga G, Ehrchen J, Brockhausen A, Weinlage T, Nippe N, Belz M, Tsianakas A, Ross M, Bettenworth D, Spieker T, et al. (2014): Immune suppression via glucocorticoid-stimulated monocytes: a novel mechanism to cope with inflammation. *J Immunol Baltim Md* 1950 193, 1090–1099
- Viglietta V, Baecher-Allan C, Weiner HL, Hafler DA (2004): Loss of functional suppression by CD4+CD25+ regulatory T cells in patients with multiple sclerosis. *J Exp Med* 199, 971–979

- Waddell DS, Baehr LM, van den Brandt J, Johnsen SA, Reichardt HM, Furlow JD, Bodine SC (2008): The glucocorticoid receptor and FOXO1 synergistically activate the skeletal muscle atrophy-associated MuRF1 gene. *Am J Physiol Endocrinol Metab* 295, E785-797
- Weber MS, Prod'homme T, Youssef S, Dunn SE, Rundle CD, Lee L, Patarroyo JC, Stüve O, Sobel RA, Steinman L, Zamvil SS (2007): Type II monocytes modulate T cell-mediated central nervous system autoimmune disease. *Nat Med* 13, 935–943
- Weinstein RS (2012): Glucocorticoid-Induced Osteoporosis and Osteonecrosis. *Endocrinol Metab Clin North Am* 41, 595–611
- Weissleder R, Nahrendorf M, Pittet MJ (2014): Imaging macrophages with nanoparticles. *Nat Mater* 13, 125–138
- Wu F, Cao W, Yang Y, Liu A (2010): Extensive infiltration of neutrophils in the acute phase of experimental autoimmune encephalomyelitis in C57BL/6 mice. *Histochem Cell Biol* 133, 313–322
- Wüst S, van den Brandt J, Tischner D, Kleiman A, Tuckermann JP, Gold R, Lühder F, Reichardt HM (2008): Peripheral T cells are the therapeutic targets of glucocorticoids in experimental autoimmune encephalomyelitis. *J Immunol Baltim Md 1950* 180, 8434–8443
- Wüst S, Tischner D, John M, Tuckermann JP, Menzfeld C, Hanisch U-K, van den Brandt J, Lühder F, Reichardt HM (2009): Therapeutic and Adverse Effects of a Non-Steroidal Glucocorticoid Receptor Ligand in a Mouse Model of Multiple Sclerosis. *PLoS ONE* 4, 12 e8202
- Xu L, Kitani A, Fuss I, Strober W (2007): Cutting edge: regulatory T cells induce CD4+CD25-Foxp3- T cells or are self-induced to become Th17 cells in the absence of exogenous TGF-beta. *J Immunol Baltim Md 1950* 178, 6725–6729
- Yuan B, Zhao L, Fu F, Liu Y, Lin C, Wu X, Shen H, Yang Z (2014): A novel nanoparticle containing MOG peptide with BTLA induces T cell tolerance and prevents multiple sclerosis. *Mol Immunol* 57, 93–99
- Zamvil S, Nelson P, Trotter J, Mitchell D, Knobler R, Fritz R, Steinman L (1985): T-cell clones specific for myelin basic protein induce chronic relapsing paralysis and demyelination. *Nature* 317, 355–358
- Zhang G, Zhang L, Duff GW (1997): A negative regulatory region containing a glucocorticosteroid response element (nGRE) in the human interleukin-1beta gene. *DNA Cell Biol* 16, 145–152
- Zhang G-X, Yu S, Gran B, Li J, Siglienti I, Chen X, Calida D, Ventura E, Kamoun M, Rostami A (2003): Role of IL-12 receptor beta 1 in regulation of T cell response by APC in experimental autoimmune encephalomyelitis. *J Immunol Baltim Md 1950* 171, 4485–4492
- Zhang X, Koldzic DN, Izikson L, Reddy J, Nazareno RF, Sakaguchi S, Kuchroo VK, Weiner HL (2004): IL-10 is involved in the suppression of experimental autoimmune encephalomyelitis by CD25+CD4+ regulatory T cells. *Int Immunol* 16, 249–256
- Zhang Z, Zhang Z-Y, Schluesener HJ (2009): Compound A, a plant origin ligand of glucocorticoid receptors, increases regulatory T cells and M2 macrophages to attenuate experimental autoimmune neuritis with reduced side effects. *J Immunol Baltim Md 1950* 183, 3081–3091

- Zindler E, Zipp F (2010): Neuronal injury in chronic CNS inflammation. *Best Pract Res Clin Anaesthesiol* 24, 551–562
- Zivadnov R, Rudick RA, Masi RD, Nasuelli D, Ukmar M, Pozzi–Mucelli RS, Grop A, Cazzato G, Zorzon M (2001): Effects of IV methylprednisolone on brain atrophy in relapsing-remitting MS. *Neurology* 57, 1239–1247

## 6 Acknowledgements

Many are the people who, in one way or another, contributed to this work.

First, I would like to thank Prof. Dr. Holger Reichardt for placing his trust in me to carry out this interesting project, offering me the opportunity to learn and grow as a scientist. I would also like to acknowledge his guidance and organizing skills in both scientific and bureaucratic matter, and his support in the ups and downs during these years. The door of his office was always open for counseling and interactive discussions, and I really appreciated it.

Many thanks to my second supervisor, PD Dr. Fred Lühder, whom I cannot officially name 'Doktorvater', but he earned at least the degree of 'Doktoronkel'. I thank him for his close supervision, his assistance in practical laboratory matters and for the refreshing scientific discussions. I am also thankful for his guidance through the lights and shadows of the German language.

I would also like to thank Prof. Dr. Hanisch and Prof. Dr. Walter as members of the Thesis Committee, and the rest of the members of the Examination Board, Prof. Dr. Stadelmann-Nessler, Prof. Dr. mult. Meyer, and Prof. Dr. Jarry. I am also thankful to the SFB TRR43 for offering the opportunity to participate in conferences and talks that gave me a broader perspective about the neuroimmunology field.

I am personally really grateful to Dr. Erik Meskauskas, coordinator of the MolMed program, for his help with the bureaucracy and his friendliness. Thanks also to the new coordinator of the PhD students, Ms. Wolfram; to our secretaries in the Immunology Department, Anika Schindler and Ingrid Teuteberg; and to Cathy Ludwig from the Institute for Multiple Sclerosis Research (IMSF).

Not to forget our collaborators in the Institute for Technology in Karlsruhe, Prof. Dr. Feldmann and Dr. Heck, and specially our colleagues in the IMSF here in Göttingen, where I conducted a big part of my experiments. Thanks to Tanja, Anne and Judith for their help in

many experiments and for their friendliness. Also to César, for making my visits to the IMSF more amusing. To the rest of the PhDs, postdocs and PIs, who were always helpful and contributed to my work with nice feedback. And of course thanks to the animal care takers and the technicians, particularly to Martina Weig, who taught me all about histology and was always willing to help whenever something went wrong.

Next, I would like to thank my colleagues from the Institute for Immunology. Thanks for the many nice moments lived together, both scientific and extra-professional. I am deeply grateful to our technicians, Julian Koch and Amina Bassibas, without them this work would have not been possible. To Amina, thanks for being not only a great technical assistant, but my personal confident and a good friend as well. To all the colleagues that in these years worked with me in the Reichardt's group: Jennifer, Xiao, Kai, Nils, Anna, Ann-Kathrin, Eric, Milena, Katharina, Henrike, Sybille, Nicky, Laura, Garrit and Tina. To the master students that were under my supervision: Sarah, Vicky, Natalie and Elena, it was great to work with you girls! Thanks to Carina, for being always by my side since we started together in the lab. Also to Julius, always friendly and helpful inside and outside the lab. To both of them and Annemarie, extra thanks for the proofreading of this work.

I also want to express my gratitude to all the friends that gave me their support throughout these years. To the ones I made in Göttingen, thank you for making me feel at home in this town.

Finally, an important part of these acknowledgements goes to my family. To my brothers Ignacio and Alberto, and especially to my parents, Toyi and Justo, to whom I dedicate this thesis. Thank you for the education you gave me, which brought me this far, and for being always there, come what may. Foremost, I want to thank you Pedro for always encouraging me to give my best, for your caring support and for making every day colorful and fun.

# Curriculum Vitae

**Name** Elena Victoria Montes Cobos  
**Date of birth** 06.02.1988  
**Nationality** Spanish  
**Contact** Institute for Cellular and Molecular Immunology  
Humboldtallee 34, 37075 Göttingen (Germany)  
Telephone: +49 (0551) 39-5816  
E-mail: elena.montes.cobos@gmail.com

## Education

09/2012 - present PhD candidate at the Institute for Cellular and Molecular Immunology - UMG, Göttingen  
09/2011 - 09/2012 Master of Science in Molecular Medicine - UMG, Göttingen  
09/2006 - 07/2011 Licentiate in Biotechnology - University of Salamanca, Spain  
09/2004 - 07/2006 Secondary School - I.E.S. Valle del Jerte, Plasencia, Spain  
09/1992 - 07/2004 Primary School - Colegio San Calixto, Plasencia, Spain

## Publications

**Montes-Cobos E**, Li X, Fischer HJ, Sasse A, Kügler S, Didié M, Toischer K, Fassnacht M, Dressel R, Reichardt HM (2015): Inducible Knock-Down of the Mineralocorticoid Receptor in Mice Disturbs Regulation of the Renin-Angiotensin-Aldosterone System and Attenuates Heart Failure Induced by Pressure Overload. *PloS One* 10, e0143954

Theiss-Suennemann J, Jörß K, Messmann JJ, Reichardt SD, **Montes-Cobos E**, Lühder F, Tuckermann JP, AWolff H, Dressel R, Gröne H-J, et al. (2015): Glucocorticoids attenuate acute graft-versus-host disease by suppressing the cytotoxic capacity of CD8 (+) T cells. *J Pathol* 235, 646–655